Substrate Targeting and Control of DNA Replication by the CUL4/DDB1 Ubiquitin Ligase

by
Chad M. McCall

A dissertation submitted to the faculty of the University of North Carolina at Chapel Hill in partial fulfillment of the requirements for the degree of Doctor of Philosophy in the Department of Biochemistry and Biophysics

Chapel Hill
2007

Approved by

Advisor: Dr. Yue Xiong

Reader: Dr. Stephen Chaney

Reader: Dr. Jeanette Cook

Reader: Dr. William Marzluff

Reader: Dr. Cam Patterson

ABSTRACT

CHAD M. MCCALL: Substrate Targeting and Control of DNA Replication by the CUL4/DDB1 Ubiquitin Ligase

(under the direction of Dr. Yue Xiong)

Ubiqutin-mediated proteolysis is an essential pathway in the cell, by which specific proteins are targeted for degradation at specific times. The small protein ubiquitin is conjugated onto targets for proteolysis by a series of three enzymatic reactions, catalyzed by an E1 ubiquitin activating enzyme, an E2 ubiquitin conjugating enzyme, and one of hundreds of E3 ubiquitin ligases. E3 ubiquitin ligases provide specificity for the reaction by interacting with specific substrates and an E2. The cullin family of ligases is particularly important because their modular domain structure allows for many ligases to be formed from a minimum of components. In this study, I describe research into the substrate-targeting mechanism of Cullin 4A. First, I identified by mass spectrometry a substrate receptor family containing a specific motif within WD-40 repeats that interacts with a common Cullin 4A adaptor, DDB1. In collaboration with others in my laboratory, we determined that more than 90 potential receptors contain this "DWD" motif. I then characterized one of these receptors, VprBP, which is required for normal cellular proliferation. VprBP silencing leads to a defect in DNA replication, whereby replication stress leads to an upregulation of cryptic origins of replication but an overall decrease in nucleotide incorporation. It also interacts with the HIV-1 accessory protein Vpr, and bridges the Vpr ubiquitination substrate UNG2 to the CUL4A ligase.

To my parents, Frank and Martha McCall

ACKNOWLEDGEMENTS

There are many people that I would like to thank for their help in countless ways over the past several years. First, I thank my advisor, Dr. Yue Xiong, for his mentorship and support. I am grateful for the opportunity to work in his lab on challenging projects, and for the example he shows in his enthusiasm and love for science. Without his guidance, I would not have become nearly the scientist that I am today. I also thank my committee members, Drs. Bill Marzluff, Cam Patterson, Steve Chaney, Jean Cook, and Christoph Borchers, for their encouragement and excellent ideas throughout my dissertation work. I would especially like to thank Jean for the close collaboration between her lab and ours over the past year; her ideas and technical assistance have immeasurably helped the final direction of my project.

I would also like to thank my collaborators in the Xiong Laboratory, without whose help, expertise, and ideas through daily conversations, this project would not have been successful: Dr. Paula Miliani de Marval, Dr. Jian Hu, Dr. Sima Zacharek, Mr. Yizhou He, and Mrs. Sarah Jackson. Especially, I would like to thank Yizhou (Joe) for his invaluable technical assistance in almost every aspect of my research, and for his colloboration that forms Chapter 2 of this dissertation. I am also grateful to the other members of the Xiong Lab, past and present, who have contributed to such an enjoyable atmosphere in which to work: Dr. Feng Bai, Dr. Xin-Hai Pei, Dr. Zhijun Li, Ms. Yaxue

Zeng, Mr. Matt Smith, Ms. Jenna Spencer, Dr. Yojiro Kotake, Dr. Paul Andrews, Dr. Stuart Shumway, Dr. Manabu Furukawa, Dr. Toru Nishikawa, Ms. Rupa Shukla, Ms. Erin Parsons, Dr. Jidong Liu, Dr. Theresa Allio, Dr. Gabrielle White Wolf, Ms. Sarah Nicholls, Ms. Deborah Brown, Dr. Jialiang Wang, and Dr. Joe McCarville.

I would also like to thank the staff of the Biochemistry Department, who have guided me throughout my PhD work, especially Dr. Tom Traut, the director of graduate studies, and Ms. Diane Harris, his secretary, who made sure that I met every deadline and stayed on track each year. Also, without the help of Mr. Mark Kramer and the staff of Lineberger Cancer Center, I would not have been successful at obtaining a predoctoral fellowship.

Finally, I would like to thank my parents, Frank and Martha McCall, and my sister, Erin, for their love and support. Without them by my side throughout my life, there is no way I would be where I am today.

TABLE OF CONTENTS

LIST OF FIGURES

Table

LIST OF ABBREVIATIONS AND SYMBOLS

AMP	Adenosine monophosphate
APC	Anaphase promoting complex
APG16L	Autophagy 16-like
APOBEC3G	Apolipoprotein B mRNA editing enzyme, catalytic polypeptide-like 3G
ATM	Ataxia Telangiectasia Mutated
ATP	Adenosine Triphosphate
ATR	ATM and Rad-3 related
BARD1	BRCA1-associated RING domain 1
Bax	BCL2-associated X protein
Bmi1	B lymphoma Mo-MLV insertion region 1
BRCA1	Breast Cancer 1
BrdU	Bromodeoxyuridine
BTB	Bric-a-brac, Tramtrack, Broad-complex
β-TrCP	Beta-transducin repeat-containing protein
CAND1	Cullin-associated Nedd8-dissociated 1
Cbl	Casitas B-lineage lymphoma
Cdc	Cell division cycle
CDT	chromatin licensing and DNA replication factor
Chk	Checkpoint kinase
Cip1	Cyclin-dependent kinase inhibitor protein 1
CldU	Chlorodeoxyuridine

COP	Constitutive Photomorphogenic
CPSF160	Cleavage and polyadenylation specific factor 160-kDa
CRL	Cullin-ROC Ligase
CSA	Cockayne Syndrome Gene A
CSB	Cockayne Syndrome Gene B
CSN	COP9 signalosome subunit
CUL	Cullin
Dbf4	DumbBell Forming 4
DNA	Deoxyribonucleic acid
DDB	Damaged DNA Binding
DET1	De-etiolated 1
DMEM	Dulbecco's Minimum Essential Medium
DWD	DDB1-binding WD-40
E1	Ubiquitin activating enzyme (enzyme 1)
E1B55K	Adenoviral protein E1B, 55-kDa
E2	Ubiquitin conjugating enzyme (enzyme 2)
E3	Ubiquitin ligase (enzyme 3)
E4orf6	Adenoviral protein E4 open reading frame 6
E6	Human papillomavirus protein E6
E6AP	E6 associated protein
Ex.x (days)	Embryonic age day x.x
FBS	Fetal bovine serum
FBXW	F-box WD-40

G1	Gap phase 1
G2	Gap phase 2
GADD45α	Growth arrest and DNA Damage protein 45 alpha
$G\beta_2$	G-protein β_2
GRWD1	Glutamine-rich WD-40 protein 1
H2A	Histone 2A
H2AX	Histone 2A variant X
H2B	Histone 2B
H3	Histone 3
H4	Histone 4
HECT	Homologous to the E6AP Carboxyl Terminus
HIF	Hypoxia-Inducible Factor
HIV	Human Immunodeficiency Virus
HPV	Human Papillomavirus
Hrt	High level expression Reduces Ty3 transpositionHus1
IdU	Iododeoxyuridine
IκBα	Inhibitor of NFκB alpha
KATNB1	Katanin subunit B1
Keap1	Kelch-like ECH-associated protein
Kip1	Cyclin-dependent kinase inhibitor protein 1 (p27)
L2DTL	Lethal (2) Denticleless homolog
LTR	Long terminal repeat
MCM	Minichromosome Maintenance

MDM2	Murine double minute chromosome protein 2
MDMX	Murine double minute chromosome protein X
M-phase	Mitotic phase
Nedd8	Neural precursor cell expressed, developmentally down-regulated 8
NF-κB	Nuclear factor κ-B
Noc	Nocodazole
Nrf2	NF-E2-related factor 2
NUP43	Nucleoporin 43-kDa
p53	53-kDa protein
PARC	Parkin-like cytoplasmic protein
PBS	Phosphate-buffered saline
PCNA	Proliferating cell nuclear antigen
Pcu	*Pombe* cullin
PPi	Phosphate
PWP1	Periodic WD-40 repeat protein 1
Rad17	Radiation-sensitive protein 17
Rb	Retinoblastoma protein
RBBP	Rb Binding Protein
Rbx	RING-box
ROC/Roc	Ring of cullin
RING	Really Interesting New Gene
Ring1B	RING protein 1B
RNAi	Ribonucleic Acid (RNA) interference

RPA	Replication Protein A
RTT101	Regulator of Ty1 Transposition 101
Rub1	Related to Ubiquitin 1
SAG	Suppressor of Apoptosis Gene
SAP130	Spliceosome-associated protein 130-kDa
SCF	SKP1-CUL1-F-box
SDS-PAGE	Sodium dodecyl sulfate-polyacrylamide gel electrophoresis
shRNA	Small hairpin RNA
siRNA	Small interfering RNA
SKP	Suppressor of Kinetochore Protein
SMUG	Single-strand selective monofunctional uracil DNA glycosylase
SOCS	Suppressor of cytokine signaling
S-phase	DNA synthesis phase
STAT	Signal transducer and activator of transcription
SUMO-1	Small Ubiquitin-like modifier 1
TSC2	Tuberous sclerosis complex gene 2
Ub	Ubiquitin
UbcH5c	Ubiquitin conjugating enzyme H5c
Ubc12	Ubiquitin conjugating enzyme 12
Ube2g2	Ubiquitin conjugating enzyme 2g2
UNG	Uracil nucleotide glycosylase
UV	Ultraviolet
VHL	von Hippel-Lindau

Vif	Viral infectivity factor
Vpr	Viral protein R
VprBP	Vpr Binding Protein
WD-40	Trytophan-aspartic acid domain – 40 residues
WDR	WD-40 Repeat Protein
WSB	WD-40 and SOCS Box Protein
XPC	Xeroderma Pigmentosum group C protein
XP-E	Xeroderma Pigmentosum group E

Chapter 1

INTRODUCTION

Covalent modification with ubiquitin alters protein fate and function

The cell targets almost all of its proteins for post-translational covalent modification, in order to rapidly change various properties, from catalytic activity to binding partners to cellular fate. These modifications take various forms, from small molecular weight additions like phosphorylation, acetylation, and methylation, to conjugation of small proteins such as ubiquitin, Nedd8, and SUMO-1. Ubiquitin is of particular interest, because its conjugation is associated with the targeted degradation of proteins at specific points in the lifetime of the cell when they are no longer needed.

Ubiquitin (Ub), a small protein of 76 amino acids, is strongly conserved throughout all eukaryotes. Via its carboxyl-terminal glycine, it may be conjugated through an isopeptide bond to the epsilon amino groups of lysine residues on specific proteins in the cell (Jentsch 1992). This conjugation occurs through a cascade of reactions requiring three enzymes: an E1 ubiquitin activating enzyme, an E2 ubiquitin conjugating enzyme, and an E3 ubiquitin ligase (Figure 1.1) (Pickart and Eddins 2004). The E1 functions by first catalyzing the ATP-dependent formation of a ubiquitin-adenylate intermediate. The catalytic cysteine residue of the E1 then attacks the adenylate intermediate, forming a high-energy thioester bond between the E1 and ubiquitin. The activated ubiquitin is then passed in an ATP-independent manner to the catalytic cysteine of the E2.

Figure 1.1

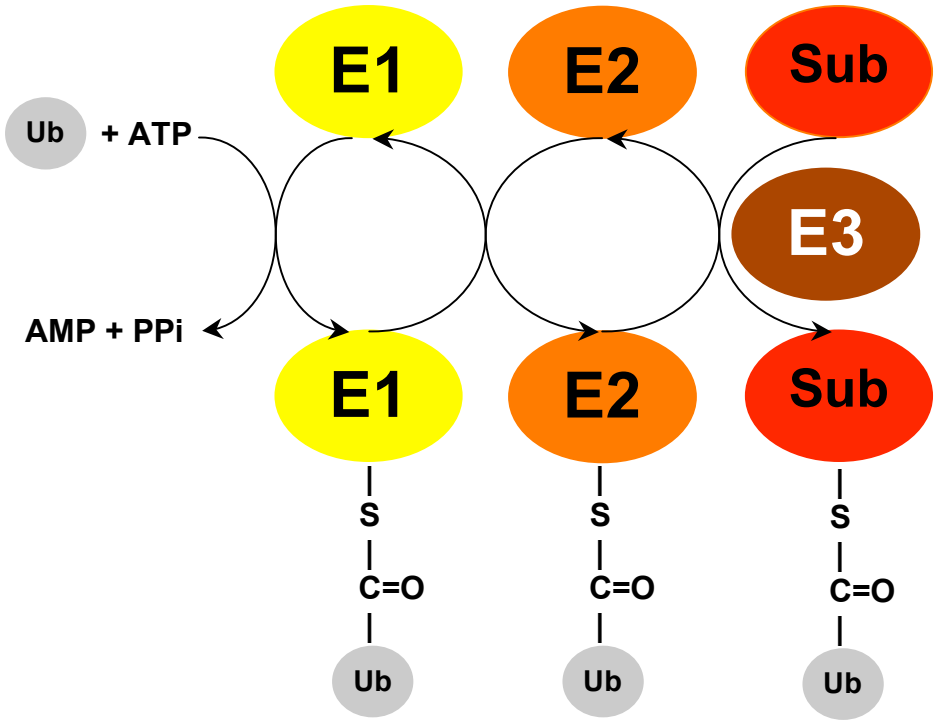

Figure 1.1 -- The Ubiquitination Cascade

Ubiquitin modification requires a series of three enzymes: the E1 ubiquitin activating enzyme (yellow), which in an ATP-dependent manner covalently binds to ubiquitin (grey) in a high-energy thioester bond. The E1 then passes ubiquitin to one of more than twenty E2 ubiquitin conjugating enzymes (orange). An E3 ubiquitin ligase (brown) interacts with a substrate (red) and the E2, allowing the E2 to transfer ubiquitin onto the substrate. For polyubiquitin chain formation, multiple ubiquitin moieties are conjugated onto a single substrate.

E3 ubiquitin ligases target substrates for ubiquitin conjugation

The E2-Ub intermediate then interacts with an E3 ubiquitin ligase in order to covalently conjugate ubiquitin to the target protein lysine. There are two broad families of E3 ligases: those containing either RING (Really Interesting New Gene) or HECT (Homologous to the E6AP Carboxyl Terminus) domains (Huibregtse et al. 1995; Jackson et al. 2000). A smaller family, the U-box ligases, are structurally and catalytically very similar to RING ligases, with the major difference being electrostatic instead of zinc-ion interactions producing structural stability to the catalytic domain (Hochstrasser 2006). Both RING and HECT domains interact with E2 enzymes; however, HECT ligases form a covalent E3-Ub thioester intermediate before ligating ubiquitin to substrates, while RING (and U-box; hereafter, any discussion of RING ligases includes U-box) ligases pass ubiquitin directly from the E2 to the substrate without a covalent intermediate. RING ligases can be subdivided into two families as well: those that contain intrinsic RING domains as well as substrate-binding domains in a single protein, and those that utilize RING and substrate-interacting domains on separate polypeptides.

The RING domain is critical for E3 ubiquitin ligase catalytic activity, but how this occurs is not as clear as in the case of HECT ligases, which form covalent E3-Ub intermediates. The characteristic structural feature of a RING domain is a "cross-brace" scaffold formed by the coordination of two zinc ions by a series of cysteine or histidine residues (Pickart 2001). The spacing of the zinc ions, and not the primary sequence, is conserved among RING family members, and as the zinc ions are inert, the domain likely

serves as a rigid scaffold, not in catalysis. Studies on the RING subunit of the cullin ubiquitin ligases, ROC1/2, have provided the most insight into this conundrum. The RING finger directly binds to the E2 ubiquitin conjugating enzyme; the residues within the RING finger required for maintaining its "cross-bridge" zinc-coordinated structure are required for its catalytic activity; and, the RING domain is sufficient to catalyze polyubiquitin chain formation (Kamura et al. 1999; Ohta et al. 1999; Seol et al. 1999; Skowyra et al. 1999; Tan et al. 1999). Moreover, studies from our laboratory have shown that the ROC1 RING domain by itself, without its cullin binding partner, is sufficient to catalyze polyubiquitin chain formation by the E2 UbcH5c (Furukawa et al. 2002). In some RING ligases, such as Cbl, the RING domain is required for binding to the E2, but in others, such as ROC1, mutating the RING domain does not abolish E2 binding but only inhibits ubiquitin chain formation (Jackson et al. 2000). Another layer of complexity is added by the specificity of E2/E3 interactions: ROC1 requires its cullin binding partner to catalyze polyubiquitination by the E2 Cdc34, but activates UbcH5C regardless of whether the cullin subunit is present or not (Seol et al. 1999; Furukawa et al. 2002). The most likely explanation for these data is that the RING domain's primary role is in E2 catalytic activation, by a heretofore-unclear mechanism, while it has a secondary role in E2/E3 interaction.

Ubiquitin ligases may, depending upon characteristics of E2 enzymes, substrates, and the ligases themselves, either conjugate a single ubiquitin or poly-ubiquitin chains onto substrates. Mono-ubiquitination serves to alter the cellular fate of various proteins, such as targeting membrane proteins for internalization, sorting nascent proteins to the

trans-Golgi network, viral budding, and altering transcriptional activity, histone modification, and DNA repair (d'Azzo et al. 2005). Poly-ubiquitination serves various roles in the cell depending upon the nature of the ubiquitin chain. Ubiquitin molecules linked in chains through lysine-63 play a poorly-characterized role in modulating cellular signaling pathways, in particular the NF-κB pathway and the regulation of error-prone vs. error-free translesion DNA synthesis by PCNA (Pickart 2004). However, lysine-48-linked polyubiquitin chains function to target modified proteins for proteolytic degradation by the 26S proteasome. It is this prominent function of polyubiquitination, to target specific proteins, at specific times, for degradation, that has been the focus of research in our laboratory for the past several years.

The formation of polyubiquitin chains proceeds by a poorly defined mechanism.

The exact mechanism by which ubiquitin chains are formed is not well defined. The classical model, whereby single ubiquitin molecules are conjugated to each other, one by one, by rounds of charged ubiquitin, has never been experimentally established (Hochstrasser 2006). However, another possibility has been recently demonstrated for one particular E2/E3 pair: mouse Ube2g2 (E2) and human gp78 (endoplasmic reticulum RING E3) (Li et al. 2007). The authors experimentally demonstrate that a polyubiquitin chain forms on the E2, in a manner that requires interaction between two E2 molecules as well as E2-E3 interaction; and, the chain is thus transferred as a unit onto a substrate. It is not clear, though, whether this model can be generalized to all E2's or ubiquitination of all substrates. Other studies have generated data that fits the sequential addition

(classical) model better than preformed chain addition, such as differential ubiquitination of different anaphase-promoting complex (APC) E3 substrates and mechanistic studies of ubiquitin chain formation by the E3 SCF^{Cdc4} and its E2 Cdc34 (Petroski and Deshaies 2005b; Rape et al. 2006). However, as Hochstrasser points out in his recent review, none of these data rules out preformed chain assembly entirely; therefore, the real mechanism of polyubiquitination may be either yet to be defined, or depend on the individual E2, E3, and/or substrate (Hochstrasser 2006).

The cullin E3 ligases function in multisubunit complexes to target a wide variety of substrates for ubiquitination

Our laboratory has focused upon the cullin family of multisubunit RING ligases, which play critical roles in a large number of cellular processes. There are six canonical cullins in mammalian cells: CUL1, CUL2, CUL3, CUL4A, CUL4B, and CUL5, as well as three more distantly-related proteins, CUL7, Parc, and APC11. Orthologous to the six canonical cullins, *C. elegans* and *Drosophila* have five cullins (a single CUL4 ortholog rather that both CUL4A and CUL4B), while *S. pombe* contains four (single CUL4 (Pcu4p) and single CUL2/5 (Pcu2p) orthologs) and *S. cerevisiae* has but three (CUL1 (Cdc53), Cul3, and the more distantly-related Cul8/RTT101) (Petroski and Deshaies 2005a). Each canonical cullin contains three characteristic features: an amino-terminal domain required for recruiting specific substrates, a carboxyl-terminal domain required for the interaction with one of the Roc/Rbx/Hrt family of small RING finger proteins (which recruit and allosterically activate E2 enzymes to ubiquitinate cullin substrates), and a lysine adjacent to the Roc binding domain, which is covalently modified by the

ubiquitin-like protein Nedd8/Rub1 to activate cullin function in a manner to be described below. The crystal structures of both CUL1 and CUL4A ligase complexes have been solved, and show a clear spatial separation of the N-terminal substrate-recruitment domain from the C-terminal ROC1-binding/catalytic domain by a rigid central scaffold (Zheng et al. 2002b; Angers et al. 2006). This rigid structure hypothetically serves to hold the activated E2 at the proper distance and orientation from the substrate, as mutations disrupting the rigidity of the central domain of CUL1 abolish ligase activity (Zheng et al. 2002b); however, there are no structures available of a full cullin-substrate complex, so the actual structural basis for interaction between the substrate and the E2 remains to be elucidated.

Each cullin recruits substrates through distinct N-terminal domains interacting with different families of substrate receptors

The canonical cullins, while quite homologous in their Roc-binding and Nedd8-modification domains, have divergent amino-terminal sequences, which are required for interaction with their substrates. However, these substrates do not bind to the cullins directly, but interact through a series of linker molecules specific to each cullin (Figure 1.2). CUL1, the first family member to be well characterized, interacts at its amino terminus with the small protein SKP1 (Feldman et al. 1997; Skowyra et al. 1997; Zheng et al. 2002b). SKP1, in turn, interacts with one of greater than 60 mammalian proteins containing an F-box domain. These secondary linkers then interact with specific substrates, often through recognition of a phosphorylation event, such as the F-box proteins β-TrCP with phosphorylated substrates IκBα and β-catenin, and SKP2 with

phosphorylated $p27^{Kip1}$ (Carrano et al. 1999; Latres et al. 1999; Tan et al. 1999; Tsvetkov et al. 1999). In this manner, the SKP1-CUL1-F-box (SCF) modular complexes can potentially ubiquitinate and target for proteasomal degradation tens, if not hundreds, of substrates. The vast majority of F-box proteins have yet to be well characterized, leaving fertile ground for future characterization of CUL1 substrates.

CUL2 and CUL5 recruit substrates in a very similar manner to CUL1. The heterodimeric linker complex of Elongins B and C (Elongin C being structurally homologous to SKP1) interacts with both the amino-terminus of CUL2/5 and secondary linkers containing either VHL- or SOCS-box domains (for CUL2 or CUL5 respectively) (Kamura et al. 1998; Stebbins et al. 1999; Zhang et al. 1999; Kamura et al. 2001; Kamura et al. 2004). These secondary linkers interact with specific substrates, such as hydroxylated HIF-1 transcription factor interacting with the linker VHL (Figure 1.2B). CUL3, on the other hand, interacts with substrates through a single hybrid linker containing both a cullin-interacting BTB domain and another domain interacting with substrates, such as the BTB-Kelch protein Keap1 interacting with the substrate Nrf2 (Figure 1.2C) (Geyer et al. 2003; Pintard et al. 2003; Xu et al. 2003; Furukawa and Xiong 2005). In the human genome, there are at least 40 VHL- or SOCS-box proteins, and over 200 BTB domain proteins, which allow CUL2/5 and CUL3 to also potentially recruit hundreds of substrates.

Figure 1.2

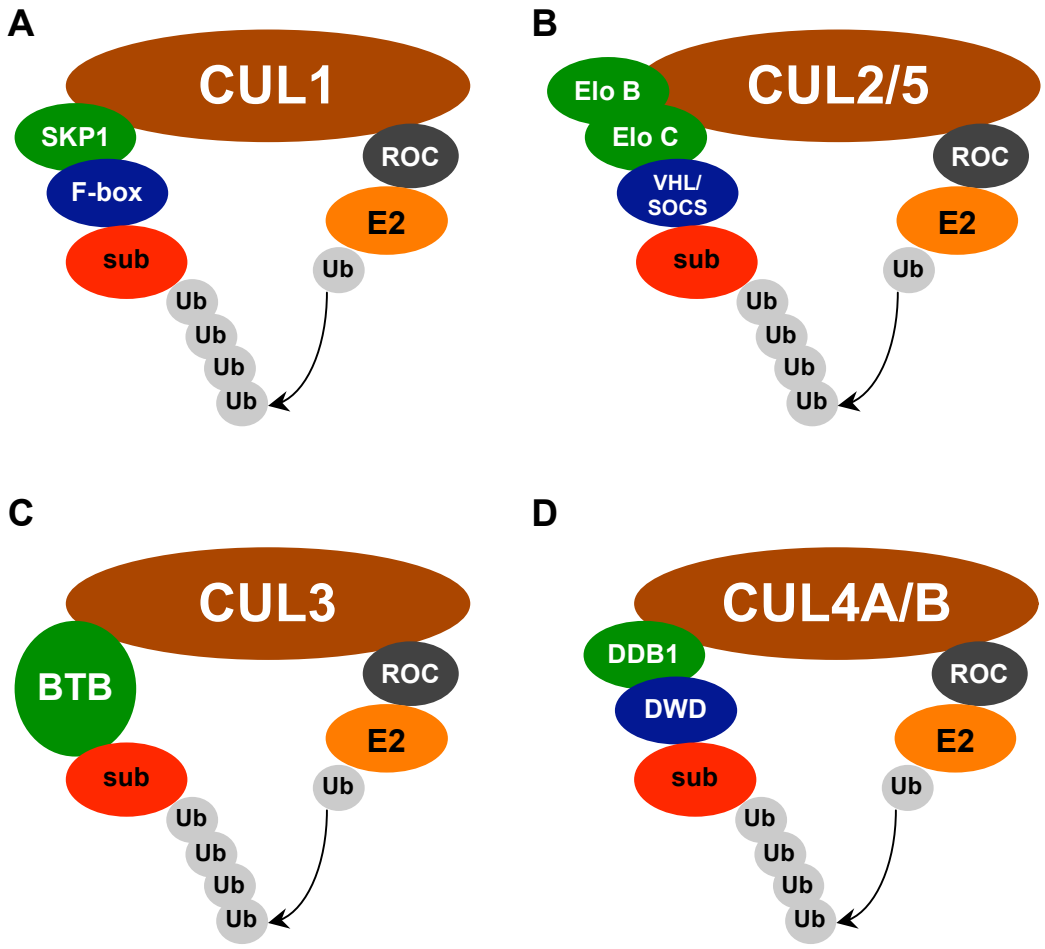

Figure 1.2 – The Cullin Family of E3 Ubiquitin Ligases

The canonical cullins form multisubunit E3 ubiquitin ligase complexes. (A) CUL1 interacts with SKP1 and one of greater than 60 F-box proteins to recruit substrates. (B) CUL2 and CUL5 interact with Elongins B and C and either VHL- or SOCS-box proteins to recruit substrates. (C) CUL3 interacts with a series of over 200 BTB-domain proteins to recruit substrates. (D) CUL4A and CUL4B interact with DDB1 and one of over 90 DWD-domain proteins to recruit substrates.

The cullins are regulated through cyclical modification by the ubiquitin-like protein Nedd8 and inhibition by the regulatory protein CAND1

Substrate recruitment and ubiquitination by the cullin ligases is tightly regulated in the cell by cyclical modification of the cullins with the small ubiquitin-like protein Nedd8 and its subsequent removal by the "deneddylase" COP9/signalosome. Several years ago, our laboratory and others discovered that CUL1 and all other canonical cullins are strongly associated with a 120-kDa protein, CAND1 (Cullin Associated Nedd8-Dissociated) (Liu et al. 2002; Zheng et al. 2002a; Oshikawa et al. 2003). CAND1 associates with cullins that are unmodified by Nedd8, and its cullin binding is mutually exclusive with binding of the cullins to their substrate receptors, such as CUL1 with SKP1 and CUL4A with DDB1 (Liu et al. 2002; Zheng et al. 2002a; Oshikawa et al. 2003; Hu et al. 2004). By an unknown mechanism, SKP1 associated with an F-box protein, but not SKP1 alone, is able to initiate the dissociation of CAND1from CUL1 and promote Nedd8 modification (Bornstein et al. 2006). Nedd8 removal, catalyzed by the metalloprotease COP9/signalosome, is also essential for normal cullin function (Lyapina et al. 2001). Failure to remove Nedd8 results in ubiquitination and degradation of not only proper substrates, but also their cognate receptors, which leads paradoxically to accumulation of various cullin substrates (Cope and Deshaies 2006; Lo and Hannink 2006). It is speculated that removal of Nedd8 preserves receptor stability by enhancing the affinity of cullins for CAND1, which then competes with the receptors for cullin binding. This "cullin cycle" of CAND1 binding, substrate recruitment, and Nedd8 modification and removal ensures both the stability of substrate receptors and, by limiting

the time each substrate receptor resides on the ligase, the availability of the ligase for ubiquitination of the correct substrates in response to cellular signals.

Cullins 4A and 4B recruit substrates through interacting with the damaged DNA binding protein DDB1

The primary focus of my research has been to characterize the substrate-recruiting functions of CUL4A/B. CUL4A is of particular interest because the gene is amplified in over 20% of primary breast tumors, and the protein is overexpressed in another 30% of breast tumors (Chen et al. 1998a). It may, therefore, have some oncogenic activity that contributes to breast cancer, or more broadly, tumor development. My laboratory first established that CUL4A interacts with ROC1, as do all other known cullins (Ohta et al. 1999). We also have firmly established that CUL4A interacts in a stoichiometric manner with the damaged DNA binding protein 1 (DDB1), and that DDB1 is required for UV-dependent degradation of the known CUL4A/B substrate CDT1 (Hu et al. 2004). (CUL4A and CUL4B both bind to DDB1 and thus may be at least partially redundant in function.) CDT1, a factor required for the licensing of DNA replication, was the first CUL4A substrate to be well-studied; *C. elegans* with RNAi against CUL-4 showed a re-replication phenotype in certain cell types, which was found to be the result of accumulation of CDT1 (Zhong et al. 2003).

Contemporaneous with our and others' work on CDT1, other labs showed that the DDB2 immunocomplex contains DDB1 and CUL4A, and a similar Cockayne Syndrome protein A (CSA) complex also contains DDB1 and CUL4A (Groisman et al. 2003). The authors demonstrated that CUL4A/DDB1 function is required for normal global genomic

repair (a function of DDB2) and transcription-coupled nucleotide excision repair (a function of CSA). They also found that the DDB2/DDB1/CUL4A complex responds differently to UV irradiation than does the CSA/DDB1/CUL4A complex; within 30 minutes of UV treatment, the DDB2 complex associates with chromatin and dissociates from the Nedd8-deconjugating enzyme COP9/signalosome, which results in increased CUL4A-Nedd8 (its putatively active state). After two hours, the signalosome reassociates, and CUL4A is de-neddylated, likely ceasing its ligase activity. CSA behaves with different kinetics—always chromatin-bound, its signalosome-bound fraction increases after UV, suggesting a different pattern of substrate degradation. DDB2 itself is also ubiquitinated by CUL4A, and its protein levels oscillate during the cell cycle while its mRNA levels stay relatively constant. This suggests that DDB2 is itself regulated by proteolysis, perhaps after targeting its substrates for ubiquitination (Nag et al. 2001).

After these initial discoveries of CUL4A mutisubunit complexes and substrates, the picture of how CUL4A/B target their substrates for degradation has gradually come into focus through a series of findings over the past few years. The transcription factor c-Jun is a CUL4A substrate, through interaction with a series of linkers: DDB1, DET1 and COP1 (Wertz et al. 2004). In an unclear manner, the homeobox protein HOXA9 is also targeted by CUL4A for polyubiquitination and degradation (Zhang et al. 2003). The CSA/DDB1/CUL4A complex targets the Cockayne Syndrome protein B (CSB) for ubiquitination as well (Groisman et al. 2006). And, the DDB2/DDB1/CUL4A complex has been shown to ubiquitinate (but not target for proteolysis) the nucleotide excision

repair factor XPC (Sugasawa et al. 2005), histones H3 and H4 (Wang et al. 2006), and histone H2A at UV-damaged DNA sites (Kapetanaki et al. 2006). Finally, the WD-40 domain protein L2DTL/CDT2 and PCNA are required for targeting of the substrate CDT1 for CUL4A-dependent ubiquitination (Higa et al. 2006a; Hu and Xiong 2006; Senga et al. 2006).

DDB1 associates with a subset of WD40-domain substrate receptors

These several findings clearly implicate DDB1 as the primary linker for CUL4A/B-based E3 ligases. However, how DDB1 recruits substrates is substantially more complex than the one- or two-linker systems used by other cullins. Several proteins known to interact with DDB1 contain WD-40 beta-propeller domains: DDB2, CSA, CDT2, and two novel proteins that I identified by mass spectrometry (see Chapters 2 and 3), VprBP and WDR23. This led Joe He in my laboratory to hypothesize that there is a specific domain within these WD-40 proteins that interacts with DDB1. His bioinformatic approach yielded a putative domain, which led to the identification of 17 novel DDB1-interacting WD (DWD) proteins (He et al. 2006). This research, to which I contributed significantly, is described in Chapter 2. At the same time, three other laboratories by mass-spectrometric and structural approaches identified the same domain and other novel DWD proteins (Angers et al. 2006; Higa et al. 2006b; Jin et al. 2006). The greater than 90 DWD proteins in the human genome suggest that there are numerous CUL4A substrates yet to be identified. And, it is also clear that not only DWD proteins recruit substrates to CUL4A/DDB1. The linker DET1 has no identifiable WD domain,

yet links c-Jun to CUL4A; and, the paramyxovirus SV5 V protein, which does not fold into a beta-propeller, hijacks the CUL4A/DDB1 ligase to degrade STAT1/2 (Ulane and Horvath 2002; Li et al. 2006).

CUL4A/DDB1 has broad and essential cellular functions

In addition to the description of the biochemical mechanism, and identification of a wide variety of WD-40 domain and other cellular substrate receptors, several groups have studied CUL4A/DDB1 function at the organismal level. CUL4A knockout mice, as would be expected for a ubiquitin ligase functioning on a broad variety of cellular substrates, die between days E4.5 and E7.5, and fewer heterozygotes are born than expected by Mendelian ratios, suggesting some haploinsufficiency (Li et al. 2002). CUL4-silenced *C. elegans* and *dCul4* mutant *Drosophila* also die in larval stages, and demonstrate a growth arrest phenotype ((Zhong et al. 2003) and unpublished data from Sima Zacharek in my laboratory). The close paralog CUL4B, however, is clearly not essential and cannot completely compensate for CUL4A function. CUL4A loss alone is embryonic lethal, and loss of CUL4B function in humans only leads to an X-linked mental retardation syndrome (Tarpey et al. 2007; Zou et al. 2007). Molecular data from the study of CDT1 degradation suggested strongly that, at least in that case, the two CUL4 ligases were redundant because silencing of both was necessary to stabilize CDT1 after UV treatment; however, the organismal data proves that the redundancy is not total (Hu et al. 2004). CUL4B also contains over 100 amino acids in its amino terminus upstream of the DDB1-interaction site, which may contribute to its specialized functions.

Most importantly for understanding CUL4A/DDB1 cellular function, DDB1 has been conditionally knocked out, in both the brain and in the epidermis. Loss of DDB1 in the brain led to widespread apoptosis of neural progenitor cells, severe brain developmental abnormalities, and neonatal lethality. Mouse embryonic fibroblasts produced from these mice had very slow growth, eventually stopping dividing, and mitotic abnormalities, increased evidence of oxidative DNA damage, and accumulation of the CUL4A substrates CDT1 and p27 (Cang et al. 2006). In the epidermis, the same group did a much more detailed characterization of DDB1 function. Loss of DDB1 led, again, to neonatal lethality due to a total loss of epidermal proliferation, and apoptosis of epidermal progenitor cells. $DDB1^{-/-}$ keratinocytes had high levels of apoptosis, G2/M accumulation, and activation of the ATM-dependent DNA damage pathway. Concomitant p53 loss rescued the apoptotic phenotype but not the accumulation of DNA damage, growth inhibition, aneuploidy, or neonatal lethality. Regardless of p53 state, c-Jun and $p21^{Cip1}$ accumulated. c-Jun is a known CUL4A/DDB1 substrate, but it will be highly interesting to examine whether p21 is also a substrate for the ligase. These DDB1 knockout studies have firmly established CUL4A/DDB1's role in DNA metabolism, cellular proliferation, and organismal development.

Viral proteins utilize cellular ubiquitin ligases to target specific cellular proteins for proteasomal degradation

Ubiquitin ligases are an excellent target for viral modification of cellular activity, because they can rapidly polyubiquitinate and signal for proteolysis specific cellular proteins. The degradation of the immune modulators STAT1 and 2 by CUL4A/DDB1

bridged by the paramyxovirus SV5 V protein is one example of many. The founding member of the HECT E3 ligase family, E6AP (E6 associated protein), is named for its association with human papillomavirus E6 protein. E6 links the tumor suppressor p53 to E6AP, causing its polyubiquitination and degradation, a critical event in the papillomavirus-mediated development of cervical cancer (Talis et al. 1998). p53 is also targeted by the adenoviral proteins E4orf6 and E1B55K to a CUL5-dependent ubiquitin ligase (Querido et al. 2001). The human immunodeficiency virus (HIV) also utilizes cellular ubiquitin ligase machinery. The accessory protein Vif also interacts with CUL5, targeting the host antiviral factor APOBEC3G for degradation (Yu et al. 2003). Recently, another HIV-1 accessory protein, Vpr, was also shown to target cellular proteins, the uracil DNA glycosylases UNG2 and SMUG, for proteolytic degradation in a CUL4A/DDB1-dependent manner (Schrofelbauer et al. 2005; Schrofelbauer et al. 2007). This interaction is physiologically significant, as Vpr's interaction with UNG2 inhibits UNG2's critical role in immunoglobulin class switch recombination, thereby impairing antibody production and possibly inhibiting an antibody-based immune response against HIV (Begum et al. 2006).

The Vpr binding protein VprBP is a major binding partner of CUL4A/DDB1

HIV-1 Vpr may have more broad effects on CUL4A/DDB1 function than has been reported. The most abundant protein that I identified by mass spectrometry in the CUL4A immunocomplex was the Vpr interacting protein VprBP (see Chapters 2-4).

This protein was initially identified through co-immunoprecipitation and peptide sequencing of HIV-1 Vpr-interacting proteins (Zhao et al. 1994; Zhang et al. 2001), and its physiological functions are the focus of my dissertation research, particularly in Chapter 3, while initial explorations into its function with Vpr are described in Chapter 4.

Vpr, a 96-amino-acid, 14-kDa protein, is dispensable for *in vitro* viral growth and replication, yet is essential for HIV function *in vivo*. It has been implicated in a number of different viral and cellular processes, from enhancing accuracy of reverse transcription to nuclear import of viral DNA, and from anti- and pro-apoptotic activities to transactivation of HIV LTR and host genes (Le Rouzic and Benichou 2005). Yet, its most well studied cellular phenotype, when expressed alone or in the context of whole viral infection, is arrest of the cell cycle in G2, followed subsequently by apoptosis (He et al. 1995; Re et al. 1995; Bartz et al. 1996; Stewart et al. 1997; Roshal et al. 2003; Andersen et al. 2005; Lai et al. 2005). There have been many studies into the mechanism of this G2 arrest, yet it is still not entirely clear how it occurs. Inhibition of either the ATR or Chk1 DNA damage checkpoint kinases inhibits this arrest (Roshal et al. 2003), which occurs regardless of the presence of the p53 or Rb stress response pathways, as HeLa cells readily arrest. The G2 arrest has characteristics of replication stress or DNA damage: Vpr binds directly to chromatin (Lai et al. 2005), it induces H2AX phosphorylation and RPA foci, requires Rad17 and Hus1 (Zimmerman et al. 2004), and activates Brca1 and its target GADD45α (which is also required for the arrest) (Andersen et al. 2005). Despite all this data, there has yet to be clear mechanistic evidence showing how Vpr activates this DNA damage/replication stress pathway. Very recent data

showed that Vpr disrupts the association of CUL4A/DDB1 with its substrate receptor DDB2, thereby disrupting nucleotide excision repair (Schrofelbauer et al. 2007). Knowing that DDB1 loss also leads to G2 cell cycle arrest, the authors speculate that the loss of DNA repair capacity by disrupting DDB1-DDB2 interaction may be the direct cause of Vpr-mediated G2 arrest. However, this remains purely correlative, as G2 arrest is not a very specific cellular phenotype.

Summary

In subsequent chapters, I explore several aspects of the function of the CUL4A/DDB1 E3 ubiquitin ligase. In Chapter 2, modified and expanded from a publication in 2006 in *Genes and Development*, Joe He and I, together with contributions from others in our lab, discovered by mass spectrometry, followed by bioinformatics and molecular biological approaches, a common motif shared by many CUL4A/DDB1-interacting WD40 (DWD) repeat proteins. In Chapter 3, soon to be reformatted into a manuscript for submission, I selected one novel DWD protein, VprBP, and characterized its interactions with CUL4A/DDB1, and have begun to explore its essential role in DNA replication. Following up on the reported interaction between VprBP and the HIV-1 protein Vpr, in Chapter 4, I have included preliminary studies into the detailed characterization of this interaction. Finally, Chapter 5 contains broad conclusions and a discussion of future prospects for research in VprBP, CUL4A/DDB1, and the cullin family in general.

CHAPTER 2

DDB1 FUNCTIONS AS A LINKER TO RECRUIT WD40 PROTEINS TO CUL4-ROC1 UBIQUITIN LIGASES

(including modified portions from He YJ, McCall CM, Hu J, Zeng Y, and Xiong Y. *Genes Dev* 20(21): 2949-2954, 2006)

Summary

Cullins assemble the largest family of ubiquitin ligases by binding with ROC1 and various substrate receptors. CUL4 function is linked with many cellular processes, but its substrate-recruiting mechanism remains elusive. We identified a protein motif, the DWD box (DDB1-binding WD40 protein), and demonstrated the binding of 15 DWD proteins with DDB1-CUL4A. We provide evidence supporting the critical function of the DWD box and DDB1's role as the linker mediating DWD protein association with CUL4A. A database search predicts that about one-third of WD40 proteins, 90 in humans, contain the DWD box, suggesting a potentially large number of DWD-DDB1-CUL4-ROC1 E3 ligases.

Background

The ubiquitin-proteasome pathway regulates the concentration and conformation of many cellular proteins in response to changes in physiological conditions. This pathway consists of a cascade of three activities performed by E1 (ubiquitin activating), E2 (ubiquitin conjugating) and E3 (ubiquitin ligase) enzymes (Hochstrasser 1996; King et al. 1996; Hershko and Ciechanover 1998). A critical step in this process is how individual protein substrates are recruited to specific E3 ligases. The RING family represents the major family of E3 ligases. Members either contain an intrinsic RING finger domain (as in MDM2 and BRCA1), or bind *in trans* with a small RING finger protein, such as ROC1 (also known as Rbx1 and Hrt1) by the cullins, to recruit and activate an E2 (Jackson et al. 2000; Petroski and Deshaies 2005a).

A remarkable aspect of cullin E3 ligases is that each cullin can assemble into many distinct cullin-RING dependent ligases (CRLs) by interacting with a conserved motif present in multiple proteins (Petroski and Deshaies 2005a). To recruit specific substrates, CUL1 utilizes an N-terminal domain to bind with a linker protein, SKP1 (Feldman et al. 1997; Skowyra et al. 1997; Zheng et al. 2002b), which does not interact with other cullins (Michel and Xiong 1998). SKP1 uses a separate domain to bind with a conserved protein motif, the F-box, which via its additional protein-protein interaction modules recruits various substrates, often phosphorylated, to the CUL1-ROC1 catalytic core. To bring specific substrates to CUL2- and CUL5-dependent ligases, a heterodimeric linker complex containing elongins B and C binds simultaneously to an analogous N-terminal domain in CUL2 and CUL5 and to two similar protein motifs, the

VHL-box and SOCS box. VHL and SOCS proteins, via their additional protein-protein interaction modules, target various substrates differentially to the CUL2-ROC1 or CUL5-ROC2 catalytic cores (Kamura et al. 1998; Stebbins et al. 1999; Zhang et al. 1999; Kamura et al. 2001; Kamura et al. 2004). Omitting a linker, CUL3 utilizes its N-terminal domain to bind to proteins with a conserved 100-residue protein motif known as a BTB domain, which via additional protein-protein interaction domains then target various substrates to the CUL3-ROC1 catalytic core (Furukawa et al. 2003; Geyer et al. 2003; Pintard et al. 2003; Xu et al. 2003). The presence of multiple substrate receptors—mammals express more than 60 F-box, 40 SOCS and 200 BTB proteins—suggests that cullins may form the largest family of E3 ligase complexes and control the ubiquitination of a wide variety of substrates. The substrate recruiting mechanism of CUL4, which has two closely related paralogues, CUL4A and CUL4B, in mammals and presents as a single gene in *S. pombe*, *C. elegans* and *Drosophila*, has remained elusive. Various reports have suggested that CUL4 may assemble multiple ligases to target many different substrates. One protein that has frequently been found in association with these various different CUL4 complexes is DDB1, first identified as a damaged DNA binding protein (Chu and Chang 1988). The emerging picture is that DDB1 functions as a critical factor for CUL4-ROC ligases and possibly acts as a linker to bridge a substrate receptor(s) to CUL4. This chapter is directed toward understanding the substrate recruiting mechanism and the architecture of DDB1-CUL4 ligases.

Experimental Procedures

Antibodies, immunopurification and mass spectrometric analysis

Antibodies to HA (12CA5, Boehringer-Mannheim), Myc (9E10, NeoMarker), T7 (Novagen), and FLAG (M2, Sigma) were purchased commercially. Rabbit polyclonal antibodies to CUL4A, DDB1 and CDT1 have been described (Hu et al. 2004). A rabbit polyclonal antibody against CUL4B was produced by injection of a synthetic peptide antigen to residues 34-62 of CUL4B (AAQEVRSATDGNTSTTPPTSAKKRKLNSS). A rabbit polyclonal antibody against DDB2 was the kind gift of Dr. Altaf Wani (Ohio State University). To purify the endogenous CUL4A complex, BT474 cells from 47 150-mm plates were lysed with a 0.5% NP-40 lysis buffer (50 mM Tris-HCl at pH 7.5, 150 mM NaCl, 0.5% NaCl, 50 mM NaF) with addition of additional inhibitors immediately before lysis (1 mM DTT, 1 mM Na_3VO_4, 1 mM PMSF, 1 mM benzamidine, 100 μg/mL trypsin inhibitor, 25 μg/mL leupeptin, 25 μg/mL aprotinin) and lysates were pooled (300 mg total). Clarified lysates were immunoprecipitated with affinity-purified anti-CUL4A antibody (2 μg per mg protein in lysate, +/- 10 μg/mg antigen peptide). Immunocomplexes were resolved by SDS-PAGE, stained with Coomassie blue, and the protein bands were digested with trypsin and subjected to mass spectrometric analysis at the UNC Proteomics Core Facility.

Plasmids, cell culture and cell transfection

Plasmids expressing human CUL4A, DDB1, and CDT1 were as previously described (Ohta et al. 1999; Liu et al. 2002; Furukawa et al. 2003; Hu et al. 2004). Plasmids expressing DDB2, CSA, and all other WD40 proteins were produced by amplifying cDNA from either human HeLa or thymus (kind gift of Dr. Lishan Su) cDNA libraries and subcloning into pcDNA3-based mammalian expression vectors. Mutations were introduced by site-directed mutagenesis using the Quick-Change Kit (Stratagene) and verified by DNA sequencing. All human cells were cultured in DMEM containing 10% FBS in a 37^0C incubator with 5% CO_2, except 293T cells, which were cultured in DMEM containing 10% newborn calf serum. Cell transfections were carried out using a calcium-phosphate buffer.

Gel filtration chromatography

To examine the elution profile of CUL4A and associated proteins, HeLa cells were lysed with the 0.5% NP-40 lysis buffer, and clarified lysate was resolved through a Superdex-200 gel filtration column (GE/Amersham). 0.5 mL fractions were collected, and 50 μL of each was resolved via SDS-PAGE and immunoblotted with antibodies as indicated. High molecular weight standards (GE/Amersham) were resolved through the same column, and the peak fraction for each was determined.

^{35}S-IP

About 80% confluent 100-mm tissue culture dishes of cells were washed with 1X PBS and then incubated in DMEM without methionine or cysteine (ICN, Inc.) + 10% dialyzed FBS, for 30 minutes. 0.5 mCi of ^{35}S-methionine (NEN) was added to each dish and incubated for 4 hours to label newly synthesized proteins. The cells were then washed twice with 5 mL of cold 1X PBS and lysed with 1 mL of 0.5% NP-40 lysis buffer per plate. Clarified lysates were divided in half, and each half was immunoprecipitated with 10 μg of anti-CUL4A antibody, +/- 50 μg of antigen peptide. The immunocomplexes were immobilized on Protein-A agarose beads, and resolved via SDS-PAGE. The gel was then dried and exposed to film.

RNA interference (RNAi)

A duplex oligonucleotide encoding human DDB1-specific shRNA (5'-CCGGCAGCATTGACTTACCAGGCATCTTCCTGTCAATGCCTGGTAAGTCAATG CTGTTTTTG-3') was ligated into the PMKO.1 vector (Addgene plasmid 8452). Retrovirus production was carried out according to a standard protocol and then used to infect U2OS and HeLa cells. The infected cell lines were then selected by puromycin (2 μg/mL) for 4 days before analyzing protein expression and complex formation.

Results

CUL4A associates with a potentially large number of cellular proteins

To begin searching for the substrate targeting mechanism of CUL4, I first examined CUL4A complexes *in vivo* by size-exclusion chromatography to gain an initial view of their size distribution. This study revealed that CUL4A exists in a number of different complexes, varying in size from approximately 250 kDa to over 700 kDa (Fig. 2.1A). Notably, two proteins that are critical partners of CUL4A, DDB1 and ROC1, also exist in many different complexes. In comparison, the distribution of most CUL1 complexes is limited to a much narrower size range smaller than 440 kDa, very similar to that of CAND1, a negative regulator of CRLs that binds to un-neddylated form of cullins and blocks the binding of SKP1 linker with CUL1 (Liu et al. 2002; Zheng et al. 2002a; Goldenberg et al. 2004). The distribution of CSN5, the catalytic subunit of the COP9/signalosome, exhibits an almost mutually exclusive pattern from that of CUL1 and CAND1, but yet overlaps significantly with CUL4A. These observations are consistent with the finding that CUL4A molecules abundantly associate with the COP9/signalosome [(Groisman et al. 2003) and Fig. 2.1C], but only a small portion is associated with CAND1, suggesting that CUL4A assembles into many different and active complexes *in vivo*.

To identify proteins that interact with CUL4A in these different complexes, I analyzed CUL4A complexes by ^{35}S-IP in various tissues (data not shown) and cell lines,

including two breast cancer lines (SKBR3 and BT474) known to overexpress CUL4A (Chen et al. 1998b), as well as two other cell lines that do not overexpress CUL4A. These analyses revealed a large number of potential CUL4A-interacting proteins as determined by antigen peptide competition (Fig. 2.1B). I then scaled up immunopurification of the CUL4A complex from BT474 cells and analyzed it by mass spectrometry. I have thus far identified 13 CUL4A-associated proteins (Fig. 2.1C). These include 11 proteins whose association with CUL4A had been previously identified (ROC1, DDB1, CAND1 and the eight COP9/signalosome subunits), and two novel proteins, WDR23 and VprBP. Coomassie blue staining indicates that CUL4A associates nearly stochiometrically with DDB1, but with the COP9/signalsome at a much lower level. Together, these results support the notion that CUL4A may associate with multiple different cellular proteins to assemble various E3 complexes and that DDB1 is a critical, if not essential, component of CUL4A ligases.

Identification of a DWD box conserved in DDB1-binding WD40 proteins

One intriguing finding from my preliminary studies of CUL4A-interacting proteins is the identification of two WD40 repeat proteins, WDR23 and VprBP. While neither protein has been functionally characterized or linked with CUL4-DDB1, the significance of this identification is appealing when considering that four previously-identified CUL4A interacting proteins, DDB2, CSA, COP1 and CDT2, also contain WD40 repeats (Groisman et al. 2003; Wertz et al. 2004; Holmberg et al. 2005; Liu et al. 2005). The WD40 repeat is loosely defined at the primary sequence level by a Gly-His

dipeptide 10-20 residues N-terminal from a Trp-Asp (WD) dipeptide, and is typically about 40 residues in length. WD40 proteins form a propeller-like structure, typically with 7 blades, each composed of four anti-parallel b-sheets. There are more than 700 human WD40 repeat protein entries in the current PFAM database (http://www.sanger.ac.uk/Software/Pfam/index.shtml), corresponding to 320 unique genes after eliminating duplicates and truncated forms. As not all WD40 repeat proteins associate with DDB1 or CUL4 even when overexpressed (see below), it is likely that only a subset of WD40 repeat proteins interact with the DDB1-CUL4A ligase.

To identify the signature motif shared by DDB1-binding WD40 proteins, Mr. He carried out extensive primary sequence alignment and computer modeling. The WD40 repeats were first compared using NCBI-Blast searches and the CLUSTAL algorithm, then adjusted manually and continuously refined as more DDB1-binding proteins were experimentally identified (see below). This analysis identified a 16-residue stretch that we refer to as the DWD box (DDB1-binding and WD40 repeat, Fig. 2.1D) and is defined by three features. (i) The first 14 residues in the DWD box correspond to the second half of a WD40 repeat that is more conserved than other WD40 repeats. These 14 residues include three highly conserved residues, Asp7, Trp13, Asp14, five hydrophobic residues (Ile, Leu or Val) at position 1, 2, 10, 12 and 15, and three small residues (Ala, Gly, Ser or Thr) at position 3, 4, and 5. (ii) Arg16 following the WD dipeptide is a signature residue of the DWD box. Notably, the Arg residue in the DWD box of DDB2 is mutated in several human patients with xeroderma pigmentosum group E (XP-E), and reduces its binding with DDB1 [(Rapic-Otrin et al. 2003), see Fig. 2.3 below]. The crystal structure

Figure 2.1

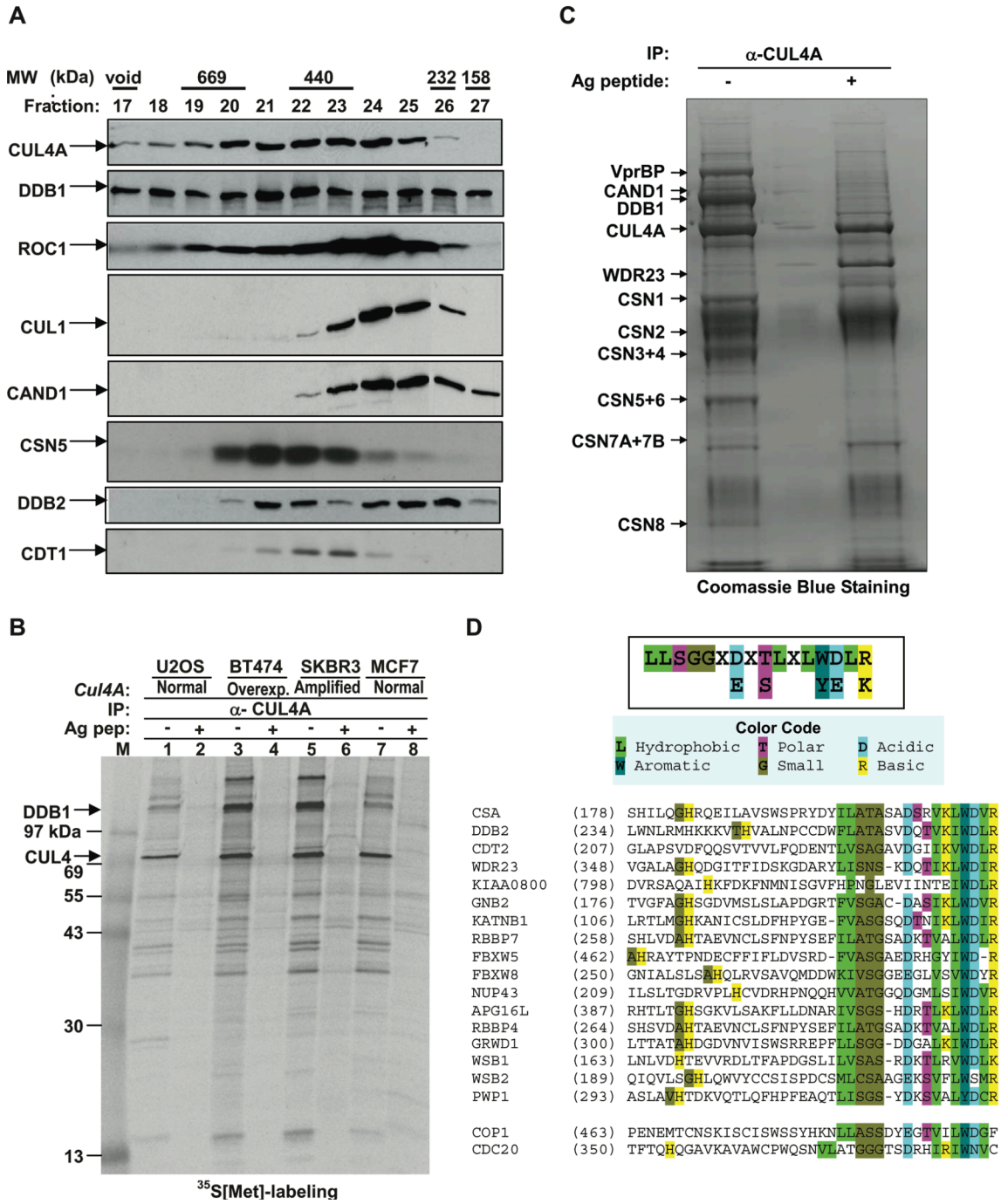
A
MW (kDa) void 669 440 232 158
Fraction: 17 18 19 20 21 22 23 24 25 26 27
CUL4A
DDB1
ROC1
CUL1
CAND1
CSN5
DDB2
CDT1
C
IP: α-CUL4A
Ag peptide: - +
VprBP
CAND1
DDB1
CUL4A
WDR23
CSN1
CSN2
CSN3+4
CSN5+6
CSN7A+7B
CSN8
Coomassie Blue Staining
B
U2OS BT474 SKBR3 MCF7
Cul4A: Normal Overexp. Amplified Normal
IP: α- CUL4A
Ag pep: - + - + - + - +
M 1 2 3 4 5 6 7 8
DDB1
97 kDa
CUL4
69
55
43
30
13
35S[Met]-labeling
D
LLSGGXDXTLXLWDLR
E S YE K
Color Code
L Hydrophobic T Polar D Acidic
W Aromatic G Small R Basic
CSA (178) SHILQGHRQEILAVSWSPRYDYILATASADSRVKLWDVR
DDB2 (234) LWNLRMHKKKVTHVALNPCCDWFLATASVDQTVKIWDLR
CDT2 (207) GLAPSVDFQQSVTVVLFQDENTLVSAGAVDGIIKVWDLR
WDR23 (348) VGALAGHQDGITFIDSKGDARYLISNS-KDQTIKLWDIR
KIAA0800 (798) DVRSAQAIHKFDKFNMNISGVFHPNGLEVIINTEIWDLR
GNB2 (176) TVGFAGHSGDVMSLSLAPDGRTFVSGAC-DASIKLWDVR
KATNB1 (106) LRTLMGHKANICSLDFHPYGE-FVASGSQDTNIKLWDIR
RBBP7 (258) SHLVDAHTAEVNCLSFNPYSEFILATGSADKTVALWDLR
FBXW5 (462) AHRAYTPNDECFFIFLDVSRD-FVASGAEDRHGYIWD-R
FBXW8 (250) GNIALSLSAHQLRVSAVQMDDWKIVSGGEEGLVSVWDYR
NUP43 (209) ILSLTGDRVPLHCVDRHPNQQHVVATGGQDGMLSIWDVR
APG16L (387) RHTLTGHSGKVLSAKFLLDNARIVSGS-HDRTLKLWDLR
RBBP4 (264) SHSVDAHTAEVNCLSFNPYSEFILATGSADKTVALWDLR
GRWD1 (300) LTTATAHDGDVNVISWSRREPFLLSGG-DDGALKIWDLR
WSB1 (163) LNLVDHTEVVRDLTFAPDGSLILVSAS-RDKTLRVWDLK
WSB2 (189) QIQVLSGHLQWVYCCSISPDCSMLCSAAGEKSVFLWSMR
PWP1 (293) ASLAVHTDKVQTLQFHPFEAQTLISGS-YDKSVALYDCR
COP1 (463) PENEMTCNSKISCISWSSYHKNLLASSDYEGTVILWDGF
CDC20 (350) TFTQHQGAVKAVAWCPWQSNVLATGGGTSDRHIRIWNVC

Fig. 2.1. Human CUL4 associates with potentially multiple WD40 repeat proteins

(A) Clarified lysate from HeLa cells was fractionated over a Superdex 200 gel filtration chromatography column, resolved by SDS-PAGE, and Western blotted with indicated antibodies.

(B) ^{35}S-labeled, clarified lysates from four cell lines were immunoprecipitated with an anti-CUL4A antibody and resolved by SDS-PAGE, followed by autoradiography. Identity of CUL4A and DDB1 were subsequently confirmed by mass spectrometric analysis.

(C) Immunopurification and mass spectrometric analysis of CUL4A complexes. CUL4A immunocomplexes were precipitated from human BT474 cells and resolved by SDS-PAGE followed by staining with Coomassie Brilliant Blue. Bands identified by mass spectrometry are indicated.

(D) Identification of a putative DDB1-binding motif in WD40 proteins, the DWD box. The DWD box is predicted to be present in more than 100 human WD40 repeat proteins. Only three reported in the literature (DDB2, CSA and COP1) and 15 demonstrated in this study are included. CDC20 does not contain a DWD box and does not detectably interact with DDB1-CUL4A.

of the heterotrimeric G protein b_1 subunit, a DWD protein (see below), has been solved and shows that several conserved residues, including the Arg16, within the DWD box are located on the protein surface (Sondek et al. 1996), suggesting that these residues might participate in binding with other proteins. (iii) A DWD protein usually contains one and sometimes two DWD boxes, but rarely three.

Multiple DWD proteins associate with DDB1-CUL4A

To experimentally test the DWD hypothesis, Mr. He and I randomly chose and expressed a number of putative DWD proteins and examined their binding with CUL4A/DDB1 by coupled IP-Western assays. Considering DDB1 as a possible linker, Mr. He triply transfected plasmids expressing CUL4A, DDB1 and individual WD40 proteins. Association between WD40 proteins and DDB1-CUL4A was determined by either Western blotting of the WD40 protein in the CUL4A immunocomplex, or conversely blotting either CUL4A or DDB1 protein in the WD40 protein immunocomplex (Fig. 2.2A and 2B). DDB2 and CSA, the two best-characterized DWD proteins, interact with DDB1 strongly and were included as positive controls. We have identified thus far 15 novel human WD40 proteins that positively bind with DDB1-CUL4A. Twelve are associated with CUL4A/DDB1 in a readily detectable manner when compared with DDB2 and CSA, including VprBP and WDR23 (Fig. 2.1C), FBXW5, RBBP7, and Gb_2 (Fig. 2.2A), WSB1, WSB2, PWP1 and GRWD1 (Fig. 2.2B), and FBXW8, APG16L and KATNB1 (Fig. 2.3B). Three WD40 proteins, NUP43, mbTrCP and RBBP4, weakly interact with DDB1 and CUL4A (Fig. 2.2B). COP1 contains

conserved WD40 repeats, but not the signature Arg16, and only associates with DDB1-CUL4A weakly in comparison with other WD40 proteins (Fig. 2.2B). It is currently not clear whether COP1 directly interacts with DDB1 or is bridged by another protein as suggested by the finding that a mutation outside the WD40 repeats in COP1 disrupted its binding with DET1 as well as with DDB1 (Wertz et al. 2004). CDC20, a WD40 protein that is missing several conserved residues including the signature Arg16 (Fig. 2.1D), did not detectably interact with DDB1-CUL4A in a reciprocal IP-Western assay (Fig. 2.2A), suggesting that only a subset of, but not all, WD40 proteins interact with DDB1-CUL4A. Thus, together with three previously reported DDB1-binding WD40 proteins, DDB2, CSA and COP1, a total of 18 DWD proteins have been demonstrated to bind with DDB1-CUL4 experimentally.

The DWD box is important for DWD proteins binding to DDB1-CUL4A

To provide evidence supporting the DWD hypothesis, Ms. Zeng first determined the *in vivo* association of endogenous CUL4A with a newly identified DWD protein, RBBP7, to which an antibody is available. RBBP7 was readily detected in the CUL4A immunocomplex and was competed off by molar excess of antigen peptide (Fig. 2.3A).

Finding that at least two F-box-containing WD40 repeat proteins, FBXW5 (Fig. 2.2A) and FBXW8 (Fig. 2.3A), interact with DDB1-CUL4A is somewhat unexpected given that F-box proteins interact with CUL1. Mr. He determined whether the F-box is

Figure 2.2

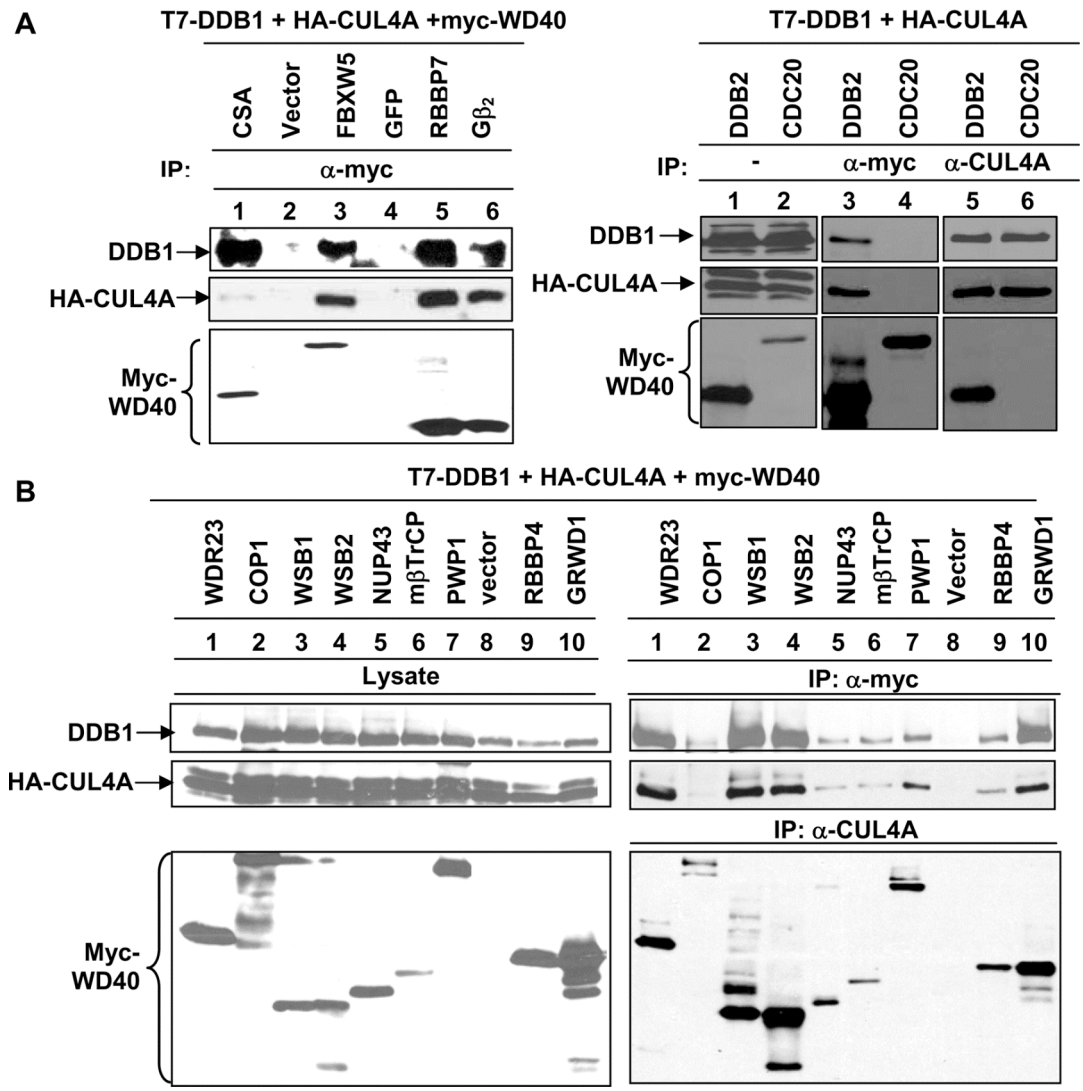

Fig. 2.2. Multiple WD40 repeat proteins bind with CUL4A/DDB1

(A, B) WD40 proteins were cloned into pcDNA3-myc3 expression vectors and co-transfected into 293T cells with plasmids expressing HA-CUL4A and T7-DDB1. Cell lysates were immunoprecipitated and Western blotted as indicated.

required for the binding of WD40 proteins with DDB1-CUL4A. Binding assays showed that the F-box protein SKP2, which does not contain WD40 repeats, did not interact with CUL4A, and that deletion of the F-box from FBXW5 did not seem to affect its binding with CUL4A (Fig. 2.3A). Two additional WD40 proteins that do not contain an F-box, APG16L and KATNB1, were readily detected in the CUL4A immunocomplex in the same binding assay. We therefore conclude that WD40 repeats, but not the F-box, are required for interacting with DDB1-CUL4A.

To directly test the DWD hypothesis, Mr. He performed site-directed mutagenesis of the DWD box of DDB2 (Fig. 2.3C). Nine residues in the DWD box were changed to alanine and individual mutant proteins were co-expressed with CUL4A. The expression of both CUL4A and DDB2 mutants were verified by direct Western blotting and DDB2-CUL4A association was determined by IP-Western analysis. DDB2-CUL4A association was nearly completely disrupted by the mutation of the signature Arg at position 16 (corresponding to Arg273 in DDB2), substantially reduced by the mutations of five conserved residues, Leu at position 2 (corresponding to Leu258 in DDB2), Asp at position 7 (Asp264), Ile at position 10 (Ile269), Trp at position 13 (Trp270) and Leu at position 15 (Leu272), and reduced to a lesser extent by the mutation of Ser at position 3 (Ser262). Mutation of Val at position 11 (Val267), which is not highly conserved among the DWD proteins, and another residue, Gln274, outside the DWD box did not appreciably affect DDB2-CUL4A binding.

To further test the DWD hypothesis, Mr. He introduced alanine substitutions targeting the signature arginine residue in the DWD box of three additional DWD proteins, CSA, PWP1 and APG16L. The Arg–to-Ala substitution nearly completely disrupted the binding of DDB1-CUL4A with CSA, and substantially reduced the binding of DDB1-CUL4A with PWP1 and APG16L (Fig. 2.3D). Together, these bioinformatic analysis and binding and mutagenesis experiments demonstrate that the DWD box not only correlates with, but is also directly involved in mediating the binding of a subset of WD40 proteins with DDB1-CUL4. Whether the DWD motif is sufficient for binding with DDB1 has not been tested due to the unique structure of WD40 proteins. Each WD40 propeller contains seven blades and every blade is made of four β-sheets, three from one WD40 repeat and one from the next repeat. The DWD box corresponds to the second and third β-sheets of one blade. These features suggest that while the DWD box is required for binding to DDB1, other residues are likely involved as well and also make it unfeasible to map the binding sequence by deletion analysis without causing conformational collapse of the entire blade.

DDB1 links the DWD protein DDB2 to CUL4A

The results from our binding assays are most consistent with a model where DDB1 functions as a linker to bridge the DWD proteins to CUL4A. To directly test this model, we examined the interaction of DDB2 with CUL4A in more detail. Two hydrophobic helical surfaces in the N-terminal tip of CUL1, H2 and H5, bind with hydrophobic and polar residues from SKP1 to form a large interface. The N-terminal

Figure 2.3

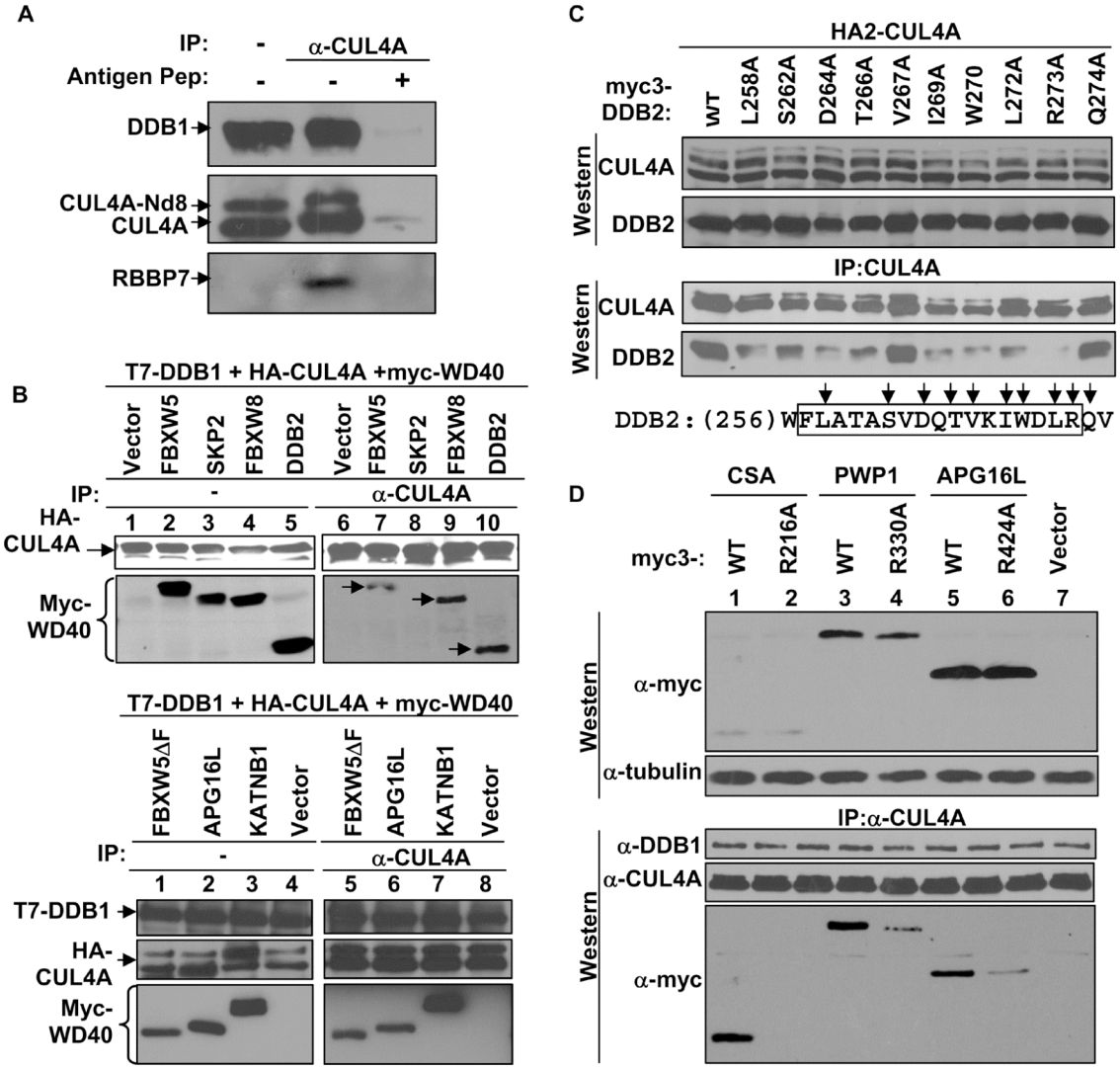
A
IP: - α-CUL4A
Antigen Pep: - - +
DDB1
CUL4A-Nd8
CUL4A
RBBP7
B
T7-DDB1 + HA-CUL4A +myc-WD40
Vector FBXW5 SKP2 FBXW8 DDB2 Vector FBXW5 SKP2 FBXW8 DDB2
IP: - α-CUL4A
1 2 3 4 5 6 7 8 9 10
HA-CUL4A
Myc-WD40
T7-DDB1 + HA-CUL4A + myc-WD40
FBXW5ΔF APG16L KATNB1 Vector FBXW5ΔF APG16L KATNB1 Vector
IP: - α-CUL4A
1 2 3 4 5 6 7 8
T7-DDB1
HA-CUL4A
Myc-WD40
C
HA2-CUL4A
myc3-DDB2: WT L258A S262A D264A T266A V267A I269A W270 L272A R273A Q274A
Western
CUL4A
DDB2
IP:CUL4A
Western
CUL4A
DDB2
DDB2:(256)WFLATASVDQTVKIWDLRQV
D
CSA PWP1 APG16L
myc3-: WT R216A WT R330A WT R424A Vector
1 2 3 4 5 6 7
Western
α-myc
α-tubulin
IP:α-CUL4A
α-DDB1
α-CUL4A
Western
α-myc

Fig. 2.3. Testing the DWD hypothesis

(A) CUL4A associates with endogenous RBBP7. 293T cells were lysed with 0.1% NP-40 lysis buffer and immunoprecipitated with an anti-CUL4A antibody, with or without molar excess of antigen peptide. The immunocomplexes were resolved by SDS-PAGE, and Western blotted with indicated antibodies.

(B) F-box-and-WD40 proteins FBXW5 and FBXW8 were characterized for binding with DDB1-CUL4A. SKP2 (F-box protein without WD40 repeats) and DDB2 were included as a negative and a positive control, respectively. A mutant of FBXW5 deleting the F-box was tested for binding with DDB1-CUL4A along with two additional DWD proteins, APG16L and KATNB1, that do not contain an F-box.

(C) Individual residues of the DWD box of DDB2 protein were changed to alanine and tested for binding with CUL4A by IP-Western analysis.

(D) The conserved arginine of the DWD box is critical for binding with DDB1-CUL4A. The arginines of three DWD proteins were changed to alanine and tested for binding with CUL4A by IP-Western analysis.

regions of other cullins form similar H2 and H5 helices, which contain residues that are invariably conserved in orthologues, but are different in paralogues (Zheng et al. 2002b). We have previously shown that the substitution of residues in the H2 (^{86}LYQAV^{90} -> ^{86}AAAAA^{90}) or H5 (^{139}WQDH^{142} -> ^{39}AADA^{142}) helices of CUL4A substantially reduced DDB1-CUL4A binding ((Hu et al. 2004) and Fig. 2.3B). Binding assays demonstrated that mutation of either the H2 or H5 helix of CUL4A almost completely abolished CUL4A-DDB2 interaction (Fig. 2.4A). Mr. He noted that the steady-state level of DDB2 was higher when co-expressed with either the H2 or H5 mutant of CUL4A, a finding that is consistent with the possibility that DDB2 is degraded by the DDB1-CUL4A-ROC1 ligase, either as a direct substrate or as a substrate receptor that is degraded after delivering the substrate. Infection of a retrovirus expressing shRNA targeting DDB1 reduced the steady state level of DDB1 by more than 85% in U2OS cells and about half in HeLa cells, and did not change the steady state level of either CUL4A or RBBP7, but substantially reduced the *in vivo* association of CUL4A-RBBP7 in both U2OS and HeLa cells (Fig. 2.4B). Together, these results support a model that DDB1 acts as a linker bridging the binding of DWD proteins and CUL4.

We previously demonstrated that like SKP1-CUL1, the DDB1-CUL4A association is also negatively regulated by CAND1 (Hu et al. 2004). The model that DDB1 acts as a linker to bring other DWD proteins to CUL4 predicts that CAND1 and DWD proteins would interact with CUL4 in a mutually exclusive manner. To test this prediction, Mr. He determined the interactions among these proteins. As expected, CAND1, DDB1 and the DWD protein DDB2 were readily detected in the CUL4A

Figure 2.4

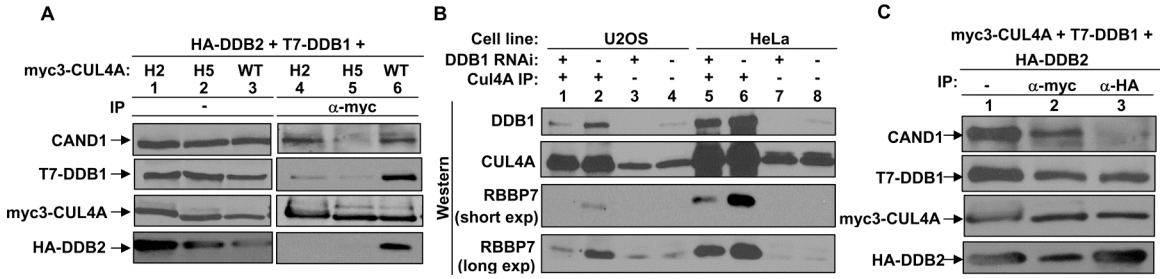

Fig. 2.4. DDB1 bridges WD40 repeat proteins to CUL4

(A) Intact H2 and H5 helices of CUL4A are required for binding with DDB1 and DDB2. 293T cells were co-transfected with plasmids expressing indicated proteins. The steady state level and protein-protein interactions were determined by direct immunoblotting and IP-Western, respectively.

(B) Silencing DDB1 reduced CUL4A-RBBP7 association. DDB1 was knocked down by the infection of a retrovirus expressing shRNA targeting DDB1. The steady state level and CUL4A-RBBP7 association were determined by direct Western and IP-Western analysis.

(C) CAND1 and DDB2 form mutually exclusive complexes with CUL4A. 293T cells were co-transfected with plasmids expressing HA-DDB2, T7-DDB1, and myc3-CUL4A. Cell lysates were immunoprecipitated and blotted with indicated antibodies.

immunocomplex (Fig. 2.4C). In the same assay, both DDB1 and CUL4A, but not CAND1, were detected in the DDB2 immunocomplex (Fig. 2.4C), further supporting the model that DDB1 acts as a linker bridging the binding of DWD proteins and CUL4.

Multiple DWD proteins interact with each other, potentially in an oligomeric cullin complex.

There is mounting evidence that RING finger ubiquitin ligases may function in dimeric complexes. Mdm2/MdmX, BRCA1/BARD1, and Bmi1/Ring1B are three recent examples (Sharp et al. 1999; Tanimura et al. 1999; Brzovic et al. 2001; Buchwald et al. 2006). Recently, CUL3 was also shown to function as a dimer, and dimerization required modification with Nedd8 (Wimuttisuk and Singer 2007). Together with our evidence that CUL4A and DDB1 exist in very high molecular weight complexes (Figure 2.1A), I hypothesized that CUL4A might also exist in dimeric complexes. To test this, I co-transfected CUL4A constructs with different epitope tags (Figure 2.5A). I found that CUL4A both homodimerizes and heterodimerizes with CUL1, and the dimerization is stabilized by additional overexpression of DDB1. To confirm this, I co-immunoprecipitated endogenous CUL1 using an anti-CUL4A antibody (Figure 2.5B). The component of such a dimeric complex are not known, but one possibility is that multiple complete CUL4A/DDB1/DWD complexes might exist in one unit. To test this, I co-transfected the DWD protein VprBP and several other DWD proteins. All tested DWD proteins co-immunoprecipitated with VprBP (Figure 2.5C). To confirm that this was not specific to VprBP, I also tested the binding of the DWD protein DDB2 to the

Figure 2.5

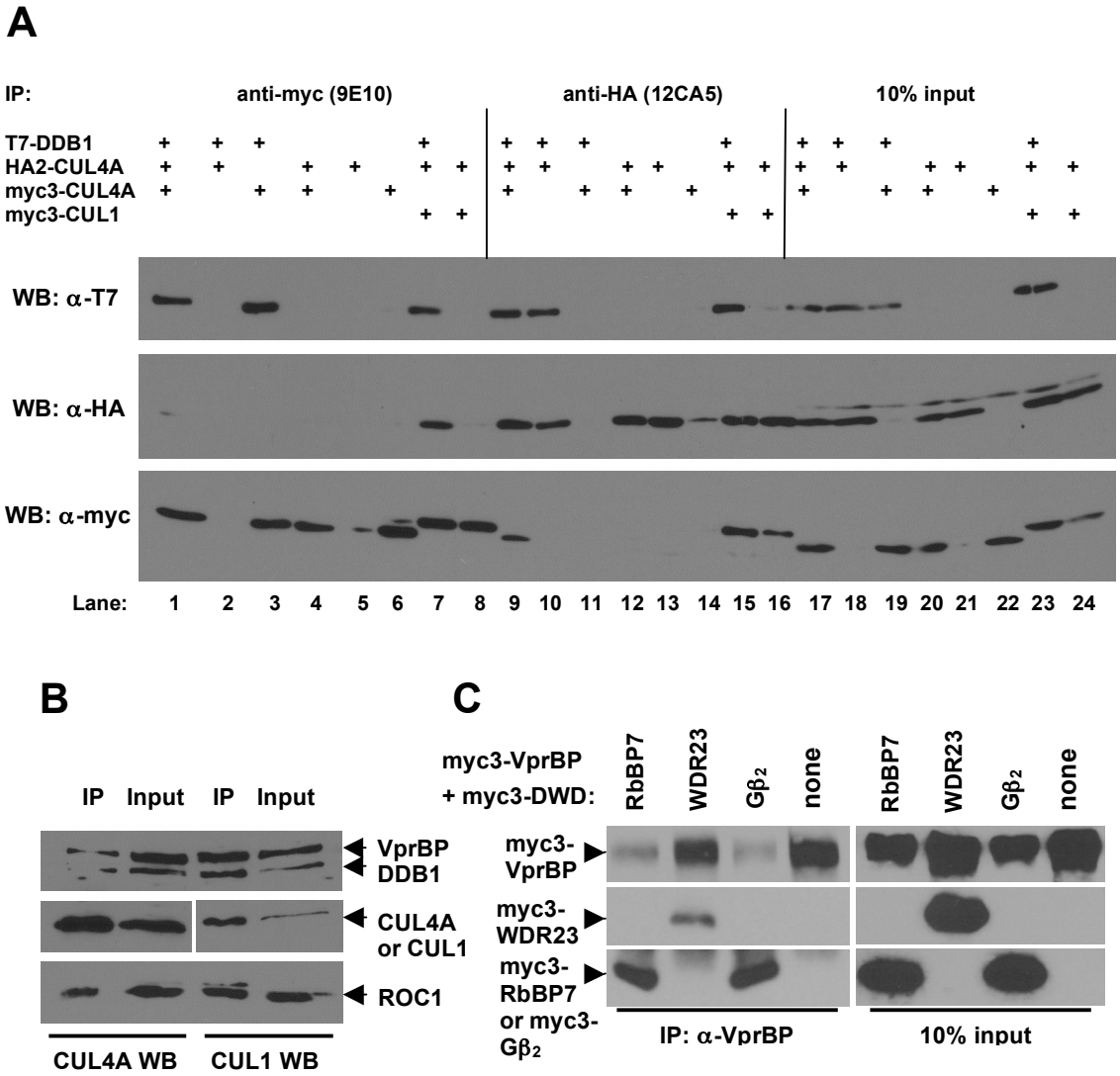
A
IP:
anti-myc (9E10)
anti-HA (12CA5)
10% input
T7-DDB1
HA2-CUL4A
myc3-CUL4A
myc3-CUL1
WB: α-T7
WB: α-HA
WB: α-myc
Lane: 1 2 3 4 5 6 7 8 9 10 11 12 13 14 15 16 17 18 19 20 21 22 23 24
B
IP Input IP Input
VprBP
DDB1
CUL4A
or CUL1
ROC1
CUL4A WB
CUL1 WB
C
myc3-VprBP
+ myc3-DWD:
RbBP7
WDR23
Gβ2
none
myc3-
VprBP
myc3-
WDR23
myc3-
RbBP7
or myc3-
Gβ2
IP: α-VprBP
10% input

Figure 2.5. CUL4A exists in homo- and hetero-dimeric complexes.

(A) Ectopically-expressed CUL4A dimerizes. 293T cells were transfected with plasmids expressing myc3- or HA-tagged CUL4A and/or myc3-tagged CUL1 and/or T7-tagged DDB1. 24 hrs after transfection, cells were lysed in 0.5% NP-40 lysis buffer, immunoprecipitated with anti-HA or anti-myc antibodies, and Western blotted as indicated.

(B) Endogenous CUL4A heterodimerizes with CUL1. U2OS cells were lysed with 0.5% NP-40 lysis buffer, and lysates were immunoprecipitated with an anti-CUL4A antibody. The immunocomplexes were split in half and resolved alongside 10% input control lanes. One set of IP and input was blotted with anti-CUL4A, the other with anti-CUL1, along with other antibodies as indicated.

(C) Multiple DWD proteins interact with each other, presumably in a cullin complex. 293T cells were co-transfected with myc3-tagged VprBP and one of a series of other DWD proteins, as indicated. Cells were lysed with 0.1% NP-40 lysis buffer, immunoprecipitated with an anti-VprBP antibody, and Western blotted with an anti-myc antibody.

same series of DWD proteins, and it also interacted with them all (data not shown). In these preliminary experiments, no negative control WD-40 protein that does not interact with CUL4A/DDB1 was included; therefore, the possibility remains that these interactions are non-specific. However, that both DDB2 and VprBP can form these dimeric complexes argues that the interaction is specific. These data suggest that CUL4A functions as an oligomeric ligase as well, but the functional consequence of this has yet to be determined.

Discussion

A remarkable feature of the cullin family of E3 ligases is the assembly of multiple E3 ligases by each individual cullin. Despite its linkage with multiple cellular pathways and many putative substrates, the substrate recruiting mechanism for CUL4 has remained elusive. The evidence presented here supports the model that a subset of WD40 proteins, defined by the presence of a DWD box, bind to DDB1, and that DDB1 functions as a linker connecting the DWD proteins to CUL4. A DWD protein could either be a substrate itself or function as a substrate receptor to recruit other protein(s) for ubiquitination by the CUL4-ROC catalytic core.

Database searches predict that there may be as many as 90 DWD proteins in humans, 74 in mice, 75 in *Drosophila*, 36 in *C. elegans*, 122 in *Arabidopsis*, 33 in *S. pombe*, and 20 in *S. cerevisiae* (see Appendix 1). These observations suggest that CUL4-ROC1 could potentially form a large family of distinct ubiquitin ligases with individual

DWD proteins and target the ubiquitination of many substrate proteins. Among the DWD proteins that have been experimentally tested positive for binding with DDB1-CUL4A are two F-box proteins, FBXW5 and FBXW8, and two SOCS proteins, WSB1 and WSB2 (Fig. 2.2). FBXW5 and WSB1 have been shown to bind with CUL1 and CUL2/5, respectively (Kamura et al. 2001; Arai et al. 2003). Whether these receptor proteins bind simultaneously with both CUL1 and CUL4 or CUL2/5 and CUL4, and whether cullin heterodimers more efficiently promote substrate polyubiquitination is an interesting possibility that is yet to be tested. Data recently presented in the dissertation of Jian Hu, a graduate student from our laboratory, shows that the F-box of FBXW5 is dispensable for the degradation of a novel cullin 4A substrate, TSC2, but this does not prove that other receptor proteins containing multiple cullin binding domains do not utilize a cullin heterodimer, or in some other way multiple cullins, to target substrates for polyubiquitination. My preliminary data (Figure 2.5) clearly indicates that CUL4A and CUL1 may form heterodimers, and CUL4A may form homodimers, but what role these dimers play in cullin function is unclear.

Furthermore, our identification of the "DWD box" as an identifiable feature of DDB1-interacting WD-40 proteins does not imply that this is the only necessary surface for DDB1 interaction. It is unlikely that one or two arginine residues are all that is necessary to interact specifically with DDB1. We may find, through more careful analysis of DWD proteins, that only a subset of these proteins actually interact with DDB1, and/or that other sequences are also required for interaction in addition to the conserved box. Preliminary data from Yaxue Zeng in our laboratory shows that

mutagenesis of the critical arginine residues in several DWD proteins does not disrupt their interaction with DDB1, which strongly suggests that other sequences are definitely required, or stabilize the DDB1-DWD interaction. However, our mutagenesis data and that of others shows that for other DWD proteins, such as DDB2 and CSA, changing even one arginine residue to alanine almost completely disrupts DDB1 interaction. At this point, all we can conclusively say is that the definition of the DWD motif is only the beginning of understanding how DDB1 interacts with its substrate receptors.

The presence of twenty WD40 proteins in the *S. cerevisiae* genome with the potential to bind with DDB1 is surprising, since there is no obvious homologue of either DDB1 or CUL4 in budding yeast. Two obvious candidate linkers for binding with these putative DWD proteins are CPSF160 (the cleavage and polyadenylation specificity factor A, 160 kDa subunit) and SAP130 (spliceosome-associated protein 130). Both CPSF160 and SAP130 are present in budding yeast, and exhibit a low level similarity with DDB1 at the primary sequence level, but contain similar β-propellers, as predicted by computational modeling (Neuwald and Poleksic 2000) and reinforced by comparison with the DDB1 crystal structure (Li et al. 2006). Even more speculatively, Joseph McCarville and Jen Michel from our laboratory discovered that *S. cerevisiae* lacking *Cul8* have an anaphase delay and mitotic defects, which are somewhat similar to the chromosome segregation and mitotic defects seen in *S. pombe* and mouse cells lacking *DDB1* (Bondar et al. 2003; Michel et al. 2003; Cang et al. 2007). It would be very interesting to see if Cul8 interacts with CPSF160 and/or SAP130 in *S. cerevisiae*.

The data presented in this chapter establishes the first evidence for a family of substrate receptor proteins that interact with the CUL4/DDB1 ubiquitin ligase. The exact composition of the "DWD box" motif remains to be firmly elucidated, however, and in the future, we may be able to more firmly establish which subset of WD-40 proteins, and which other possible proteins, may interact with DDB1 and form functional ubiquitin ligase complexes.

Contributions of individuals to work in this chapter:

Figure 2.1: A-C, Chad McCall. D, Yizhou He

Figure 2.2: cDNA cloning and plasmid preparation: Chad McCall and Yizhou He.

Western blotting: Yizhou He.

Figure 2.3: Yizhou He

Figure 2.4: A and C: Yizhou He, B: Yaxue Zeng

Figure 2.5: Chad McCall

CHAPTER 3

VprBP, A CUL4/DDB1-INTERACTING DWD PROTEIN, IS ESSENTIAL FOR NORMAL DNA REPLICATION

Summary

The CUL4/DDB1 E3 ubiquitin ligase interacts with a set of WD40 repeat proteins containing a specific motif, the DWD box. The most abundant of these DWD box proteins in the CUL4A immunocomplex, VprBP, has yet to be fully characterized. VprBP interacts with CUL4A/DDB1 through its WD40 domain, and binds stoichiometrically with DDB1, suggesting that its major cellular function is acting through the CUL4A/DDB1 ligase. Silencing of VprBP results in inhibition of cellular growth in a partially p53-dependent manner, and this inhibition is due to a defect in DNA replication. VprBP-deficient cells incorporate significantly less BrDU than controls, do not respond to S-phase or M-phase chemical cell cycle inhibitors, and activate cryptic origins of replication, an indicator of replication stress. In the absence of Rb function, VprBP loss results in G2 accumulation and cell death, while in the presence of wildtype p53 and Rb, its loss results in G1 accumulation and little evidence of cell death. Ongoing studies in my laboratory are aimed at discovering the CUL4A/DDB1 substrates whose dysregulation results in the DNA replication stress found in VprBP-silenced cells.

Background

Ubiquitin ligases play a critical role in cellular function, by recruiting various protein substrates for covalent modification by the small protein ubiquitin (Hochstrasser 1996; King et al. 1996; Hershko and Ciechanover 1998). Ubiquitin modification, either monomeric or in polyubiquitin chains, leads to various changes in cellular protein function, most prominently the targeting of polyubiquitin-conjugated proteins to the 26S proteasome for proteolytic degradation. The cullin family of ubiquitin ligases have particularly broad function, due to their ability to recruit a wide variety of substrates through modular interaction with substrate receptors containing specific protein-protein interaction motifs (Petroski and Deshaies 2005a). Cullins interact with their substrate receptors either directly, as in the case of CUL3 with one of over 200 BTB-domain-containing receptors (Geyer et al. 2003; Pintard et al. 2003; Xu et al. 2003; Furukawa and Xiong 2005), or indirectly through a conserved linker protein, such as SKP1 bridging one of more than 70 F-box-containing receptors to CUL1 (Feldman et al. 1997; Skowyra et al. 1997; Zheng et al. 2002b) and the heterodimer of elongins B and C linking one of the more than 30 VHL-box or SOCS-box receptors with CUL2 or CUL5 (Kamura et al. 1998; Stebbins et al. 1999; Zhang et al. 1999; Kamura et al. 2001; Kamura et al. 2004). Through interaction with these common motifs, the cullins may target hundreds of substrates for ubiquitination.

We and other groups recently identified a family of substrate receptors that interact with the CUL4A and CUL4B ligases through a single linker protein, DDB1: a

subclass of WD-40 repeat proteins containing a specific motif, which we term the DWD box (Angers et al. 2006; He et al. 2006; Higa et al. 2006b; Jin et al. 2006). The most critical feature of this motif is the presence of surface arginine residues immediately adjacent to the WD (Trp-Glu) of consecutive WD-40 repeats (WDxR). These DWD-box proteins include the CUL4A substrate receptors DDB2, which targets histones H2A, H3, and H4 for ubiquitination (Kapetanaki et al. 2006; Wang et al. 2006), the Cockayne syndrome protein CSA, which targets CSB for degradation (Groisman et al. 2006), and L2DTL/CDT2, which targets the DNA licensing factor CDT1 (Zhong et al. 2003; Hu et al. 2004; Arias and Walter 2005; Arias and Walter 2006; Higa et al. 2006b; Hu and Xiong 2006; Jin et al. 2006; Nishitani et al. 2006; Senga et al. 2006). Notably, all these substrates are involved in DNA repair or replication, though this common feature could simply be due to the systems focused on by laboratories investigating CUL4A/DDB1 ligases. However, there are more than 90 DWD proteins in the human genome, and the most abundant of these in the CUL4A immunocomplex, VprBP/DCAF1, has yet to be fully characterized.

VprBP was initially identified through co-immunoprecipitation and peptide sequencing of HIV-1 Vpr-interacting proteins (Zhao et al. 1994; Zhang et al. 2001), but its function has yet to be explored beyond the initial binding observations. Vpr, a 96-amino-acid, 14 kDa HIV-1 accessory protein, is dispensible for *in vitro* viral growth and replication, yet is essential for HIV function *in vivo*. It has been implicated in a number of different viral and cellular processes, from enhancing accuracy of reverse transcription to nuclear import of viral DNA, and from anti- and pro-apoptotic activities to

transactivation of HIV LTR and host genes (Le Rouzic and Benichou 2005). Yet, its most well studied cellular phenotype, when expressed alone or in the context of whole viral infection, is arrest of the cell cycle in G2, followed subsequently by apoptosis (He et al. 1995; Re et al. 1995; Bartz et al. 1996; Stewart et al. 1997; Roshal et al. 2003; Andersen et al. 2005; Lai et al. 2005).

In this chapter, I have initiated the characterization of the roles of VprBP in the cell apart from its function in HIV biology. I first verified by binding experiments that VprBP behaves much as other DWD-box proteins in its interactions with CUL4A and DDB1. Then, turning to RNA interference studies, I first noticed growth inhibition and cell death, which led me to examine whether VprBP played a role in the cell cycle, which was reasonable given the function of all other known DWD substrates, as well as the physiological effect of HIV-1 Vpr expression. I demonstrated that loss of VprBP causes a partially p53-dependent G1 and growth arrest in primary human cells, and causes failure of DNA replication associated with presence of double-strand breaks and likely firing of cryptic origins of replication in HeLa cells lacking p53- or Rb-pathway checkpoints.

Experimental Procedures

Antibodies, immunopurification, and mass spectrometric analysis

Antibodies to HA (12CA5, Boehringer-Mannheim), Myc (9E10, NeoMarkers), T7 (Novagen), FLAG (M2, Sigma), p53 (DO-1, NeoMarkers), p21 (NeoMarkers), Bax (N-20, Santa Cruz), and CSN5 (JAB1, GeneTex) were purchased commercially. Rabbit polyclonal antibodies to CUL4A, DDB1, and CDT1 have been described (Hu et al. 2004). A rabbit polyclonal antibody against VprBP was produced by injection of a synthetic peptide antigen to residues 1493-1507 of VprBP (DNSDLEDDIILSLNE). To purify the endogenous CUL4A complex, BT474 cells from 47 150-mm plates were lysed with a 0.5% NP-40 lysis buffer (50 mM Tris-HCl at pH 7.5, 150 mM NaCl, 0.5% NaCl, 50 mM NaF), and lysates were pooled (300 mg total). Clarified lysates were immunoprecipitated with affinity-purified anti-CUL4A antibody (2 μg/mg lysate, ±10 μg/mg antigen peptide). Immunocomplexes were resolved by SDS-PAGE and stained with Coomassie blue, and the protein bands were digested with trypsin and subjected to mass spectrometric analysis at the University of North Carolina Proteomics Core Facility. To purify the endogenous VprBP complex, an analogous protocol was used, but with U2OS cells.

Plasmids, cell culture, and cell transfection

Plasmids expressing human CUL4A and DDB1 were as previously described (Ohta et al. 1999; Liu et al. 2002; Furukawa et al. 2003; Hu et al. 2004). pFSZ2-VprBP-

FLAG was the kind gift of Dr. L.J. Zhao (St. Louis University), and was used to subclone VprBP into a pcDNA3-based mammalian expression vector. Mutations were introduced by site-directed mutagenesis using the QuickChange Kit (Stratagene) and verified by DNA sequencing. Cell lines were cultured as follows: HeLa cells in DMEM containing 10% FBS in a 37°C incubator with 5% CO2, U2OS cells in McCoy's 5A medium containing 15% FBS, WI-38 cells in MEM with sodium pyruvate, non-essential amino acids, and 10% FBS, and 293T cells in DMEM containing 10% newborn calf serum. Cell transfections were carried out using a calcium-phosphate buffer.

Gel filtration chromatography

To examine the elution profile of CUL4A and associated proteins, HeLa cells were lysed with the 0.5% NP-40 lysis buffer, and clarified lysate was resolved through a Superdex-200 gel filtration column (GE/Amersham). Fractions (0.5 mL) were collected, and 50 μL of each was resolved via SDS-PAGE and immunoblotted with antibodies as indicated. High-molecular-weight standards (GE/Amersham) were resolved through the same column, and the peak fraction for each was determined.

RNA interference (RNAi)

r-Dicer-generated siRNA to VprBP was generated by first amplifying nt 4008-4625 of VprBP cDNA using PCR primers with 5' overhangs with T7 promoter sequences. This PCR product was then used as a template for *in vitro* transcription of

both strands of a dsRNA using the T7 RiboProbe kit (Promega), then annealing the dsRNA by heating the transcribed mixture to 95ºC and slowly cooling to room temperature. This double-stranded RNA was then immediately added, without purification, to a reaction mixture containing 8 U of recombinant Dicer (Stratagene) and Dicer reaction buffer to a total of 500 mL. After digesting for 18 hrs at 37ºC, the Dicer products were purified by a series of three spin columns (G-25 (Amersham, Piscataway, NJ), EZ-pure (Millipore, Bedford, MA), Microcon-100 (Millipore)) (Myers et al. 2003). The final product was resolved on a 15% native polyacrylamide gel along with a known quantity of a synthetic siRNA to estimate final concentration. Control GFP r-Dicer siRNA were prepared as described in Myers et al, 2003.

Two duplex oligonucleotides encoding human VprBP-specific shRNA (sh1: 5'-CCGG GAA TAC TCT TCA AGA ATG ATG CCTCCTGTCA CAT CAT TCT TGA AGA GTA TTC TTTTTG-3' and sh2: 5'-CCGG GAA ATA CCT CGT CCT TCT ATG CTTCCTGTCA CAT AGA AGG ACG AGG TAT TTC TTTTTG), one duplex encoding human DDB1-specific shRNA (5'-CCGG CAG CAT TGA CTT ACC AGG CAT CCTCCTGTCA ATG CCT GGT AAG TCA ATG CTG TTTTTG-3') and one duplex oligonucleotide encoding firefly luciferase-specific shRNA (5'-CCGG GAGCT GTTTC TGAGG AGCC CCTCCTGTCA GGCT CCTCA GAAAC AGCTC CCGG TTTTTG-3') were ligated into the PMKO.1 vector (Addgene plasmid 8452). Retrovirus production was carried out according to a standard protocol and then used to infect WI-38, U2OS, and HeLa cells. Twenty-four hours after infection, cell lines were selected by puromycin

(2 μg/mL) for 2 d before cell cycle analysis, replating for cell proliferation assays, or analyzing protein expression and complex formation.

Flow cytometry

To analyse DNA content by propidium iodide staining, WI-38, U2OS, or HeLa cells were fixed in 75% ethanol overnight at 4ºC, then washed once in 1X PBS + 1% fetal bovine serum, and permeabilized for 30-45 mins at 37ºC in 1X PBS + 0.1 mg/mL RNAse A + 0.1% Triton X-100. The fixed and permeable cells were stained with 50 μg/mL propidium iodide for at least 90 mins at room temperature, shielded from light.

To analyze ongoing replication of DNA by bromodeoxyuridine (BrDU) labeling, HeLa cells were fixed in 80% ethanol overnight at 4ºC, then washed once in 1X PBS. Nuclei were isolated by incubating cells in 0.1M HCl/0.08% pepsin for 20 min at 37ºC, then DNA was denatured by incubating cells in 2M HCl for a further 20 mins at 37ºC. After neutralizing the HCl with 2 volumes of 0.1M sodium borate, pH 8.5, the cells were washed once with IFA buffer (10 mM HEPES (pH 7.3), 150 mM NaCl, 4% FBS) + 0.5% Tween-20. The cells were labeled with FITC-conjugated anti-BrDU (BD Biosciences) at 1:10 in IFA + Tween for 45 min at room temperature, then washed once with IFA + Tween. Finally, cells were stained for DNA content by incubating for 30 mins at room temperature with IFA + 0.1 mg/mL RNase A + 50 mg/mL propidium iodide. Stained cells were analyzed at the UNC School of Medicine Flow Cytometry Facility on either a

FACScan (Becton Dickinson) or CyAN (Dako Cytomation) flow cytometer, and data analyzed using Summit 4.3 software (Dako Cytomation).

Molecular combing

To analyze the properties of replication forks, HeLa cells were double labeled by incubation, first in medium with 100 μM IdU for 10 min, and second in 50 μM CldU for 20 min. DNA spreads were stained for IdU and CldU and analyzed for individual replication tracks as described previously (Unsal-Kacmaz et al. 2007).

Results

VprBP is a CUL4A/DDB1-interacting DWD protein.

We previously used large scale immunoprecipitation and mass spectrometry to identify a series of CUL4A/DDB1-interacting proteins, and used this to define a common motif found in potential CUL4A/DDB1 substrate receptors, the DWD box (He et al. 2006). The most abundant of these DWD proteins in our CUL4A immunocomplex was VprBP (Figure 3.1A, left panel). To further characterize the interaction partners of VprBP, I generated a rabbit polyclonal antibody and used it to perform a large-scale immunoprecipitation (Figure 3.1A, right panel), and submitted bands that were specifically competed off by antigen peptide for mass spectrometric identification. I found that VprBP associated with almost stochiometric amounts of DDB1 and smaller amounts of CUL4A and the subunits of the COP9/signalosome deneddylase. In order to verify the specificity of these interactions, I performed immunoprecipitation-Western blot experiments (Figure 3.1B). VprBP co-immunoprecipitated preferentially with Nedd8-modified CUL4A, which was more noticeable upon enrichment of CUL4A-Nedd8 by proteasome inhibition.

The Coomassie blue-stained immunocomplex suggested to me that VprBP might exist in a large multisubunit complex. To examine that, I separated HeLa lysate by gel filtration chromatography (Figure 3.1C). VprBP exists in complexes of more than 450

Figure 3.1

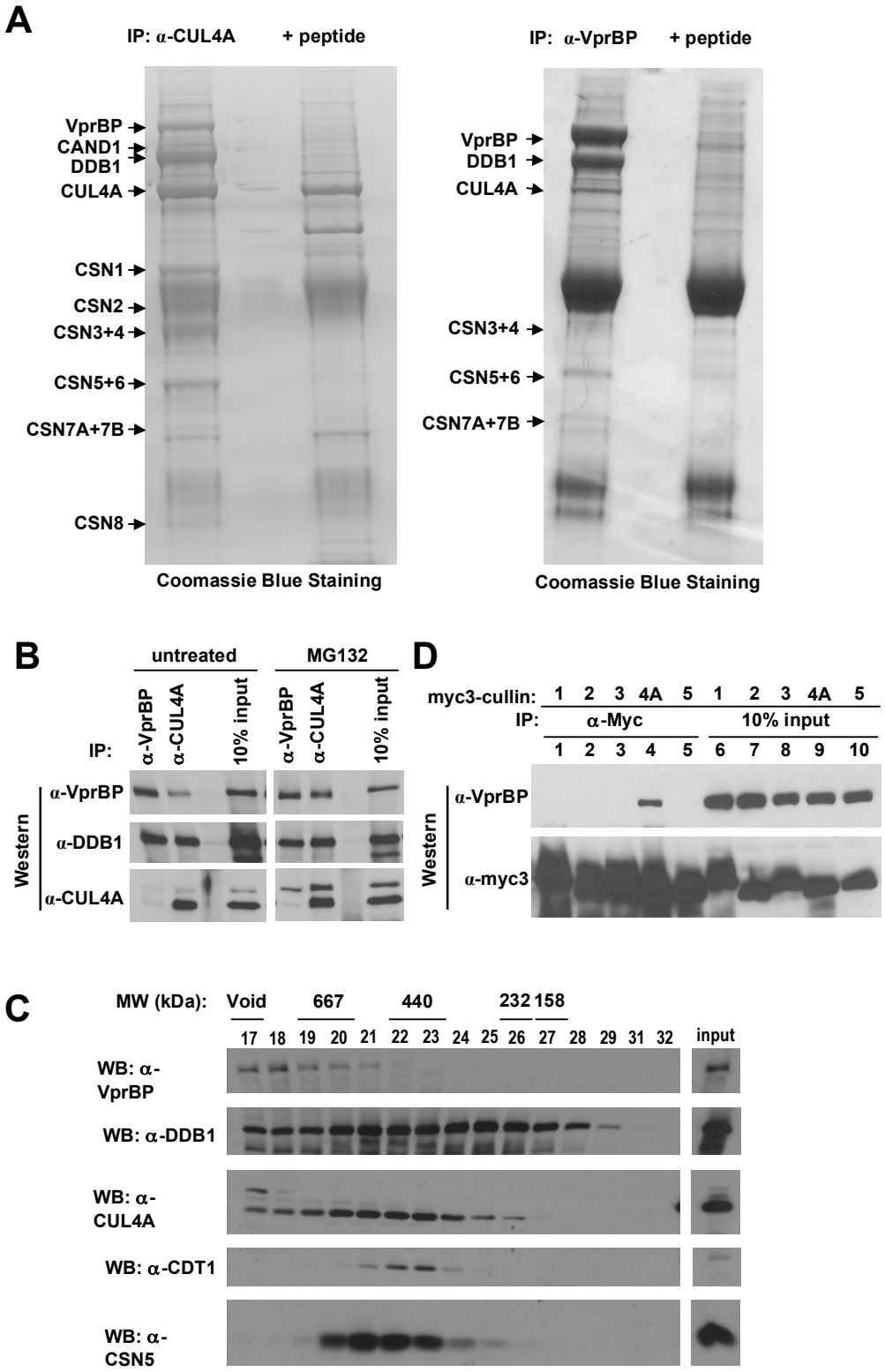
A
IP: α-CUL4A
+ peptide
VprBP
CAND1
DDB1
CUL4A
CSN1
CSN2
CSN3+4
CSN5+6
CSN7A+7B
CSN8
Coomassie Blue Staining
IP: α-VprBP
+ peptide
VprBP
DDB1
CUL4A
CSN3+4
CSN5+6
CSN7A+7B
Coomassie Blue Staining
B
untreated
MG132
IP:
α-VprBP
α-CUL4A
10% input
α-VprBP
α-CUL4A
10% input
Western
α-VprBP
α-DDB1
α-CUL4A
D
myc3-cullin: 1 2 3 4A 5 1 2 3 4A 5
IP: α-Myc
10% input
1 2 3 4 5 6 7 8 9 10
Western
α-VprBP
α-myc3
C
MW (kDa): Void 667 440 232 158
17 18 19 20 21 22 23 24 25 26 27 28 29 31 32
input
WB: α-VprBP
WB: α-DDB1
WB: α-CUL4A
WB: α-CDT1
WB: α-CSN5

Figure 3.1. VprBP is a CUL4A/DDB1-interacting DWD protein.

(A) VprBP is one of the most abundant binding partners of CUL4A/DDB1. The CUL4A immunocomplex was precipitated from human BT474 cells and resolved by SDS-PAGE, followed by staining with Coomassie Brilliant Blue. Bands identified by mass spectrometry are indicated.

(B) Endogenous VprBP and CUL4A co-immunoprecipitate. U2OS cells were treated with MG132 (25 μM x 5 hrs), then lysed with 0.5% NP-40 lysis buffer and immunoprecipitated with antibodies against VprBP or CUL4A. Immunocomplexes were resolved by SDS-PAGE and Western blotted with the indicated antibodies.

(C) VprBP exists in very large molecular weight complexes. HeLa S3 0.5% NP-40 lysate was resolved into 32 fractions on a Superdex-200 gel filtration column, along with molecular weight standards as indicated. The void volume corresponded to a molecular weight over 700 kDa, and the input control was 100 μg of HeLa S3 lysate. Equal volumes of each fraction were resolved by SDS-PAGE and Western blotted as indicated.

(D) The VprBP immunocomplex contains stoichiometric amounts of DDB1, and substoichiometric amounts of other CUL4A ligase components. U2OS cells (48 150-mm dishes) were lysed with 0.5% NP-40 lysis buffer, immunoprecipitated with anti-VprBP (antibody generated in our laboratory) with or without excess of antigen peptide. The immunocomplexes were resolved by SDS-PAGE, stained with Coomassie Brilliant Blue, and specific bands were submitted for mass spectrometric identification. Identified bands are indicated.

(E) VprBP associates with CUL4A but not other cullins. 293T cells were transfected with pcDNA3-myc3-cullin plasmids, and lysates were immunoprecipitated and Western blotted as indicated.

kDa to greater than 700 kDa in size, and I was unable to detect any VprBP in size fractions corresponding to a monomeric form. This, combined with the very abundant DDB1 in the VprBP immunocomplex, implies that VprBP primarily functions through its interactions with the CUL4A ubiquitin ligase.

In order to rule out that VprBP functions with other cullin ubiquitin ligase family members, I also immunoprecipitated ectopically-expressed cullins, and Western blotted for endogenous VprBP (Figure 3.1D). I was only able to detect VprBP in the CUL4A immunocomplex, which verifies that it, like other "DWD proteins," serves as a modulator of CUL4A ligase function.

The WD40 domain of VprBP is required and sufficient to interact with DDB1-CUL4A

We have also previously shown that CUL4A interacts with DDB1 and its DWD substrate receptors through its N-terminus (Hu et al. 2004; He et al. 2006), and I sought to verify that VprBP functions similarly. I co-expressed VprBP with a panel of CUL4A mutants (Figure 3.2A), and found that deletion of the N-terminal 52 or 100 amino acids, which constitute the DDB1- and DWD-interaction domain, completely abrogated the VprBP-CUL4A interaction (Figure 3.2B). Moreover, VprBP contains conserved domains in its N-terminus in addition to its C-terminal WD-40 domain. I examined whether these domains might influence its binding with CUL4A/DDB1. Expression of the C-terminus of VprBP alone, containing the WD repeats and a highly acidic "tail," was sufficient to

Figure 3.2

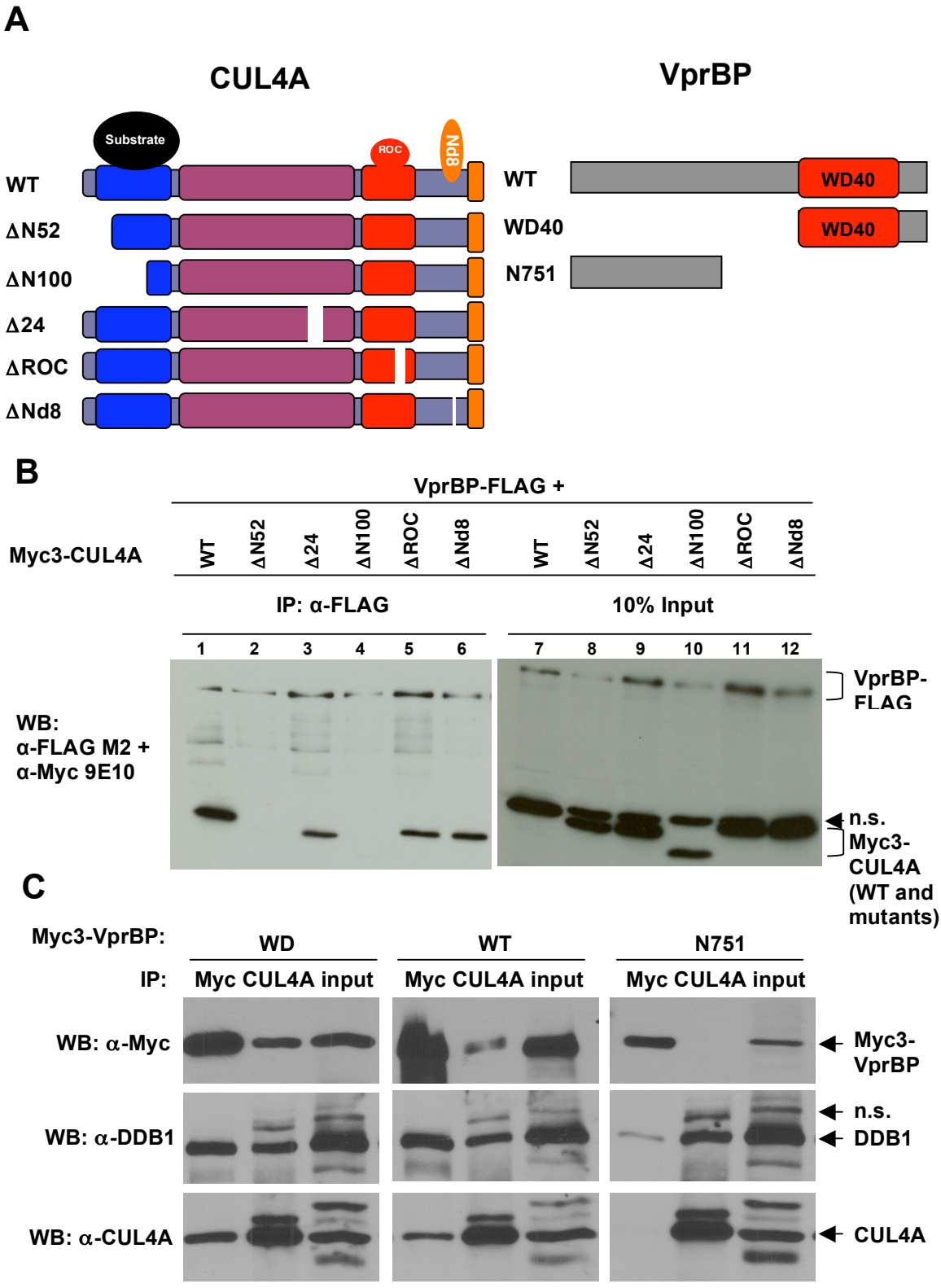
A
CUL4A
VprBP
Substrate
ROC
Nd8
WT
ΔN52
ΔN100
Δ24
ΔROC
ΔNd8
WT
WD40
WD40
WD40
N751
B
VprBP-FLAG +
Myc3-CUL4A
WT
ΔN52
Δ24
ΔN100
ΔROC
ΔNd8
WT
ΔN52
Δ24
ΔN100
ΔROC
ΔNd8
IP: α-FLAG
10% Input
1 2 3 4 5 6
7 8 9 10 11 12
WB:
α-FLAG M2 +
α-Myc 9E10
VprBP-FLAG
n.s.
Myc3-CUL4A (WT and mutants)
C
Myc3-VprBP:
WD
WT
N751
IP:
Myc CUL4A input
Myc CUL4A input
Myc CUL4A input
WB: α-Myc
WB: α-DDB1
WB: α-CUL4A
Myc3-VprBP
n.s.
DDB1
CUL4A

Figure 3.2. The WD domain of VprBP is sufficient to interact with CUL4A/DDB1.

(A) CUL4A and VprBP mutants used in B and C.

(B) VprBP interacts with the substrate-recruiting N-terminus of CUL4A. 293T cells were transfected with pFSZ2-VprBP-FLAG and pcDNA3-myc3-CUL4A plasmids as indicated. 0.5% NP-40 lysates were immunoprecipitated with anti-FLAG (M2), resolved by SDS-PAGE, and Western blotted as shown. The CUL4A mutants used are diagrammed in (A) above.

(C) The WD domain of VprBP is sufficient to interact with CUL4A/DDB1. 293T cells were transfected with pcDNA3-myc3-VprBP, wildtype or mutants as indicated. 0.5% NP-40 lysates were immunoprecipitated with anti-Myc (9E10) or anti-CUL4A, resolved by SDS-PAGE, and Western blotted as shown. VprBP mutants used are diagrammed in (A) above.

bind endogenous CUL4A and DDB1, indeed even more abundantly than full-length VprBP (Figure 3.2C). This, combined with the inability of the conserved N-terminal domain (N751) to interact with CUL4A or DDB1, strongly suggests that VprBP interacts with CUL4A/DDB1 through its WD-40 domain.

VprBP expression is essential for normal proliferation and DNA replication.

After identifying VprBP as a potential substrate receptor, or otherwise modulator, of the CUL4A/DDB1 ubiquitin ligase, I then sought to explore its cellular function through the use of RNA interference. First, I used recombinant Dicer to generate siRNA to VprBP (Figure 3.3A). Silencing was very efficient, and led to an immediately obvious growth phenotype. To quantify that phenotype, I plated equal numbers of VprBP siRNA-treated cells 72 hours after transfection, alongside DDB1 siRNA (which our unpublished data had already indicated had a growth arrest) and several controls. We found that VprBP-treated cells had essentially ceased proliferating.

Due to concerns about toxicity of transfected oligonucleotides and the transient nature of siRNA, I then sought to confirm this result by the use of small hairpin RNAs produced by retroviral infection. I produced three hairpin RNA sequences targeting different regions of VprBP, and two were very successful at silencing and at reproducing the siRNA growth arrest phenotype (Figure 3.4). Because of the potential of checkpoint pathways masking the phenotype of VprBP siRNA (leading to growth arrest), I infected HeLa cells with one of the two shRNA constructs, which produced nearly

Figure 3.3

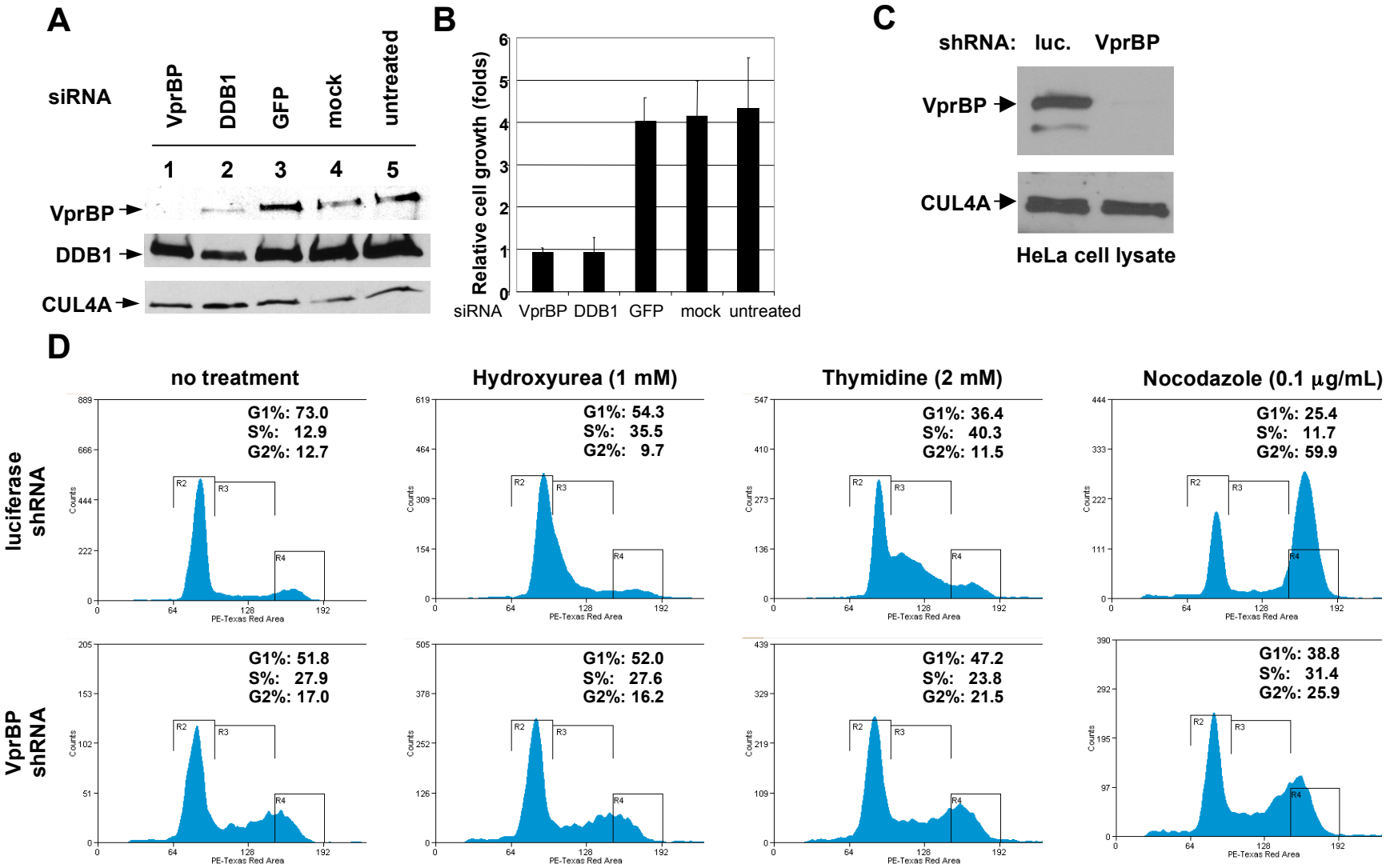
A
siRNA
VprBP
DDB1
GFP
mock
untreated
1 2 3 4 5
VprBP
DDB1
CUL4A
B
Relative cell growth (folds)
siRNA VprBP DDB1 GFP mock untreated
C
shRNA: luc. VprBP
VprBP
CUL4A
HeLa cell lysate
D
no treatment
Hydroxyurea (1 mM)
Thymidine (2 mM)
Nocodazole (0.1 μg/mL)
luciferase shRNA
VprBP shRNA
G1%: 73.0
S%: 12.9
G2%: 12.7
G1%: 54.3
S%: 35.5
G2%: 9.7
G1%: 36.4
S%: 40.3
G2%: 11.5
G1%: 25.4
S%: 11.7
G2%: 59.9
G1%: 51.8
S%: 27.9
G2%: 17.0
G1%: 52.0
S%: 27.6
G2%: 16.2
G1%: 47.2
S%: 23.8
G2%: 21.5
G1%: 38.8
S%: 31.4
G2%: 25.9
Counts
PE-Texas Red Area
R2
R3
R4

Figure 3.3. VprBP is required for normal cellular proliferation and DNA replication.

(A) r-Dicer-generated VprBP siRNA is efficient in silencing. U2OS cells were transfected with r-Dicer-generated VprBP siRNA or GFP siRNA, or synthetic DDB1 siRNA, and 72 hrs after transfection, cells were lysed using 0.5% NP-40 lysis buffer. Lysates were resolved by SDS-PAGE and Western blotted as indicated.

(B) VprBP and DDB1 siRNA inhibit cellular proliferation. 72 hrs after transfection in (A), equal numbers of siRNA-transfected U2OS cells were plated, and counted after 72 more hours of growth. The amount of proliferation over the number plated were plotted, with standard error of >4 separate counts indicated.

(C) shRNA retroviruses to VprBP efficiently silence expression. HeLa cells were infected with pMKO.1 retroviruses encoding shRNA to VprBP or luciferase (as a negative control). 24 hrs after infection, cells were selected for 48 hrs with 2 μg/mL puromycin. Dead cells were washed away with PBS, and selected cells were trypsinized, lysed in 0.5% NP-40 lysis buffer, resolved by SDS-PAGE, and Western blotted as indicated, using CUL4A as a loading control.

(D) VprBP-silenced HeLa cells are arrested in S-phase and unable to further respond to chemical inhibitors. Trypsinized cells from (C) above were replated into new dishes. 24 hrs later (96 hrs post-infection), cells were treated with 1 mM hydroxyurea, 2 mM thymidine, or 0.1 μg/mL nocodazole as indicated. 24 hrs after treatment, cells were trypsinized, and fixed overnight in 75% ethanol. After propidium iodide staining, the cell cycle was analyzed by flow cytometry.

Figure 3.4

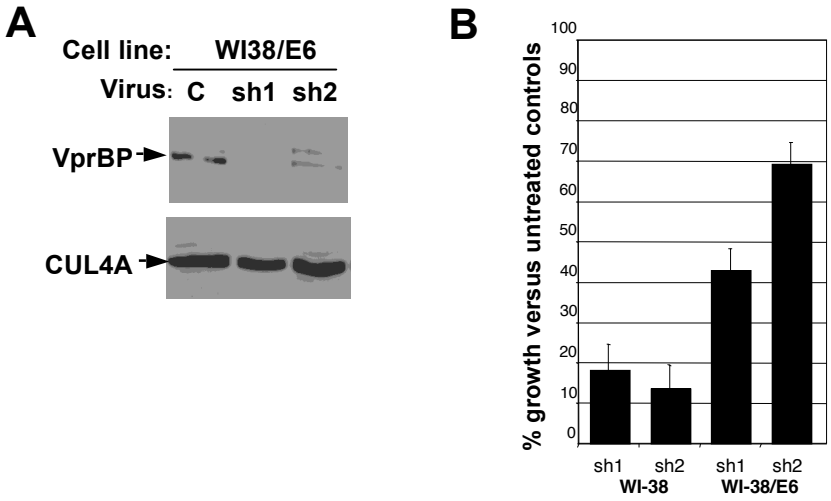

Figure 3.4. Two VprBP shRNA constructs silence protein expression efficiently.

(A) Both VprBP shRNA efficiently silence expression. WI-38/E6 cells were infected with retroviruses expressing empty pMKO.1 vector or vectors expressing two different shRNA sequences to VprBP. 24 hrs after infection, the cells were selected with 2 mg/mL puromycin for 48 hrs, then viable cells were lysed in 0.5% NP-40 lysis buffer. Lysates were resolved by SDS-PAGE and Western blotted as indicated.

(B) Both VprBP shRNA contribute to an inhibition of cellular proliferation. 72 hrs after infection with shRNA against VprBP or empty viral vector (48 hrs after selection), equal numbers of viable WI-38 or WI-38/E6 cells were replated. 72 hrs after plating, cell numbers were counted and normalized against empty vector control cells. Standard error of >4 counts indicated.

complete silencing (Figure 3.3C). To my surprise, the HeLa cells also ceased proliferating, as dramatically as in p53-competent U2OS and WI-38 cells (data not shown). I examined the cellular DNA content of fixed, stably shRNA-infected HeLa cells 72 hrs after infection, and found a pronounced S-phase accumulation compared with control luciferase shRNA-infected cells (Figure 3.3D). This arrest was not altered by treatment with the S-phase inhibitors hydroxyurea or thymidine (Figure 3.3D) or aphidicolin (not shown), and only mildly shifted to G2/M by the metaphase inhibitor nocodazole, indicating an almost complete cessation of DNA synthesis.

Defects in DNA synthesis often result in double-strand breaks, leading to phosphorylation of H2AX on Ser-139 and the ATM-dependent phosphorylation of Chk2 on Thr-68. I measured the levels of each phosphorylated species in whole-cell extracts from VprBP-silenced HeLa cells. Chk2 phosphorylation increased significantly, while H2AX phosphorylation increased less dramatically (Figure 3.5A). I was unable to detect any increase in Chk1 phosphorylation (data not shown). These data suggest that stalled replication due to VprBP silencing might lead to collapsed replication forks, which produce double-strand breaks and the phosphorylation of the markers shown.

VprBP silencing decreased the incorporation of nucleotides throughout S phase.

To further characterize the S-phase phenotype of cells lacking VprBP, I pulse labeled HeLa cells with bromodeoxyuridine (BrDU) and examined the pattern of its

Figure 3.5

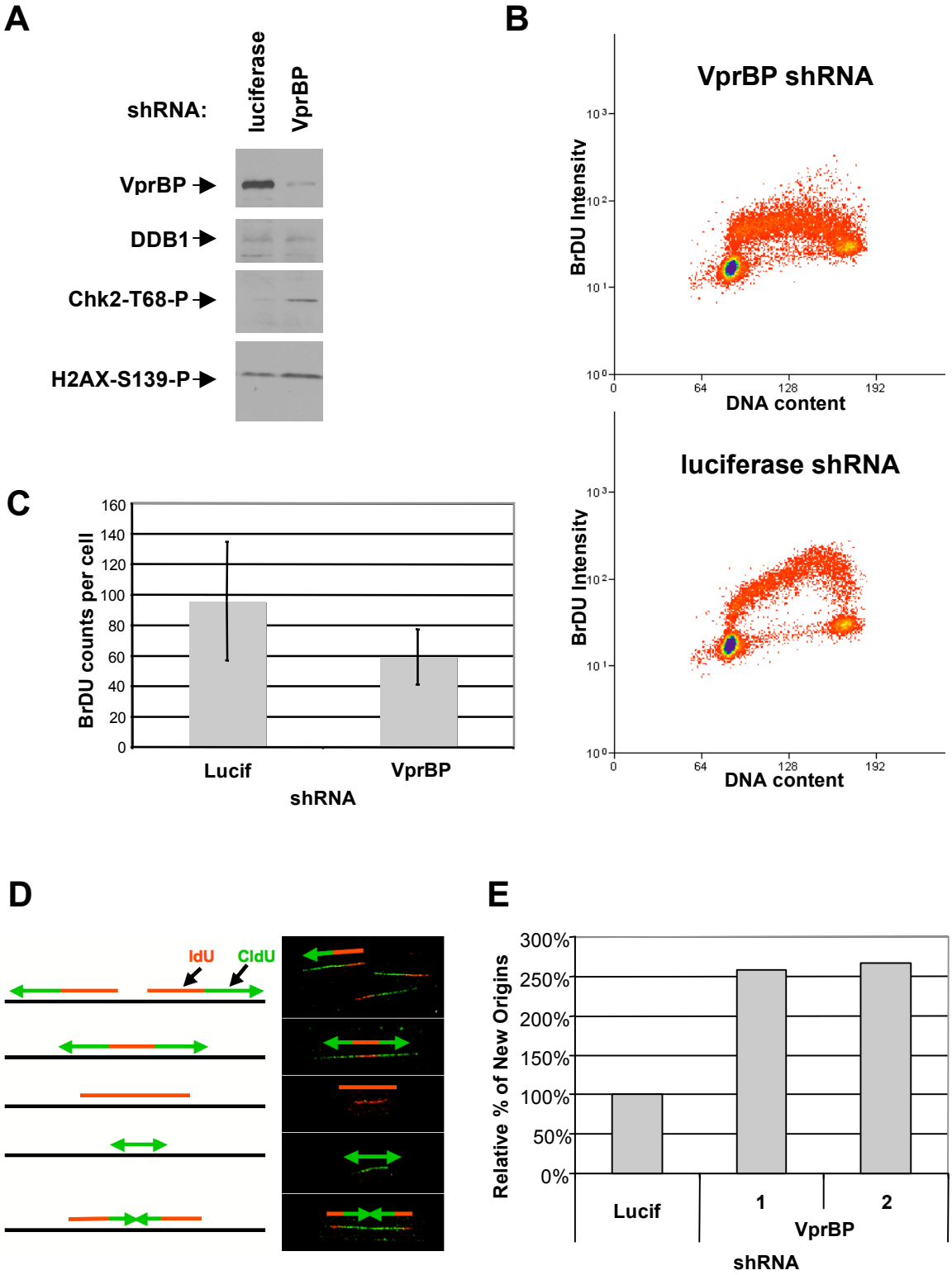
A
shRNA:
luciferase
VprBP
VprBP
DDB1
Chk2-T68-P
H2AX-S139-P
B
VprBP shRNA
BrDU Intensity
DNA content
luciferase shRNA
BrDU Intensity
DNA content
C
BrDU counts per cell
Lucif
VprBP
shRNA
D
IdU
CldU
E
Relative % of New Origins
Lucif
1
2
VprBP
shRNA

Figure 3.5. VprBP silencing reduces overall DNA replication but increases the firing of new replication forks.

(A) Silencing of VprBP leads to formation of double-strand breaks. . HeLa cells were infected with pMKO.1 retroviruses encoding shRNA to VprBP or luciferase (as a negative control). 24 hrs after infection, cells were selected for 48 hrs with 2 μg/mL puromycin. Dead cells were washed away with PBS, and selected cells were trypsinized. Cells were then lysed in a x% SDS lysis buffer, sonicated for 45 secs, and then Western blotted as indicated.

(B) Silencing of VprBP produces a decreased overall rate of DNA replication. Cells from (A), 80 hrs after infection and 56 hrs after puromycin selection, were pulse-labeled with 10 μM BrDU for 30 min. After labeling, the cells were washed with 1X PBS, trypsinized, and fixed in 80% ethanol/20% 1X PBS overnight. After staining with a FITC-conjugated anti-BrDU antibody and propidium iodide, the cells were analyzed by flow cytometry as shown.

(C) Silencing of VprBP results in decreased BrDU incorporation. Mean BrDU staining intensity was extracted from (B) by gating for BrDU-positive cells, and graphed +/- standard deviation.

(D) DNA combing allows for analysis of individual replication forks. HeLa cells, 90 hrs after VprBP shRNA infection (with both shRNA sequences), were labeled for 10 mins with iododeoxyuridine (IdU), then washed, and labeled for 20 mins with chlorodeoxyuridine (ClDU). The cells were then trypsinized and resuspended in 1X PBS. After fixing cells, combing DNA out onto slides, and staining for IdU (red) and ClDU (green), individual replication tracks were counted and analyzed. Representative data is shown here to demonstrate the types of tracks possible to distinguish.

(E) VprBP silencing leads to a relative increase in the proportion of newly fired origins of replication. After combing as described in (D), the number of ClDU-only tracks (representing origins which fired during the labeling period), increased in VprBP-silenced cells by over 250%. For other combing data, see Table 3.1.

incorporation. Consistent with our data showing a lack of response to S- and G2/M-phase inhibitors, BrDU incorporation was markedly reduced in VprBP-silenced cells (Figure 3.5B). The pattern of decreased BrDU incorporation is present in cells throughout S-phase based on DNA content measured by propidium iodide staining, and BrDU intensity is inversely correlated with increase in DNA content, as compared with a gradual increase in BrDU intensity throughout S-phase in control cells. The mean BrDU intensity in VprBP-silenced cells averaged slightly more than half that of control cells (Figure 3.5C). These data strongly suggest that VprBP is required for normal replication of DNA, and the pattern of BrDU incorporation—relatively normal in early S phase but much reduced later—suggests that the impairment is strongest in mid- to late-S phase, which is most consistent with a role in the maintenance or firing of forks throughout S, not initiation.

VprBP silencing results in firing of cryptic origins of replication.

To better examine the physical mechanism by which VprBP is functioning in DNA replication, Dr. Paul Chastain performed DNA combing experiments to examine the replication of DNA at individual replication forks (see Figure 3.5D for a diagram of the experimental design). In VprBP-silenced HeLa cells, with either of the two VprBP shRNA constructs, the proportion of newly fired DNA replication forks increased two- to three-fold over control cells, and the relative number of actively replicating forks correspondingly decreased (Figure 3.5E). Neither the relative number of terminated forks nor the track length (therefore the rate of replication of active forks) had statistically

Table 3.1

Distribution of DNA tracks with CldU-only, IdU-only, or containing both labels.

	Hours (h)	Red-only (IdU)	Green-only (CldU)	Red-Green (Idu-CldU)	Total Tracks Scored
Luc	72	87 (15%)	72 (12%)	435 (73%)	594
VprBP sh #1	72	41 (10%)	85 (22%)	269 (68%)	395
Luc	90	22 (6%)	20 (5%)	339 (89%)	381
VprBP sh #1	90	43 (8%)	72 (14%)	416 (78%)	531
VprBP sh #2	90	49 (12%)	55 (14%)	294 (74%)	398

Figure 3.6

A

B

	Average Relative Length		
	Green[i] (72 h)	Green[ii] (90 h)	Number Analyzed
Luciferase shRNA	100%	100%	60, 54
VprBP shRNA	143%	91%	50, 54
Tipin siRNA		82%	-, 57

[i] Relative to the green portion of the luciferase control red-green tracks produced at 72H.
[ii] Relative to the green portion of the luciferase control red-green tracts produced at 90H.

Figure 3.6. VprBP shRNA does not consistently affect the rate of elongation of replication forks.

(A) Diagram of the tracks measured in (B).

(B) VprBP shRNA inconsistently affects the rate of DNA elongation. The length of individual green (ClDU-stained) sections of actively elongating (red-green) tracks of VprBP and control shRNA-transduced HeLa cells were measured, as indicated. As a comparison, Paul Chastain included results from previously published experiments on Tipin (Unsal-Kacmaz et al. 2007).

significant changes (see Table 3.1 and Figure 3.6). The most likely explanation for an increase in the relative number of newly fired forks combined with a decrease in overall DNA replication (measured by BrDU incorporation per cell) is that VprBP-silenced cells are firing cryptic origins of replication as a result of replication stress, similar to what has been seen for cells with depleted Mcm2-7 licensing helicases (Woodward et al. 2006).

VprBP associates with chromatin in a cell-cycle-dependent manner.

Due to the effect that VprBP silencing has upon DNA replication, I reasoned that it might associate with chromatin in a cell-cycle specific manner. To test this, I synchronized HeLa cells by arresting them at the G1-S boundary by a double-thymidine block, then releasing them and taking fractions throughout the cell cycle. After Dr. Jean Cook isolated chromatin-bound proteins from each fraction, I found that VprBP is chromatin-bound, and its association with chromatin increases from early S through G2, and decreases again upon return to G1 phase (Figure 3.7A-B). This is in contrast to MCM2, which, as expected, leaves chromatin during S phase progression as DNA is replicated. CUL4A follows a very similar pattern to VprBP, and both proteins (and MCM2 as well) were not detectable on chromatin after arrest of cells in prometaphase by nocodazole block (Figure 3.7A). These results suggest that VprBP and CUL4A are recruited to chromatin as DNA is being replicated, and are released from chromatin in mitosis. However, they do not establish which of these proteins is required for the other to be chromatin-associated.

Figure 3.7

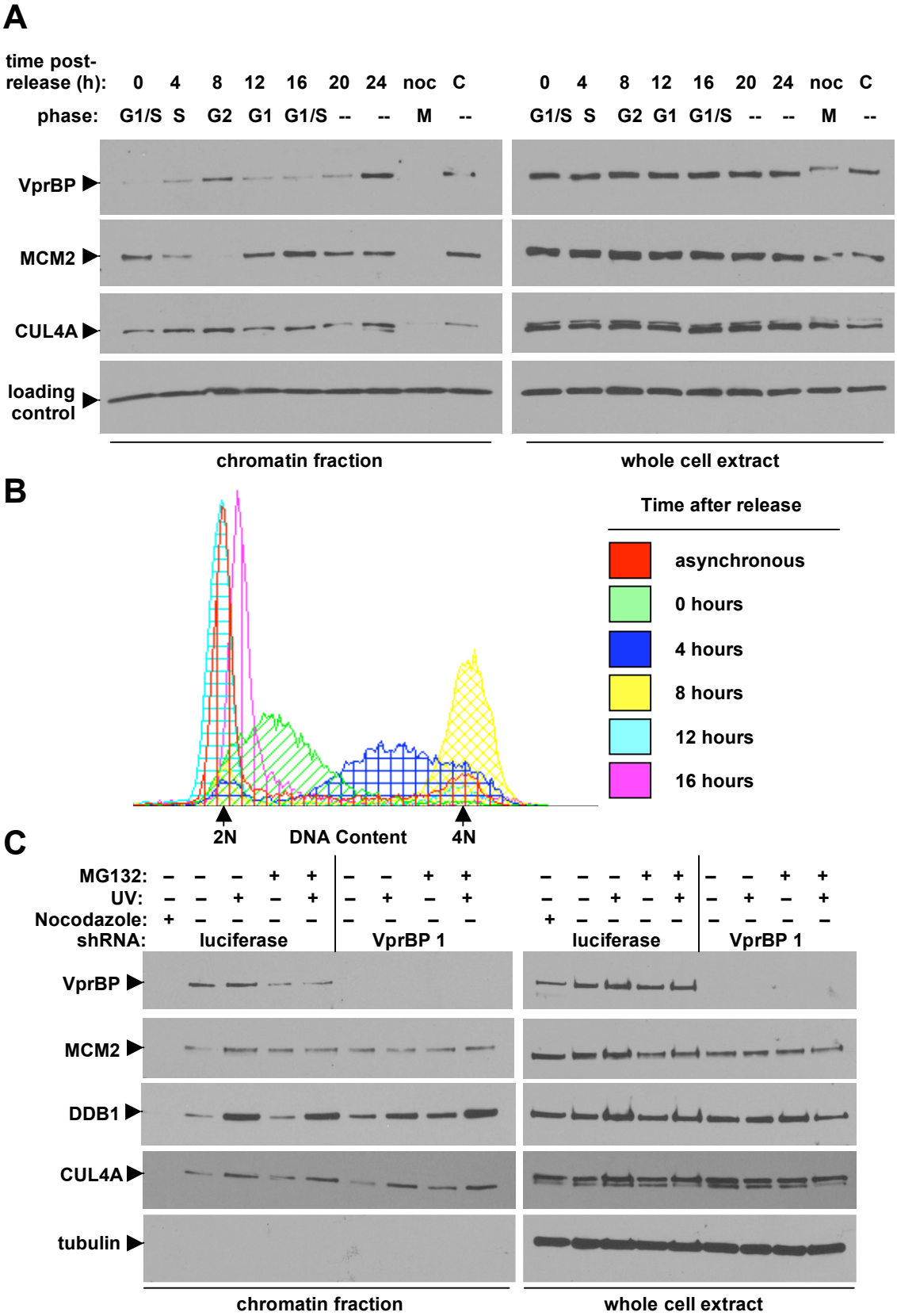
A
time post-release (h): 0 4 8 12 16 20 24 noc C 0 4 8 12 16 20 24 noc C
phase: G1/S S G2 G1 G1/S -- -- M -- G1/S S G2 G1 G1/S -- -- M --
VprBP
MCM2
CUL4A
loading control
chromatin fraction
whole cell extract
B
Time after release
asynchronous
0 hours
4 hours
8 hours
12 hours
16 hours
2N
DNA Content
4N
C
MG132: – – – + + – – + + – – – + + – – + +
UV: – – + – + – + – + – – + – + – + – +
Nocodazole: + – – – – – – – – + – – – – – – – –
shRNA: luciferase VprBP 1 luciferase VprBP 1
VprBP
MCM2
DDB1
CUL4A
tubulin
chromatin fraction
whole cell extract

Figure 3.7. VprBP and CUL4A progressively associate with chromatin during S and G2 phases of the cell cycle.

(A) VprBP and CUL4A progressively associate with chromatin during S and G2 phases of the cell cycle, but are not associated with chromatin after mitotic block. HeLa cells were synchronized at the G1-S boundary by double thymidine block, then released into fresh media. Time points were collected as indicated, with a fraction of cells being fixed for flow cytometry analysis, and the rest pelleted at frozen at -80ºC. The frozen pellets were then chromatin fractionated (see Materials and Methods), and whole cell extract and chromatin-associated proteins were resolved by SDS-PAGE and Western blotted as indicated.

(B) Propidium iodide staining reveals good synchronization in (A). After fixing with 75% ethanol for 30+ minutes, cells were permeabilized and stained with propidium iodide, then analyzed by flow cytometry. An overlay of different time points is shown. After 16 hours, the cells became asynchronous, with an increasing percentage in G2 by 24 hours.

(C) VprBP shRNA does not affect CUL4A, DDB1 or MCM2 loading onto chromatin. HeLa cells were transduced with VprBP shRNA, then selected with puromycin for 24 hours starting 24 hours after transduction. The cells were then passaged, and 36 hours later, were trypsinized and pelleted. Pellets were fractionated as in (A), resolved by SDS-PAGE, and Western blotted as indicated.

To test this, Dr. Cook again chromatin fractionated HeLa cells, this time after VprBP shRNA, with the added conditions of MG132 and/or UV treatment to examine whether proteasome inhibition or UV-damaged DNA influences VprBP association with chromatin damage. I established that VprBP shRNA does not affect CUL4A, DDB1 or MCM2 association with chromatin (Figure 3.7C). Moreover, VprBP shRNA does not change CUL4A's or DDB1's increased association with chromatin 30 minutes after UV treatment, which is well established in the literature (Groisman et al. 2003). That VprBP does not affect MCM2 loading strongly suggests that its effect on replication must come after formation of the pre-replication complex. However, the lack of any change in CUL4A/DDB1 association with chromatin, either with or without UV damage, alongside CUL4A and VprBP's very similar pattern of cell cycle association with chromatin, implies that VprBP may require interaction with CUL4A for its chromatin-based cellular functions, but may not be required for the UV-damaged DNA repair functions of CUL4A.

Cell proliferation arrest after VprBP silencing is partially p53-dependent.

Because of the growth arrest and replication stress phenotype of VprBP-silenced cells (Figures 3.3D and 3.5), I examined what role the p53 pathway might play in response to loss of this protein. I found that, in both U2OS (Figure 3.8A) and WI-38 (Figure 3.8B) cells, loss of VprBP led to moderate but consistent accumulation of p53, and significant upregulation of the cell cycle inhibitor p21. Consistent with the lack of sub-G1 cells seen in flow cytometric analysis (data not shown), I did not see any increase

in the expression of the pro-apoptotic protein Bax in either cell line, which points toward a p53-dependent cell cycle arrest, but not significant induction of apoptosis. I then examined the cell proliferation characteristics of WI-38 cells versus WI-38 cells stably infected with a retrovirus expressing HPV E6 to eliminate p53 function. The WI-38/E6 cells proliferated at a higher baseline rate, and the inhibition of growth due to loss of VprBP was reduced (Figure 3.8C). However, U2OS, WI-38, and WI-38/E6 cells all have G1 accumulation (Figure 3.9, 3.10, and data not shown) and growth inhibition in response to VprBP silencing, which clearly suggests, along with the HeLa data (Figure 3.3D), that the growth arrest is not entirely p53-dependent. Interestingly, WI-38 cells expressing HPV E7 to inhibit pocket protein function do not arrest in G1, but rather, have G2 accumulation, strong induction of p53, and massive cell death (by observation that within seven days after infection, essentially no cells remained adherent), which suggests that Rb function is critical for cell survival and G1 arrest after VprBP silencing in the presence of p53 (Figure 3.10).

VprBP silencing correlates with decreased levels of the CUL4A/DDB1 substrate CDT1

In addition to the replication stress and p53 activation phenotypes, we further examined what role VprBP might be playing in normal CUL4A/DDB1 cellular function. Its extreme abundance in the CUL4A immunocomplex, orders of magnitude more than any other DWD protein (we have only identified two others, DDB2 and WDR23, in the CUL4A immunocomplex by mass spectrometry ((He et al. 2006) and data not shown), suggests the possibility that it might be playing a regulatory, not a substrate-recruiting,

role. Consistent with that interpretation, we found that protein levels of the CUL4A/DDB1 substrate CDT1 are reduced in both VprBP siRNA- and shRNA-treated cell lines (Figure 3.11A and 3.11B). However, this CDT1 reduction could be the product of transcriptional or other indirect regulation; therefore, these preliminary studies must be followed up by future assays to determine the effect of VprBP loss on CDT1 ubiquitination, *in vivo* and/or *in vitro*, by CUL4A/DDB1.

Figure 3.8

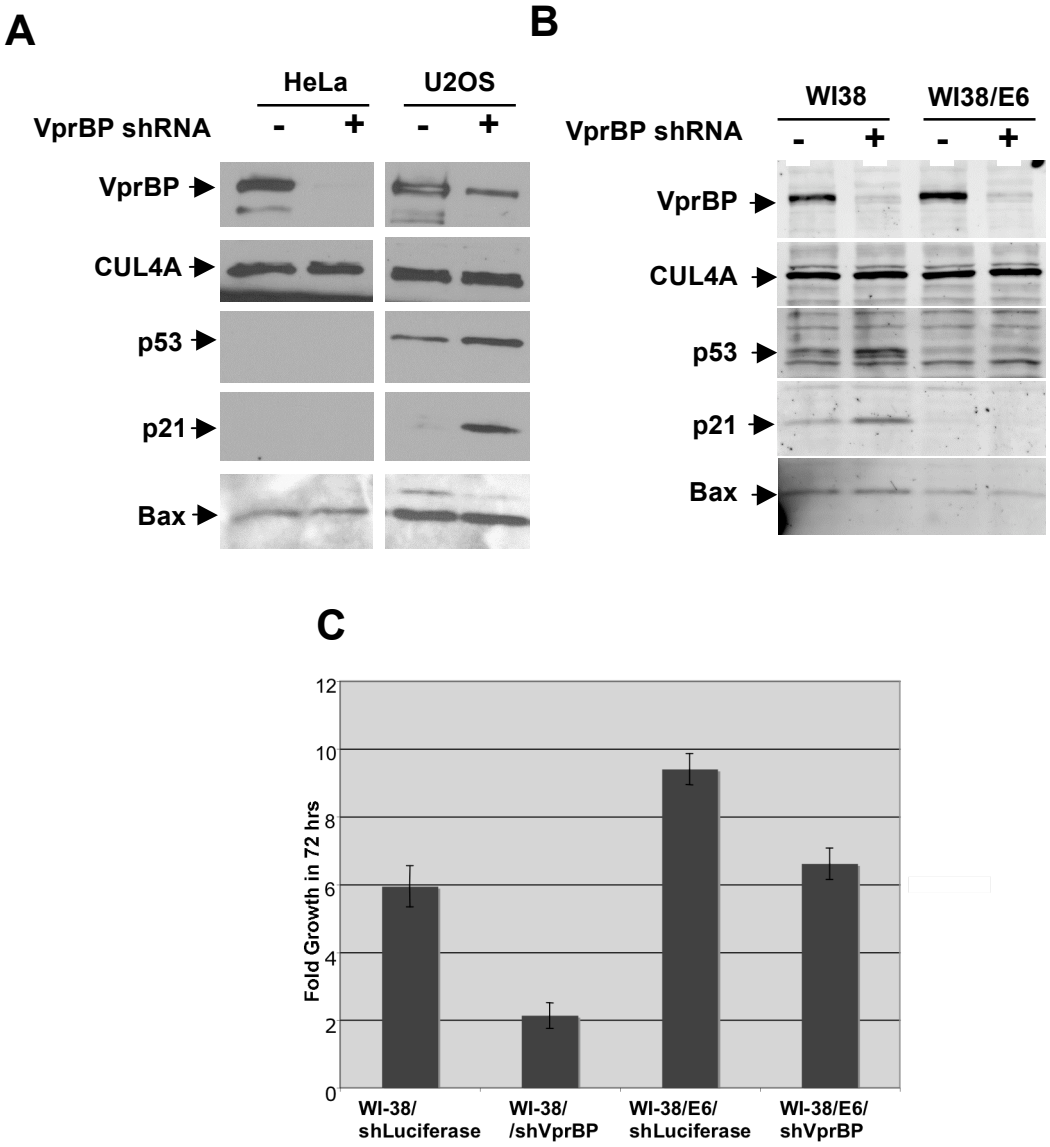
A
HeLa
U2OS
VprBP shRNA
-
+
-
+
VprBP
CUL4A
p53
p21
Bax
B
WI38
WI38/E6
VprBP shRNA
-
+
-
+
VprBP
CUL4A
p53
p21
Bax
C
Fold Growth in 72 hrs
0
2
4
6
8
10
12
WI-38/ shLuciferase
WI-38/ /shVprBP
WI-38/E6/ shLuciferase
WI-38/E6/ shVprBP

Figure 3.8. Arrest of cellular proliferation after VprBP silencing is partially p53-dependent.

(A) VprBP shRNA activates p53 and p21. HeLa (p53 negative) and U2OS (p53 wildtype) cells were infected with pMKO.1 shRNA retroviruses to VprBP or luciferase 24 hrs after infection, cells were selected with 2 μg/mL puromycin for 48 hrs (HeLa) or 24 hrs (U2OS). U2OS cells were grown for 24 hrs in normal growth medium after selection. 72 hrs after infection, cells were lysed with 0.1% NP-40 lysis buffer, resolved by SDS-PAGE, and Western blotted as shown.

(B) WI-38 cells expressing HPV E6 abrogate the VprBP shRNA-dependent activation of p53 and p21 expression. WI-38 cells, or WI-38 cells stably expressing HPV E6 (WI-38/E6) were infected with pMKO.1 shRNA retroviruses to VprBP or luciferase 24 hrs after infection, cells were selected with 2 μg/mL puromycin for 48 hrs. After selection, cells were lysed with 0.1% NP-40 lysis buffer, resolved by SDS-PAGE, and Western blotted as shown.

(C) Inactivation of p53 partially rescues the VprBP growth arrest phenotype. 48 hrs after selection with puromycin, shRNA-infected WI-38 or WI-38/E6 cells were trypsinized, and equal numbers were replated. 72 hrs later, cells were again trypsinized and counted. The amount of growth over the number plated is indicated, with standard error of 16 separate counts each.

Figure 3.9

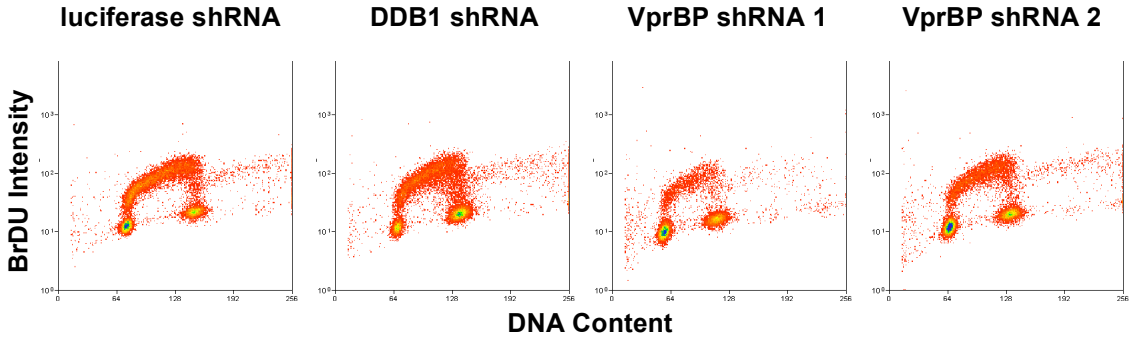

shRNA	luciferase	DDB1	VprBP 1	VprBP 2
G1% (BrDU neg)	23.9	13.8	46.6	37.0
S% (BrDU pos)	56.2	52.5	22.9	36.6
G2/M% (BrDU neg)	18.4	30.8	28.2	24.1

Figure 3.9. VprBP silencing leads to G1 accumulation and reduction of S phase in U2OS cells.

U2OS cells were transduced with retroviruses encoding shRNA hairpins as indicated. 24 hours after transduction, transduced cells were selected with puromycin for 48 hours, then passaged 1:4 into fresh media. 24 hours later, the cells were labeled for 30 mins with 10 μM BrDU, then fixed overnight and stained with FITC-conjugated anti-BrDU and propidium iodide. BrDU intensity and DNA content (propidium iodide intensity) were measured by flow cytometry. BrDU positive and negative (2N and 4N DNA content) cell populations were quantified using Summit 4.3 software.

Figure 3.10

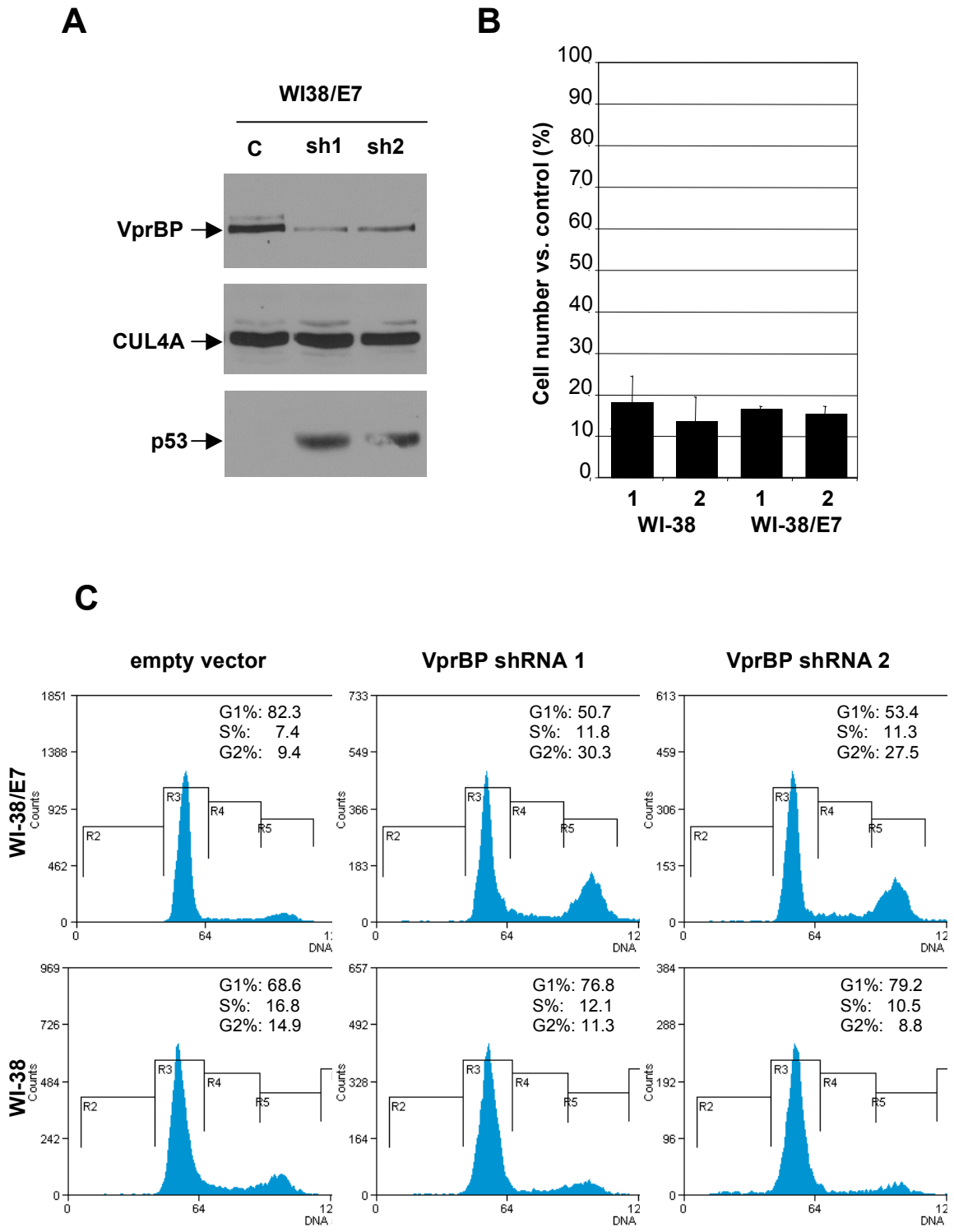
A
WI38/E7
C
sh1
sh2
VprBP
CUL4A
p53
B
Cell number vs. control (%)
100
90
80
70
60
50
40
30
20
10
0
1
2
1
2
WI-38
WI-38/E7
C
empty vector
VprBP shRNA 1
VprBP shRNA 2
WI-38/E7
WI-38
G1%: 82.3
S%: 7.4
G2%: 9.4
G1%: 50.7
S%: 11.8
G2%: 30.3
G1%: 53.4
S%: 11.3
G2%: 27.5
G1%: 68.6
S%: 16.8
G2%: 14.9
G1%: 76.8
S%: 12.1
G2%: 11.3
G1%: 79.2
S%: 10.5
G2%: 8.8
Counts
DNA
R2
R3
R4
R5

Figure 3.10. VprBP silencing in cells with active p53 but not Rb leads to G2/M accumulation and dramatic activation of p53.

(A) Silencing of VprBP in WI-38 cells expressing HPV E7 leads to high induction of p53. WI-38/E7 cells were infected with retroviruses expressing empty pMKO.1 vector or vectors expressing two different shRNA sequences to VprBP. 24 hrs after infection, the cells were selected with 2 mg/mL puromycin for 48 hrs, then viable cells were lysed in 0.5% NP-40 lysis buffer. Lysates were resolved by SDS-PAGE and Western blotted as indicated.

(B) Silencing of VprBP in WI-38/E7 cells leads to loss of cell proliferation. 72 hrs after infection with shRNA against VprBP or empty viral vector (48 hrs after selection), equal numbers of viable WI-38 or WI-38/E7 cells were replated. 72 hrs after plating, cell numbers were counted and normalized against empty vector control cells. Standard error of >4 counts indicated.

(C) VprBP silencing in WI-38/E7 cells leads to G2/M accumulation. When cells were collected for lysis in (A), an aliquot of each sample was fixed in 75% ethanol, stained with propidium iodide, and analyzed for DNA content by flow cytometry.

Figure 3.11

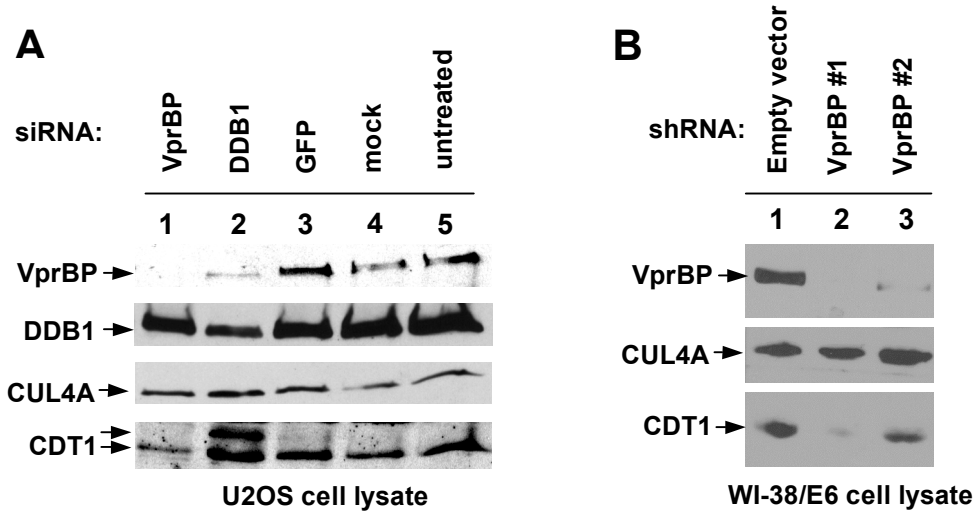

Figure 3.11. VprBP silencing correlates with decreased levels of CDT1.

(A) siRNA to VprBP decreases steady-state levels of CDT1 under the same conditions where siRNA to DDB1 accumulates CDT1. . U2OS cells were transfected with r-Dicer-generated VprBP siRNA or GFP siRNA, or synthetic DDB1 siRNA, and 72 hrs after transfection, cells were lysed using 0.5% NP-40 lysis buffer. Lysates were resolved by SDS-PAGE and Western blotted as indicated.

(B) shRNA to VprBP decreases steady-state levels of CDT1 proportional to the level of silencing of VprBP. WI-38/E6 cells were infected with retroviruses expressing empty pMKO.1 vector or vectors expressing two different shRNA sequences to VprBP. 24 hrs after infection, the cells were selected with 2 mg/mL puromycin for 48 hrs, then viable cells were lysed in 0.5% NP-40 lysis buffer. Lysates were resolved by SDS-PAGE and Western blotted as indicated.

Discussion

In this chapter, I examined the cellular function of the novel CUL4A/DDB1 interacting protein VprBP. I confirmed that VprBP interacts with CUL4A/DDB1 in a manner analogous to other DWD-box proteins that have been described, binding through DDB1 with the N-terminus of CUL4A, and requiring only its WD-40 domain (Figures 1 and 2). VprBP preferentially interacts with the active, Nedd8-modified form, of the CUL4A ligase, which suggests that it plays a role in either recruiting specific substrates, or regulating the recruitment of other substrates, to the ligase. I have yet to identify these substrates, but the cellular phenotype and subcellular localization data I have accumulated can narrow down the possibilities.

First, I can speculate on the function of VprBP in the CUL4A ligase based on the extensive characterization we have done of the cellular phenotype upon VprBP silencing by both transfected siRNA and stably infected shRNA oligonucleotides. Recently, two manuscripts have been published describing the effects of DDB1 conditional knockout in three mouse tissues: the brain, lens, and the epidermis (Cang et al. 2006; Cang et al. 2007). In both manuscripts, loss of DDB1 resulted in inhibition of cellular proliferation, and in induction of apoptosis. In the epidermis, concurrent loss of p53 resulted in rescue of the apoptotic phenotype, but did not rescue the loss of cellular proliferation and also led to the accumulation of aneuploid and polyploid cells (Cang et al. 2007). Similarly, in the $p53^{-/-}$;$DDB1^{-/-}$ mouse brain, there was a reduction in apoptosis and increase in cells

with abnormal nuclear morphology, although proliferation was not completely impeded (Cang et al. 2006).

My VprBP data are similar, yet not completely overlapping, with these results. Loss of VprBP in p53 wildtype cells did result in p53 accumulation and inhibition of proliferation (Figure 3.8 and 3.9), but we see no evidence of induction of apoptosis unless Rb function is also lost (Figure 3.10). We see induction of p21, but not in the context of p53-null cells (Figures 3.8A and 3.8B), unlike the p53-independent induction of p21 that was reported in $p53^{-/-}$;$DDB1^{-/-}$ epidermal cells (Cang et al. 2007). These results suggest that VprBP might be partially mediating the regulation of DNA replication that is a major function of DDB1, particularly since VprBP silencing in p53 and Rb-deficient HeLa cells results in inhibition of DNA replication and proliferation (Figures 3 and 4). But, functional DDB1 must, in the absence of VprBP, be enough to prevent an apoptotic response when Rb activity is present. In addition, our experiments in WI-38 cells and the same cells stably expressing E6 to remove p53 clearly indicate a partial rescue of the VprBP proliferation defect, though the WI-38/E6 cells proliferate quite slowly (Figure 5C). This response may be analogous to the partial rescue of DDB1 knockout phenotypes by p53 loss. An obvious future experiment is to silence VprBP in DDB1-deficient cells to further dissect the relationship between these two proteins.

The replication stress phenotype produced by VprBP silencing may, in the future, lead to the identification of the substrate(s) regulated by VprBP in the cell. That MCM proteins are still loaded onto chromatin in the absence of VprBP suggests that initial licensing of replication origins is intact in silenced cells. The *increased* relative firing of

origins (Figure 3.5E) also supports this notion. However, that the total level of BrDU incorporation is greatly reduced, and the cells are clearly not responsive to further inhibition by S-phase blocking agents, strongly indicates that VprBP is required for normal DNA replication. The BrDU incorporation phenotype is similar to the silencing of two other genes: Chk1 (personal communication from Dr. Jean Cook) and Cdc7 (Montagnoli et al. 2004). Chk1 inhibition also causes an increase in the rate of replication origin firing, measured by increased Cdc45 loading onto chromatin (Syljuasen et al. 2005). I have been unable to detect any changes in Chk1 protein level in VprBP-silenced HeLa cells, nor activation of Chk1 by phosphorylated Ser-345 (data not shown), which may be consistent with an inhibition of Chk1 activity by VprBP. However, what, if any, link there is between the two remains to be seen. Cdc7, a kinase required for initiation of replication at each fork, when silenced produces similar phenotypes to VprBP inhibition: HeLa cells have decreased BrDU incorporation, S-phase arrest, and apoptosis; primary human fibroblasts deficient in Cdc7 activate p53 and p21, and arrest in G1 (Montagnoli et al. 2004). The decreased BrDU incorporation in Cdc7-silenced cells is throughout S phase, and there is no report in the literature of increased firing of replication forks after Cdc7 silencing or loss, therefore it is somewhat questionable whether VprBP acts at the same level as Cdc7 in regulation of replication. We are currently examining whether the Cdc7 activator Dbf4, a known target of the anaphase-promoting complex E3 ligase (Ferreira et al. 2000), has altered protein levels and/or chromatin association in VprBP-silenced cells. These two pathways, Chk1 and Cdc7/Dbf1, represent two possible avenues for VprBP regulation, but as we have yet to establish any mechanistic link, VprBP could be acting in an entirely novel manner.

My preliminary results indicate a clear biochemical relationship between CUL4A/DDB1 and VprBP, since VprBP is the major binding partner of CUL4A and DDB1 in the CUL4A immunocomplex (Figure 3.1A). Furthermore, I can co-immunoprecipitate VprBP and other DWD proteins (Figure 2.5C), which along with evidence for CUL4A oligomerization (Figure 2.5A and 2.5B), may present a mechanism by which VprBP can either target other proteins for degradation, or regulate the degradation of other DWD substrates in an oligomeric cullin complex. I have also seen a correlation between VprBP silencing and reduction of the level of the CUL4A substrate CDT1 (Figure 3.11), but it is not at all clear whether that correlation is due to a regulation of ligase activity, or an indirect mechanism due to the perturbation of the cell cycle by silencing of VprBP. However, that UV treatment does not increase VprBP chromatin association as it does DDB1 and CUL4A (Figure 3.7C) suggests that VprBP may not function in the active CUL4A/DDB1/DDB2 and CUL4A/DDB1/CSA complexes, although the similar chromatin association profiles throughout the cell cycle for VprBP and CUL4A (Figure 3.7A) are consistent with a CUL4A/DDB1/VprBP complex present on chromatin during S- and G2-phases of the normal cell cycle. The substrates this complex regulates, as described earlier, are yet to be determined.

These observations provide the first detailed characterization of a DWD protein, VprBP, which is essential for normal DNA replication and cellular proliferation. Its abundant association with the CUL4A/DDB1 ligase, along with the well-characterized defects in DNA replication and repair associated with the loss of DDB1, suggests that VprBP may function to regulate the replication aspect of DDB1 function. These

preliminary studies have generated many questions, first and foremost being how the replication phenotype seen in VprBP-silenced cells relates to dysfunction of the CUL4A/DDB1 ligase, if at all. Identification of the DNA replication pathway modulated by VprBP will go a long way toward identifying the potential CUL4A/DDB1 substrates involved.

CHAPTER 4

VprBP INTERACTS WITH HIV-1 Vpr AND LINKS THE Vpr UBIQUITINATION SUBSTRATE UNG2 TO THE CUL4A/DDB1 LIGASE

Summary

VprBP was originally discovered as a protein that interacts abundantly with the HIV-1 accessory protein Vpr. In this chapter, I present preliminary data exploring how this interaction relates to the CUL4A/DDB1 E3 ubiquitin ligase. I have further characterized the binding between Vpr and VprBP, showing that the association is through the WD40 domain of VprBP. I then examined whether the cellular ubiquitination substrate of Vpr, UNG2, is able to interact with VprBP in the presence of Vpr. It does so, and this interaction is stabilized by proteasome inhibition. A Vpr mutant that does not interact with UNG2 still interacts with VprBP, so these two activities are separable. I attempted to also examine the role VprBP might play in Vpr's G2 cell cycle arrest phenotype, but the G1/S arrest produced byVprBP silencing alone precluded that possibility. These data form the groundwork for future experimentation into the role VprBP may be playing in the degradation of UNG2, and possibly in the G2 arrest caused by Vpr.

Background

The HIV-1 genome encodes for several accessory proteins in addition to the characteristic retroviral reverse transcriptase, protease, envelope, and capsid core proteins. Vpr, a 96-amino-acid, 14 kDa HIV-1 accessory protein, is dispensible for *in vitro* viral growth and replication, yet is essential for HIV function *in vivo*. It has been implicated in a number of different viral and cellular processes, from enhancing accuracy of reverse transcription to nuclear import of viral DNA, and from anti- and pro-apoptotic activities to transactivation of HIV LTR and host genes (Le Rouzic and Benichou 2005). Yet, its most well studied cellular phenotype, when expressed alone or in the context of whole viral infection, is arrest of the cell cycle in G2, followed subsequently by apoptosis (He et al. 1995; Re et al. 1995; Bartz et al. 1996; Stewart et al. 1997; Roshal et al. 2003; Andersen et al. 2005; Lai et al. 2005).

The G2 cell cycle arrest caused by Vpr expression is evidently the result of activation of a DNA damage response pathway, yet what is the initial insult or activation of the pathway remains a mystery. Vpr binds directly to chromatin (Lai et al. 2005), it induces H2AX phosphorylation and RPA foci, requires Rad17 and Hus1 (Zimmerman et al. 2004), and activates BRCA1 (Andersen et al. 2005), which is strongly suggestive of the actual damage of DNA. Inhibition of either the ATR or Chk1 DNA damage checkpoint kinases inhibits this arrest (Roshal et al. 2003), as would be expected from other signs of DNA damage, and the G2 arrest does not require functional p53 or Rb pathways, as HeLa cells readily arrest.

However, the G2 arrest phenotype is not the only one relevant to our studies. Recently, Vpr was also found to target two cellular substrates, the uracil DNA glycosylases UNG2 and SMUG, for polyubiquitination and proteasome-dependent degradation (Schrofelbauer et al. 2005), and this interaction is physiologically significant, as Vpr's interaction with UNG2 inhibits UNG2's critical role in immunoglobulin class switch recombination, thereby impairing antibody production (Begum et al. 2006). The authors of the UNG2 degradation manuscript also reported association of ectopically expressed CUL4A with Vpr, but did not pursue the significance of that association. The same group very recently published a manuscript showing that CUL4A or DDB1 silencing inhibits UNG2 and SMUG degradation, and Vpr physically interacts with DDB1 (Schrofelbauer et al. 2007). They also found that Vpr disrupted DDB1-DDB2 interaction and, consequently, global genomic repair of UV-damged DNA, and speculate that the G2 arrest caused by Vpr is due to the inability to repair this damage, since DDB1 silencing also produces G2 accumulation. However, they have not causally established such a link between Vpr's cell cycle arrest and DDB1.

As described in Chapter 3, I have focused my research on the characterization of VprBP (Vpr binding protein), which was, obviously by its name, originally discovered as a cellular protein that abundantly associated with Vpr (Zhao et al. 1994; Zhang et al. 2001). The combination of this physical link and the aforementioned evidence linking Vpr and the CUL4A/DDB1 ligase led me to examine the link between VprBP and Vpr function. In this chapter, I present some preliminary data describing in greater detail the interaction between VprBP and Vpr, and the bridging of UNG2, Vpr's ubiquitination

substrate, to VprBP. These results would be greatly enhanced by evidence showing a requirement for VprBP in UNG2 degradation, experiments that are ongoing at the time of this writing. I also present evidence that suggests a possible link between VprBP and the G2 arrest phenotype of Vpr expression, but is confounded by the cell cycle arrest produced by VprBP silencing alone.

Experimental Procedures

Antibodies and immunopurification

Antibodies to HA (12CA5, Boehringer-Mannheim), Myc (9E10, NeoMarkers), and UNG1/2 (Abcam) were purchased commercially. Rabbit polyclonal antibodies to CUL4A and DDB1 have been described (Hu et al. 2004). A rabbit polyclonal antibody against VprBP was produced by injection of a synthetic peptide antigen to residues 1493-1507 of VprBP (DNSDLEDDIILSLNE).

Plasmids, cell culture, and cell transfection

A plasmid expressing UNG2 was produced by amplifying cDNA from a human HeLa cDNA library and subcloning into a pcDNA3-based mammalian expression vector. pFSZ2-VprBP-FLAG was the kind gift of Dr. L.J. Zhao (St. Louis University), and was used to subclone VprBP into a pcDNA3-based mammalian expression vector. pLHAVprSN was the kind gift of Dr. Wei Chun Goh (Tufts-New England Medical Center), and was used to subclone into a pcDNA3-based mammalian expression vector. Once in pcDNA3, HA-Vpr was subcloned into a pBABE-based retroviral expression vector for retrovirus production and transduction. Mutations were introduced by site-directed mutagenesis using the QuickChange Kit (Stratagene) and verified by DNA sequencing. Cell lines were cultured as follows: U2OS cells in McCoy's 5A medium

containing 15% FBS, and 293T cells in DMEM containing 10% newborn calf serum. Cell transfections were carried out using a calcium-phosphate buffer.

RNA interference (RNAi)

Two duplex oligonucleotides encoding human VprBP-specific shRNA (sh1: 5'-CCGG GAA TAC TCT TCA AGA ATG ATG CCTCCTGTCA CAT CAT TCT TGA AGA GTA TTC TTTTTG-3' and sh2: 5'-CCGG GAA ATA CCT CGT CCT TCT ATG CTTCCTGTCA CAT AGA AGG ACG AGG TAT TTC TTTTTG), one duplex encoding human DDB1-specific shRNA (5'-CCGG CAG CAT TGA CTT ACC AGG CAT CCTCCTGTCA ATG CCT GGT AAG TCA ATG CTG TTTTTG-3') and one duplex oligonucleotide encoding firefly luciferase-specific shRNA (5'-CCGG GAGCT GTTTC TGAGG AGCC CCTCCTGTCA GGCT CCTCA GAAAC AGCTC CCGG TTTTTG-3') were ligated into the PMKO.1 vector (Addgene plasmid 8452). Retrovirus production was carried out according to a standard protocol and then used to infect WI-38, U2OS, and HeLa cells. Twenty-four hours after infection, cell lines were selected by puromycin (2 μg/mL) for 2 d before cell cycle analysis, replating for cell proliferation assays, or analyzing protein expression and complex formation.

Flow cytometry

To analyse DNA content by propidium iodide staining, WI-38, U2OS, or HeLa cells were fixed in 75% ethanol overnight at 4ºC, then washed once in 1X PBS + 1% fetal

bovine serum, and permeabilized for 30-45 mins at 37ºC in 1X PBS + 0.1 mg/mL RNAse A + 0.1% Triton X-100. The fixed and permeable cells were stained with 50 μg/mL propidium iodide for at least 90 mins at room temperature, shielded from light. Stained cells were analyzed at the UNC School of Medicine Flow Cytometry Facility on either a FACScan (Becton Dickinson) or CyAN (Dako Cytomation) flow cytometer, and data analyzed using Summit 4.3 software (Dako Cytomation).

Results

HIV-1 Vpr interacts in mammalian cells with VprBP.

VprBP was originally named for its initial identification as an HIV-1 Vpr binding protein (Zhao et al. 1994; Zhang et al. 2001). I further examined this interaction with the goal of ascertaining how Vpr's interaction with VprBP might be potentiating its cellular effects. The major phenotype of cells expressing Vpr is accumulation in the G2 phase of the cell cycle, in a manner requiring the ATR signaling pathway, followed subsequently by apoptosis. However, because silencing of VprBP leads to cell cycle arrest without the presence of Vpr—in particular, I have observed a lack of response to the mitotic inhibitor nocodazole in every cell line I have tested (Figure 3.3D and data not shown)—it is impossible by this method to examine whether loss of VprBP inhibits this function of Vpr (Le Rouzic et al. 2007).

However, Vpr has also been reported to target a specific cellular substrate, the uracil DNA glycosylase UNG2, for polyubiquitination and proteasome-dependent degradation, and Vpr co-purifies with overexpressed CUL4A (Schrofelbauer et al. 2005). These results led me to examine whether VprBP functioned to bridge Vpr and UNG2 to the CUL4A ubiquitin ligase machinery. I first confirmed the Vpr-VprBP interaction, and that the WD-40 domain of VprBP is sufficient for this interaction, by overexpressing both proteins in mammalian cell culture (Figure 4.1). These results are completely consistent with data published by another research group after I completed this series of

Figure 4.1

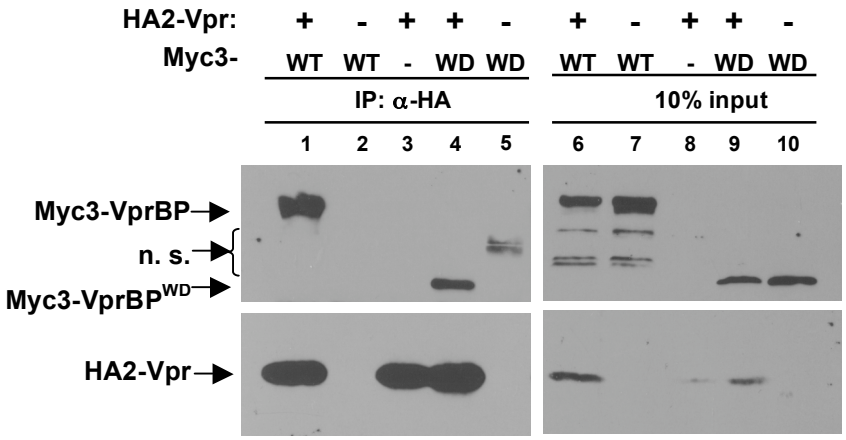

Figure 4.1. VprBP interacts with HIV-1 Vpr through its WD domain.

293T cells were transfected with plasmids expressing myc3-tagged VprBP (full-length or WD domain only) and HA2-tagged Vpr. 24 hours after transfection, cells were lysed in 0.1% NP-40 lysis buffer, immunoprecipitated with an anti-HA antibody, and Western blotted as indicated.

experiments (Le Rouzic et al. 2007). Further characterization within the WD domain of VprBP to determine the exact region of Vpr binding, as opposed to the DWD motif known to interact with DDB1, remains to be done.

UNG2 interacts with VprBP when Vpr is co-expressed.

I then examined UNG2's interaction with Vpr and VprBP by ectopically expressing Vpr and UNG2 in 293T cells. UNG2 only interacts with VprBP when Vpr is co-expressed, and this interaction is greatly stabilized by MG132 proteasome inhibition, as expected for a ubiquitin ligase substrate (Figure 4.2). Vpr's interaction with VprBP is not affected by co-expression of UNG2, suggesting that the complex is linked together by Vpr, but interestingly, in the presence of overexpressed UNG2, Vpr is significantly less stable, which may be due to its proteasomal degradation alongside its target (Figure 4.2).

Figure 4.2

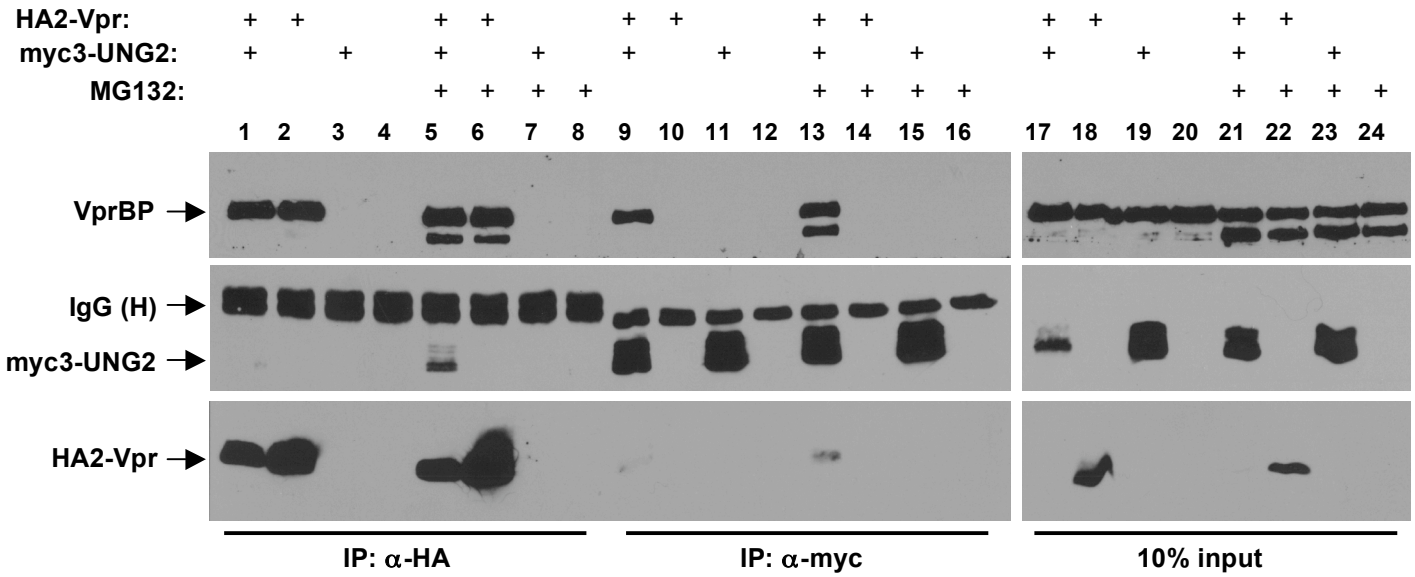
HA2-Vpr:
myc3-UNG2:
MG132:
1 2 3 4 5 6 7 8 9 10 11 12 13 14 15 16 17 18 19 20 21 22 23 24
VprBP
IgG (H)
myc3-UNG2
HA2-Vpr
IP: α-HA
IP: α-myc
10% input

Figure 4.2. Vpr expression is required for UNG2-VprBP interaction, which is stabilized by proteasome inhibition.

293T cells were co-transfected with plasmids expressing HA2-tagged Vpr and/or myc3-tagged UNG2. 24 hours after transfection, cells were lysed with 0.1% NP-40 lysis buffer and immunoprecipitated with anti-HA or anti-myc antibodies. After SDS-PAGE and transfer onto nitrocellulose membranes, the samples were Western blotted as indicated.

Endogenous UNG2 is not significantly stabilized by silencing of VprBP or DDB1.

To better understand the role that VprBP may play in UNG2 ubiquitination, I examined endogenous UNG2 stability in U2OS cells after silencing of VprBP and Vpr expression (Figure 4.3). Although I was unable to detect expression of Vpr, a retrovirus expressing Vpr produced strong G2 arrest (Figure 4.4), indicating that the protein was expressed. Vpr with arginine-90 mutated to lysine (R90K), which does not cause G2 arrest (Selig et al. 1997), reduces UNG levels somewhat less efficiently than wildtype, but because of an inability to detect the Vpr protein, I cannot conclude anything from this result. However, any stabilization of endogenous UNG2 after VprBP or DDB1 shRNA is minimal, which suggests two possibilities: either Vpr—not VprBP—is rate-limiting in this reaction, and whatever residual VprBP remaining after shRNA is sufficient to degrade UNG2; or, Vpr has additional transcriptional regulation activities that lower UNG2 expression. My data cannot distinguish between these two, but after I performed these experiments, Schrofelbauer and colleagues clearly demonstrated that, using plasmid-based expression of UNG2, DDB1 and CUL4A siRNA inhibited its degradation (Schrofelbauer et al. 2007). Their data are more consistent with additional regulation of endogenous UNG2, although this has yet to be demonstrated. Vpr with tryptophan-54 mutated to arginine (Vpr W54R) greatly reduces its interaction with UNG2 and does not promote its degradation (Schrofelbauer et al. 2005), but yet this mutant has complete interaction with VprBP, further suggesting that the interaction between Vpr and VprBP is not dependent upon association with their substrate UNG2 (Figure 4.5).

Figure 4.3

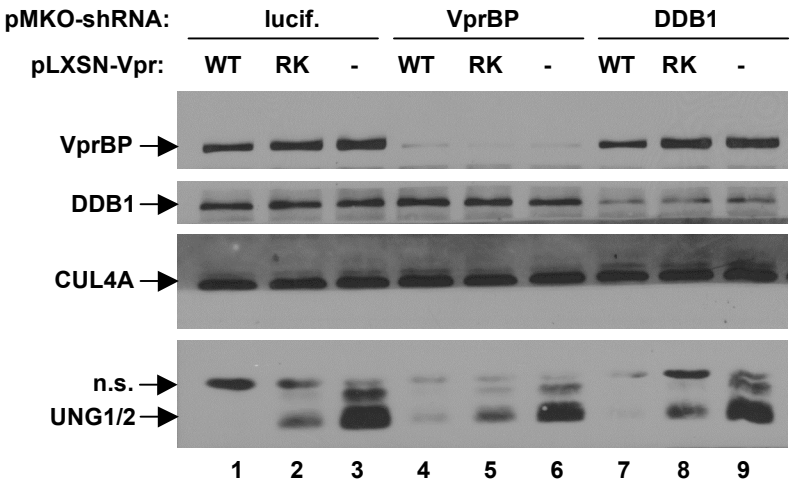

Figure 4.3. Vpr is capable of downregulating endogenous UNG after VprBP or DDB1 silencing.

U2OS cells were transduced with two retroviruses: one expressing shRNA to DDB1 or VprBP with puromycin resistance, and another expressing Vpr, either wildtype (WT) or R90K (RK). 24 hrs after transduction, the cells were selected with puromycin, and 48 hrs after selection, they were lysed in 0.1% NP-40 lysis buffer and Western blotted as indicated.

Figure 4.4

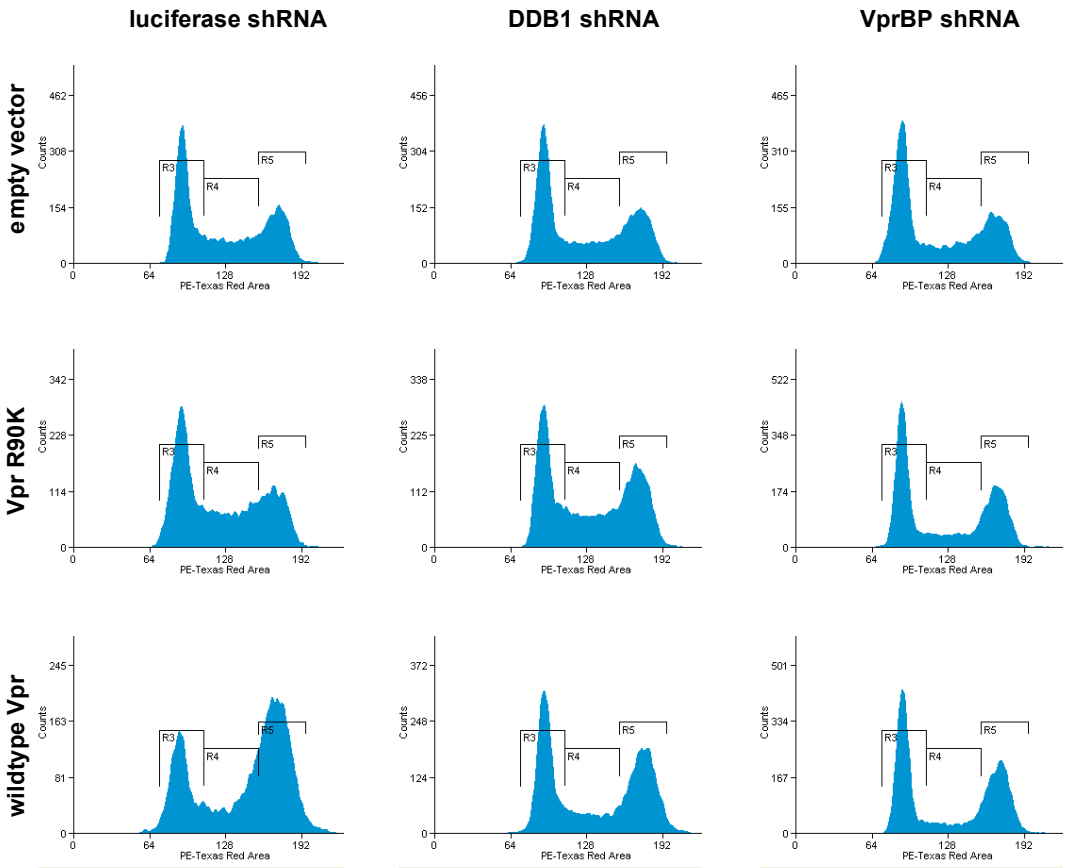

Figure 4.4. A Vpr-expressing retrovirus leads to G2 arrest, which is inhibited by VprBP shRNA.

U2OS cells were transduced with two retroviruses: one expressing shRNA to luciferase (as a negative control), DDB1, or VprBP with puromycin resistance, and another expressing Vpr, either wildtype (WT) or R90K (RK). 24 hrs after transduction, the cells were selected with puromycin, and 48 hrs after selection, they were trypsinized, fixed, and stained with propidium iodide. A flow cytometer was used to analyze the DNA content based upon propidium iodide levels.

Figure 4.5

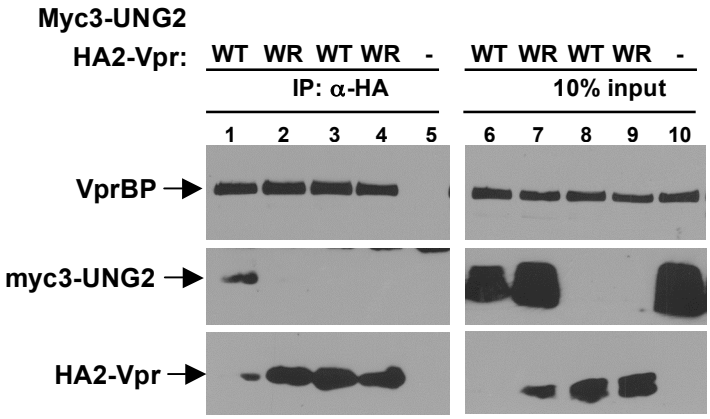

Figure 4.5. Vpr W54R interacts normally with VprBP but no longer binds UNG2.

293T cells were co-transfected with plasmids expressing HA2-tagged Vpr (wildtype or W54R mutant) and/or myc3-tagged UNG2. 24 hours after transfection, cells were lysed with 0.1% NP-40 lysis buffer and immunoprecipitated with anti-HA or anti-myc antibodies. After SDS-PAGE and transfer onto nitrocellulose membranes, the samples were Western blotted as indicated.

Discussion

The results presented in this chapter point toward future experiments to characterize how VprBP may mediate the cellular functions of HIV-1 Vpr. I have shown conclusively that VprBP does interact in mammalian cells with Vpr, and this interaction is required for the binding of VprBP and Vpr's cellular ubiquitination substrate, uracil DNA glycosylase. However, I have been unable to better characterize the functional consequences of VprBP-Vpr interactions.

While I was conducting my studies, two manuscripts have been published that both shed further light on this subject, and make future prospects for understanding this system more confusing. First, le Rouzic and colleagues examined the *in vivo* and *in vitro* interaction between Vpr and VprBP, and its consequences for the G2 cell cycle arrest that has been well-documented with Vpr expression (Le Rouzic et al. 2007). The authors clearly define, in accordance with my data, that Vpr and VprBP interact, through VprBP's WD-40 domain, and they also add yeast two-hybrid data to confirm the interaction. However, they also claim that silencing of VprBP prevents Vpr-dependent G2 arrest. As shown in this chapter, I generated very similar data, however, as described in Chapter 3, VprBP-silenced cells do not respond to G2 arrest by nocodazole, either. Therefore, the conclusions they reach based upon this data are not sound. Moreover, they demonstrate that a Vpr mutant that does not bind to VprBP also does not cause a G2 cell cycle arrest. However, as I demonstrate in this chapter, another Vpr mutant (R90K) that does not cause G2 cell cycle arrest readily interacts with VprBP. Therefore, the link between Vpr-VprBP interaction and G2 arrest is tenuous at best.

More importantly, Schrofelbauer and colleagues examined the link between Vpr and DDB1 (Schrofelbauer et al. 2007). They clearly demonstrate that Vpr interacts with DDB1 and VprBP, though they do not explore the VprBP link further. But, in a series of experiments, they showed clearly that Vpr disrupts DDB1-DDB2 interaction and DDB2-dependent nucleotide excision repair. Moreover, DDB1 and CUL4A are required for Vpr-dependent degradation of uracil DNA glycosylase UNG2. This is somewhat at odds with my data, where DDB1 and VprBP shRNA do not appreciably affect endogenous UNG2 degradation by Vpr, but their data is exclusively with ectopically-expressed UNG2 and SMUG. Perhaps there is another endogenous mechanism besides proteolytic degradation that downregulates UNG2 upon Vpr expression, which is eliminated by plasmid-based expression. Another possibility is that, due to the inefficient silencing of my DDB1 shRNA construct, that I missed this effect in my experiments, and VprBP is not required for the Vpr-DDB1 association. There is ample opportunity for future experiments along these lines. Finally, the authors speculate that, due to the known phenotype of G2 accumulation after DDB1 silencing or knockout, that perhaps DDB1 mediates Vpr's G2 arrest, but they provide no experimental evidence to support this speculation.

Future directions for this research include establishing whether VprBP is required for UNG2 degradation, by using the same system as Schrofelbauer et al, overexpressing UNG2 to eliminate any transcriptional downregulation upon Vpr expression. Furthermore, by better characterizing Vpr mutants, or perhaps VprBP point mutants that

do not interact with Vpr, it should be possible to determine whether VprBP is required for the G2 arrest and/or apoptosis produced by Vpr.

CHAPTER 5

CONCLUSIONS AND PERSPECTIVES

Over the past four years, my studies have been focused on elucidating the substrate-targeting mechanism of CUL4A. As shown in Chapter 2, I contributed to the discovery of a common motif found in many CUL4A/DDB1-interacting proteins, the "DWD box." With more than ninety proteins in the human genome containing this motif, there are many opportunities for future studies exploring the substrates targeted by any number of the heretofore-uncharacterized DWD proteins. I then took the most abundant of these DWD proteins found in the CUL4A immunocomplex, VprBP, and carefully characterized its binding with CUL4A/DDB1 and have begun to explore its cellular functions, shown in Chapter 3. VprBP also interacts with the HIV-1 accessory protein Vpr, hence its name, and I made preliminary investigations into the role that Vpr might play in recruiting a cellular substrate to CUL4A/DDB1, which I described in Chapter 4. In each of these chapters, I have discussed the future prospects for each, but taking them as a whole, and using them as a lens to examine the entire cullin field, in this final chapter I will examine some of the future prospects for studying this intriguing family of ubiquitin ligases.

VprBP as a substrate receptor for a protein (or proteins) involved in regulation of DNA replication

Because it contains a DWD box similar to that in other CUL4A/DDB1-interacting substrate receptors—DDB1, CSA, and Fbw5—the most obvious hypothesis for how VprBP functions in the CUL4A ligase is as another substrate receptor (Figure 5.1). If not a receptor itself, in a dimeric cullin complex VprBP may serve as a regulator of other DWD protein function, but as of yet, I cannot distinguish between these two possibilities

(receptor or regulator of other receptors). Examining the data I have accumulated over the past several years, what might be the targets of VprBP regulation? The major phenotype of VprBP loss is inhibition of DNA replication, yet I did not identify any proteins known to be involved in DNA replication or metabolism in a large-scale immunocomplex purification (Figure 3.1A). My laboratory will continue to explore this avenue to identify potential substrates, using advances in mass spectrometric technology since my initial screens. But, at this point, the only way I can propose substrates is through the biological functions I have identified for VprBP.

Chromatin fractionation shows that VprBP is associated with chromatin in asynchronous cells actively replicating DNA, but not in cells arrested by nocodazole in mitosis (Figure 3.7A, 3.7C). VprBP and CUL4A follow an almost identical pattern of chromatin association along the cell cycle, lowest in M and G1, and increasing through S into G2, which is consistent with VprBP functioning alongside CUL4A in regulation of DNA replication. However, VprBP silencing does not affect CUL4A or DDB1 chromatin localization, and its chromatin association is not affected by UV damage unlike CUL4A or DDB1, therefore it is unlikely to function in the regulation of UV-dependent CUL4A/DDB1 substrates (Figure 3.7C). These fractionation data are most consistent with a heretofore undefined, VprBP-dependent, role for CUL4A/DDB1 in regulation of DNA replication. This is also consonant with the inhibition of replication seen after VprBP silencing.

The chromatin fractionation data also help to narrow down where VprBP may be functioning in replication. In VprBP-silenced cells, MCM2-7 loading onto chromatin is normal; therefore, whatever substrates might be targeted for ubiquitination must act after the assembly of the pre-replication complex in G1. MCM2-7 loading requires the function of another CUL4A substrate, CDT1 (Nishitani et al. 2000), thus it is unlikely that VprBP acts on CDT1 as does another DWD protein, CDT2/L2DTL (Higa et al. 2006a). Thus, the decrease in CDT1 levels seen in two cell lines, both with and without functional p53 (Figure 3.11), is unlikely to be the cause of the VprBP S-phase arrest phenotype. VprBP's function occurs temporally after pre-replication complex formation (MCM2-7 loading), but it also must occur before actual elongation of replication forks. As shown in Table 3.1 and Figure 3.6, Dr. Paul Chastain has found no consistent change in the actual rate of fork progression in silenced cells. Once a fork is fired, therefore, it is unlikely that the mechanics of replication are adversely affected. Hence, the most likely candidates for regulation by VprBP are proteins involved in the steps between the loading of the pre-replication complex on origins of replication and actual replication of DNA by polymerases.

There are several potential CUL4A/DDB1/VprBP substrates that function in these initiatory steps in replication. First, Mcm10, which is recruited to chromatin after DNA origin licensing and is required for the assembly of factors required for replication (Cdc45 and pol α), is diubiquitinated in G1 and throughout S phase in budding yeast (Das-Bradoo et al. 2006). This diubiquitination is required for its binding to PCNA and functioning in DNA replication, yet it has not been studied in higher eukaryotes.

Figure 5.1

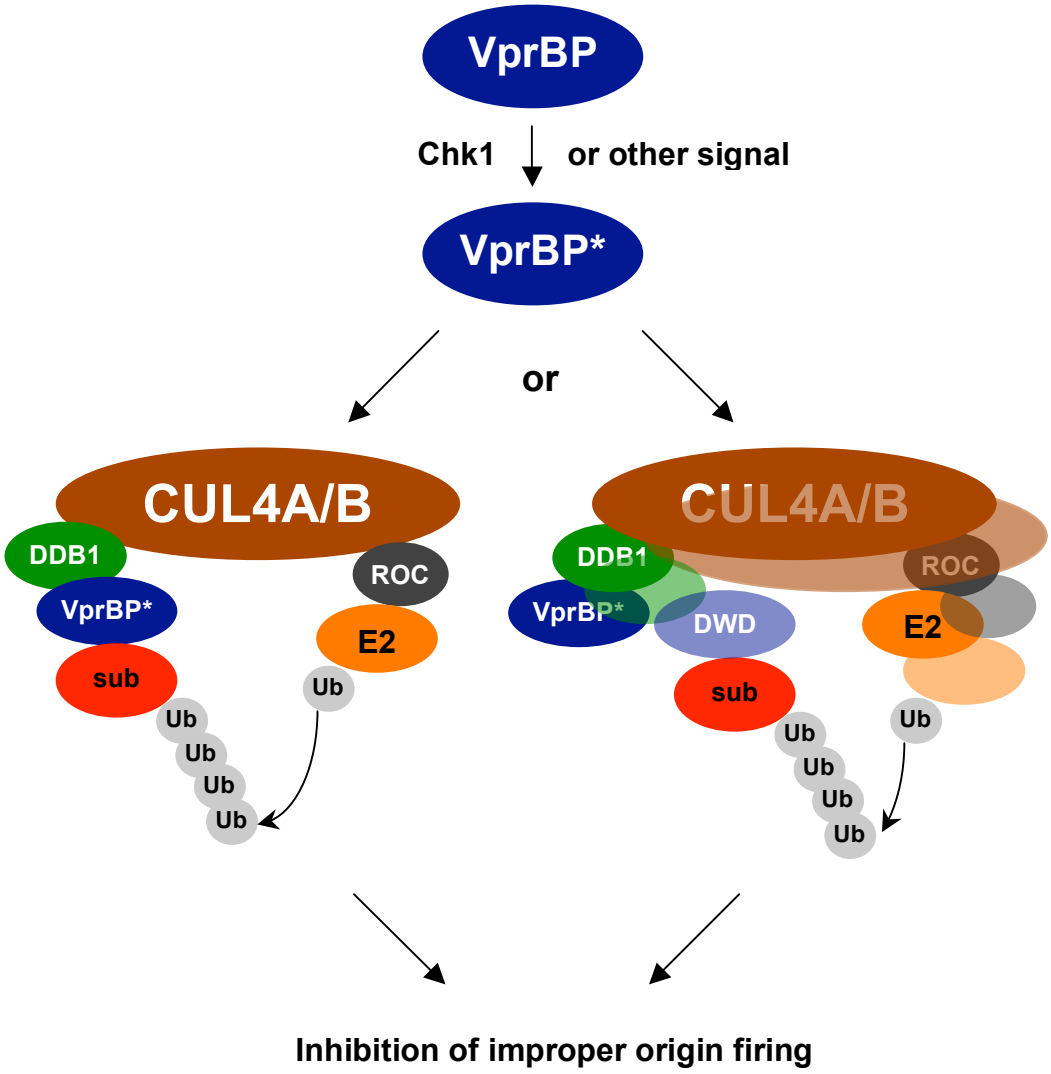

Figure 5.1. A model for VprBP function in the CUL4A/DDB1 ubiquitin ligase.

VprBP silencing results in decreased overall DNA synthesis in mid- and late S-phase, as measured by BrdU incorporation (Figure 3.5B), but a two to threefold increase in firing of new origins of replication (Figure 3.5E). One possible model is that VprBP acts to prevent improper origin firing in normal cells, either by targeting a heretofore unknown substrate for ubiquitination directly by the CUL4A/DDB1 ligase (left) or by regulating substrate ubiquitination in a targeted manner (right) in a dimeric cullin complex.

Perhaps VprBP is required for or modulates CUL4A-dependent ubiquitination of Mcm10? As discussed earlier in Chapter 3, the Cdc7 kinase, also required for initiation of replication at individual forks, is another potential target of VprBP function. The phenotype after Cdc7 silencing is similar to that of VprBP silencing in HeLa and in primary cells; however, that phenotype—a reduction in BrDU labeling and S-phase arrest—is not very specific and could just indicate a broad inhibition of DNA synthesis (Montagnoli et al. 2004). Cdc7 is not known to be regulated by ubiquitination, but its co-factor, Dbf4, is an APC substrate, therefore is a potential VprBP/CUL4A target (Ferreira et al. 2000). If VprBP were a negative regulator of a CUL4A-dependent degradation of Dbf4, then loss of Dbf4 would be expected in VprBP-silenced cells. This possibility remains to be tested. Cdc45 loading onto chromatin, which is required for polymerase loading and initiation of replication at forks throughout S phase, may also be disrupted (Bell and Dutta 2002). As antibodies are readily available for these potential substrates, they can be rapidly examined in the future.

In addition to the possibility that VprBP is disrupting initiation of replication at licensed forks, careful examination of VprBP-silenced BrDU incorporation and combing data suggests other possibilities: that VprBP might be involved in the regulation of timing of origin firing, recovery from naturally stalled forks throughout S phase, or progression through regions of chromatin that replicate slowly. I have consistently seen a decrease in overall BrDU incorporation per cell (Figure 3.5B, 3.5C), and the BrDU staining profile shows that cells with an early S-phase DNA content have almost normal incorporation, but BrdU staining per cell rapidly decreases with progression through DNA replication.

One explanation of this data is that VprBP is not required for initiation of replication at the beginning of S phase, but is required for ongoing maintenance of replication. Two possibilities for this function are the firing of forks that are initiated in the middle of S phase, or resumption of fork progression after stalling, which occurs naturally in all cells even without additional DNA damage.

Maintenance of normal S phase progression in eukaryotes requires the ATR/Chk1 pathway. In the same HeLa cell line as Dr. Chastain and I used to examine the S-phase phenotype of VprBP-silenced cells, Chk1 inhibition results in increased firing of new origins of replication, but decreased overall rate of fork progression (Petermann et al. 2006; Maya-Mendoza et al. 2007). Chk1 inhibition also results in the early firing of late origins of replication, indicating a loss of normal replication timing (Miao et al. 2003). Chk1-deficient cells also have decreased incorporation of BrDU per cell during S phase, similar to my findings (personal communication of Dr. Jean Cook). However, VprBP deficiency is not entirely analogous to Chk1 deficiency, as VprBP loss does not appreciably affect fork progression. A possible hypothesis is that VprBP is responsible for regulating, through targeting an unknown substrate for ubiquitination or regulating its CUL4A-dependent ubiquitination, the proper order of origin firing. One can imagine that, if far too many origins fire, which we see in the combing experiments (Figure 3.5E), that replication might fail due to disruption of the stoichiometry of replication factors, or collision of forks firing too near to each other, or any number of other possibilities. But, at this point, there is no obvious ubiquitination substrate to test; future experiments clarifying VprBP's role in replication, along with continuing efforts to identify VprBP-

associated proteins by immunopurification, will have to be done to further this line of research.

Substrate recruiting by CUL4A/DDB1-DWD and other CUL4A/DDB1 complexes

In addition to the numerous experiments needed to ascertain the exact role of VprBP in the cell, there are still several avenues of research open in the general field of CUL4-DDB1 biology. First and foremost, the DWD motif, which may not be all that is necessary for CUL4A/DDB1 binding, needs to be more carefully characterized, and a more systematic examination of the substrates targeted by these proteins might be possible (Angers et al. 2006; He et al. 2006; Higa et al. 2006b; Jin et al. 2006). This would be a major undertaking, and perhaps the most efficient use of the DWD proteins identified by us and other groups would be simply their identification, for use by other laboratories whose focus is on particular candidate substrates. As discussed in Chapter 2, another issue is the existence of DDB1-interacting substrate receptors, such as DET1/COP1 and the paramyxovirus SV5 V protein, which do not contain WD domains. The binding site of SV5 V, for example, compared with the DWD interacting surface, strongly suggests that multiple DDB1 binding pockets might be able to function in cullin substrate recruitment (Angers et al. 2006; Li et al. 2006). The large size and multiple domains of DDB1 at the very least makes its potential functioning in a cullin complex significantly more complicated than that of the small proteins which function as linkers for the other cullins.

Regulation of COP9/signalosome association with CUL4A/DDB1

Besides the problem of substrate recruitment and the identification of novel substrates, several lines of evidence suggest that CUL4A/DDB1 may be regulated at additional levels from the common regulatory machinery of all cullins. The original description of the CUL4A/DDB1/DDB2 and CUL4A/DDB1/CSA complexes in 2003 illustrated two unique features of these complexes: regulated association of the COP9 signalosome and regulated binding with chromatin (Groisman et al. 2003). The first observation, signalosome regulation, could potentially be a novel level of CUL4A/DDB1 regulation. In the case of DDB2, the authors showed that in the absence of UV treatment, there is a stable CUL4A/DDB1/DDB2/COP9 complex, and CUL4A is not Nedd8-modified. After UV treatment, this complex relocates to chromatin, the signalosome dissociates, and CUL4A becomes neddylated. Within 2 hours of treatment, the signalosome reassociates with the DDB2 complex on chromatin, which correlates with loss of neddylation of CUL4A. What contributes to this level of regulation—is it the association of DDB2 with its targets (histones H2B, H3, H4, and/or XPC) upon UV treatment, which leads to the dissociation of the signalosome, and then their subsequent ubiquitination and release, which allows its return? The CSA complex has different properties of chromatin association and signalosome regulation upon UV damage, which may reflect the differences in the functions of its substrate, CSB, in transcription-coupled repair. Future studies are necessary to examine what additional factors or post-translational modifications might be required for this unique regulation, and furthermore, whether other CUL4A/DDB1 substrate receptors/substrates exhibit similar properties.

Functional consequences of CUL4A/DDB1-DWD dimerization

As described earlier (Figure 2.5), I have accumulated some evidence showing that CUL4A forms dimeric complexes, both homodimers and heterodimers with CUL1. In addition, both VprBP and DDB2, two DWD proteins, are capable of interacting with other DWD proteins. These data, along with the large molecular weight size of CUL4A/DDB1 macromolecular complexes by gel filtration chromatography (Figure 2.1A), imply that CUL4A/DDB1 does not function as a single unit. But what role might this dimerization play in cullin function? Are oligomeric complexes more active as ligases? Evidence from E2 studies suggest that E2-E2 dimers are required for at least some instances of polyubiquitination (Li et al. 2007). CUL4A/DDB1 oligomers would have two molecules of the RING domain protein ROC1, therefore could promote the interaction of two E2 molecules as well. It should be possible to test this hypothesis experimentally: by mutational analysis, CUL4A and/or DDB1 mutants required for dimerization may be identified, and then examined to see what effect they have on *in vivo* or *in vitro* ubiquitination of substrates. The potential of hetero-dimerization with CUL1 adds another layer of complexity to CUL4A/DDB1 function, which could also be studied by mutagenesis, binding experiments, or the effects of CUL1 silencing on the ubiquitination and degradation of known CUL4A substrates.

Moreover, we have yet to examine carefully what role CUL4B may play in CUL4/DDB1 biology. As I discussed earlier, CUL4B loss, unlike that of CUL4A and DDB1, is not embryonic lethal but causes an X-linked mental retardation syndrome in

humans (Tarpey et al. 2007; Zou et al. 2007). However, it may play a role in the degradation of CUL4A/DDB1 substrates, like CDT1 (Hu et al. 2004). Since it clearly utilizes the same substrate-recruiting molecule, DDB1, several experiments might be designed to examine what role CUL4B is playing. First, its tissue, developmental, cell cycle, and/or subcellular localization specificity should be examined, since this could easily explain its lack of redundancy on an organismal level. Its binding properties also may be examined, particularly looking at the CUL4B immunocomplex to determine whether other factors interact with its unique 100 amino acid N-terminal extension. From an evolutionary perspective, since CUL4A and CUL4B diverged in vertebrates, as opposed to a single CUL4 in *Arabidopsis, Drosophila*, *C. elegans*, and *S. pombe*, it is logical that CUL4B might play some higher developmental role, such as is apparent in the nervous system, as opposed to the pervasive and essential role of CUL4A in mammals and CUL4 in other organisms.

Regulation of all cullins by CAND1 and ROC selectivity

In addition to the remaining questions about the regulation and function of CUL4A/B, not all is known about the general properties of the cullin ligases. CAND1, the negative regulator of cullins identified in our lab and others, remains incompletely characterized (Liu et al. 2002; Zheng et al. 2002a; Oshikawa et al. 2003). While we know that CAND1 must be dissociated from cullins in order for substrate receptors to bind, how this occurs is a mystery. CAND1 binding to CUL1 obscures binding sites to both SKP1 and Ubc12, the Nedd8 E2, while Nedd8 modification of cullins inhibits

CAND1 binding (Liu et al. 2002; Goldenberg et al. 2004). However, more recent studies have shown that, in an unknown manner, SKP1 complexed with an F-box protein, SKP2, is able to prompt the dissociation of CAND1 from CUL1, but SKP1 alone is unable to do so (Bornstein et al. 2006). The physical mechanism by which this occurs—for example, whether the F-box protein increases SKP1 affinity for CUL1 to a sufficient extent to compete off CAND1—has yet to be determined.

Another aspect of the "cullin cycle"—the deneddylation of cullins after substrate recruitment and degradation, allowing the rebinding of CAND1 and resumption of an inhibited state, is also incompletely understood. Deneddylation, catalyzed by the COP9/signalosome, must also be tightly regulated. Recently, Bornstein et al found that *in vitro*, addition of the substrate $p27^{Kip1}$ to a CUL1-SKP1-SKP2 complex prevented signalosome-dependent deneddylation under conditions where CUL1-SKP1-SKP2 was accessible for deneddylation (Bornstein et al. 2006). They propose that substrate addition causes a conformational change in the cullin, leading to inhibition of signalosome association. The actual location of COP9/signalosome binding to the cullins has never been conclusively ascertained, however. Studies in budding yeast and in our lab have shown that mutation of two conserved residues, R473 and L474 in human CUL1, leads to hyperneddylation and inhibition of CAND1 association (Lammer et al. 1998; Patton et al. 1998; Liu et al. 2002). Unpublished data from Jidong Liu in our laboratory shows that these residues are required for signalosome association. Whether this is because these residues are required for physical interaction, or whether their mutation leads to a change in CUL1 conformation, has not been established. These unanswered questions make it

clear that the "cullin cycle," while we understand it roughly, is much more complex than our initial characterization revealed.

A final poorly understood area of cullin biology is the presence of multiple ROC/Rbx RING finger proteins. In studies in our laboratory of cullin function, we have treated them as essentially interchangeable, but recent reports have called that into question. In *Drosophila*, there are three ROC proteins: Roc1a, Roc1b, and Roc2. When mutated, these have differing effects on *Drosophila* development, and they have markedly different patters of cullin binding: CUL-1 and CUL-2 preferentially bound to Roc1a, CUL-3 to Roc1b, and CUL-5 to Roc2 (Donaldson et al. 2004). What significance this has for cullin biology in higher eukaryotes has yet to be investigated. Humans have two ROCs, ROC1 and ROC2, but evidence for their differing function is less clear. ROC2 was first identified as "SAG"—"sensitive to apoptosis gene," and its silencing reduces the CUL1-dependent degradation of substrates pro-caspase-3 and c-Jun (Tan et al. 2006; Gu et al. 2007). ROC2's global effects on cullin function have yet to be examined—does it form a heterodimer with ROC1, promoting ubiquitination with certain cullin and at different catalytic rates than, for example, ROC1/ROC1 homodimers? The *Drosophila* evidence strongly suggests that the ROCs are no more than partially redundant; therefore, this is another fertile area for future research.

Summary

In summary, while the general mechanism of ubiquitination and proteasomal degradation is fairly well understood, there are many avenues of investigation remaining. My research into the function of VprBP shows that the investigation of individual substrate receptors and/or regulators of cullin ligase activity will proceed as these receptors are identified and linked with particular cellular pathways. We have only scratched the surface in the characterization of cullin ubiquitination substrates. The number of DWD box, F-box, SOCS- and VHL-box, and BTB proteins in the human genome approaches a thousand in total, therefore we will likely continue to identify novel substrates for years to come. Systematic approaches for identifying substrates have been singularly unproductive, but labs studying individual pathways will certainly discover links to proteins containing one of these motifs. Improvements in mass spectrometric technology combined with a better understanding of methods of inhibiting ubiquitination and degradation may allow us to systematically identify substrates one day, but a candidate gene approach is currently the most efficient.

On the other end from substrate identification, I have discussed several areas of general cullin mechanism that, while broadly understood, are not well characterized on a mechanistic level. How CAND1 and COP9/signalosome association are regulated, and how different RING finger proteins may play essential roles in cullin function, have not thoroughly been examined. These mechanistic studies may not allow for major new insights into cullin function, but understanding cullin biology on a molecular level may

allow for better design of pharmacological inhibitors, which are of potentially great benefit to medicine.

In the end, the cullin family may become a very interesting target for molecular medicine. We know that CUL4A is overexpressed in many breast, liver, and other cancers (Chen et al. 1998b; Yasui et al. 2002), but why increased ubiquitination of CUL4A substrates would promote carcinogenesis is unclear. Perhaps disruption of DNA repair and metabolism would create increased genomic instability, which is a known hallmark of increasing malignancy in cancer. Other cullins also have substrates that are of therapeutic potential: CUL1 degrades multiple cell cycle regulators; disrupting the cell cycle by its inhibition might be of general use as a cancer therapy; and, the CUL2 target HIF1α, which promotes response to hypoxia by driving vascular development and metabolic changes, is essential for tumor growth and blood supply. As we better understand cullin biology, we will be in a better position to take this knowledge to the clinical bedside by developing therapeutics, which might be effective against cancer and other diseases.

APPENDICES

APPENDIX 1: DWD-BOX PROTEINS IN DIFFERENT SPECIES

1.1. *Homo sapiens* DWD box proteins.

Red = confirmed by immunoprecipitation with CUL4A/DDB1; Black = putative

```
A16L1_HUMAN:   (0399) LRHTLTGHSGKVLSAKFLLDNARIVSGSHDRTLKLWDLRSKVCI  Autophagy-related protein 16-1
DDB2_HUMAN:    (0234) LWNLRMHKKKVTHVALNPCCDWFLATASVDQTVKIWDLRQVRGK  DNA damage-binding protein 2
ERCC8_HUMAN:   (0178) SHILQGHRQEILAVSWSPRYDYILATASADSRVKLWDVRRASGC  DNA excision repair protein ERCC-8
FBXW8_HUMAN:   (0464) GNIALSLSAHQLRVSAVQMDDWKIVSGGETGLVSVWDYRMNQKL  F-box/WD-repeat protein 8
GBB2_HUMAN:    (0174) QTVGFAGHSGDVMSLSLAPDGRTFVSGACDASIKLWDVRDSMCR  Guanine nucleotide-binding protein beta subunit 2
Q59ET5_HUMAN:  (0325) RAHRAYTPNDECFFIFLDVSRDFVASGAEDRHCYIWDRHYNICL  F-box and WD-40 domain protein 5
Q5VYB6_HUMAN:  (0270) ILSLTGDRVPLHCVDRHPNQQHVVATGCQDGMLSIWDVRQGTMP  Nucleoporin 43kDa
Q9NZJ0_HUMAN:  (0207) GLAPSVDFQQSVTVVLFQDENTLVSAGAVDGILKVWDLRKNYTA  L2DTL protein
RBBP4_HUMAN:   (0264) SHSVDAHTAEVNCLSFNPYSEFILATGSADKTVALWDLRNLKLK  Histone-binding protein RBBP4
RBBP7_HUMAN:   (0264) SHLVDAHTAEVNCLSFNPYSEFILATGSADKTVALWDLRNLKLK  Histone-binding protein RBBP7
WDR23_HUMAN:   (0406) PVGALAGHQDGITFIDSKGDARYLISNSKDQTIKLWDIRRFSSRE WD-repeat protein 23
WSB1_HUMAN:    (0162) LLNLVDHTEVVRDLTFAPDGSLILVSASRDKTLRVWDLKDDGNM  WD repeat and SOCS box-containing protein 1
WSB2_HUMAN:    (0189) QIQVLSGHLQWVYCCSISPDCSMLCSAAGEKSVFLWSMRSYTLI  WD repeat and Socs Box-containing protein 2
GRWD1_HUMAN:   (0253) QRPFVGHTRSVEDLQWSPTENTVFASCSADASIRIWDIRAAPSK  Glutamate-rich WD repeat-containing protein 1
KTNB1_HUMAN:   (0096) ILRTLMGHKANICSLDFHPYGEFVASGSQDMNIKLWDIRRKGCV  Katanin p80 WD40-containing subunit B1
PWP1_HUMAN:    (0292) AASLAVHTDKVQTLQFHPFEAQTLISGSYDKSVALYDCRSPDES  Periodic tryptophan protein 1 homolog
FBXW1_HUMAN:   (0000) LQRIHCRSETSKGVYCLQYDDQKIVSGLRDNTIKIWD-KNTLEC  F-box/WD-repeat protein 1A
ARC1A_HUMAN:   (0319) ETLHQNSITQVSIYEVDKQDCRKFCTTGIDGAMTIWDFKTLESS  Actin-related protein 2/3 complex subunit 1A
ARC1B_HUMAN:   (0320) DSLHKNSVSQISVLSGGKAKCSQFCTTGMDGGMSIWDVKSLESA  Actin-related protein 2/3 complex subunit 1B
COPA_HUMAN:    (0042) LIDKFDEHDGPVRGIDFHKQQPLFVSGGDDYKIKVWNYKLRRCL  Coatomer subunit alpha
DYI4_HUMAN:    (0256) TIESSHRDPVYGTIWLQSKTGTECFSASTDGQVMWWDIRKMSEP  Dynein intermediate chain 2, axonemal
EMAL4_HUMAN:   (0500) ISKQIKAHDGSVFTLCQMRNGMLLTGGGKDRKIILWD-HDLNPER Echinoderm microtubule-associated protein-like 4
FBXW7_HUMAN:   (0613) LQTLQGPNKHQSAVTCLQFNKNFVITSSDDGTVKLWDLKTGEFI  F-box/WD-repeat protein 7
FBXW9_HUMAN:   (0154) YFCLAEGHVASVDSVLLLQGGSLCLSGSRDRNVNLWDLRQLGTE  F-box/WD-repeat protein 9
GBB1_HUMAN:    (0174) QTTTFTGHTGDVMSLSLAPDTRLFVSGACDASAKLWDVREGMCR  Guanine nucleotide-binding protein beta subunit 1
GBB3_HUMAN:    (0175) QKTVFVGHTGDCMSLAVSPDFNLFISGACDASAKLWDVREGTCR  Guanine nucleotide-binding protein beta subunit 3
GBB4_HUMAN:    (0174) QTTTFTGHSGDVMSLSLSPDMRTFVSGACDASSKLWDIRDGMCR  Guanine nucleotide-binding protein beta subunit 4
GBB5_HUMAN:    (0230) QSFHGHGADVLCLDLAPSETGNTFVSGGCDKKAMVWDMRSGQCV  Guanine nucleotide-binding protein beta subunit 5
LIS1_HUMAN:    (0370) CMKTLNAHEHFVTSLDFHKTAPYVVTGSVDQTVKVWECR-----  Platelet-activating factor acetylhydrolase IB alpha subunit
NLE1_HUMAN:    (0404) YLASLRGHVAAVYQIAWSADSRLLVSGSSDSTLKVWDVKAQKLA  Notchless homolog 1
PK1IP_HUMAN:   (0031) LVADFTHHAHTASLSAVAVNSRFVVTGSKDETIHIYDMKKKIEH  p21-activated protein kinase-interacting protein 1
PRP19_HUMAN:   (0341) TKVTDETSGCSLTCAQFHPDGLIFGTGTMDSQIKIWDLKERTNV  Pre-mRNA-splicing factor 19
Q3MII9_HUMAN:  (0489) KYIMCGSDEMNIRLWKANASEKLGVLTSREKAAKDYNQKLKEKF  WD repeats and SOF1 domain containing
Q4G115_HUMAN:  (0113) TIESSHRDPVYGTIWLQSKTGTECFSASTDGQVMWWDIRKMSEP  DNAI2 protein
Q59GA8_HUMAN:  (0189) HIQTLEGHHQEIWCLAVSPSGDYVVSSSHDKSLRLWE-RTREPLI WD repeat-containing protein 3
Q59GD6_HUMAN:  (0307) TQAQPPGPGRELTHCTLAHTAGVVLTATADHNLLLYEARSLRLQ  Transducin beta-like 3
Q5JTN6_HUMAN:  (0012) RVKFFGQHGGEVNSSAFSPDGQMLLTGSEDGCVYGWETRSGQLL  OTTHUMP00000022116
Q5VTH9_HUMAN:  (0738) PSLSFYPATSVVYDVAWSPKSSYIFAAANENRVEIWDLHISTLD  Novel protein
Q5VU06_HUMAN:  (0126) IHMFGDHTNRVKRIATAPMWPNTFWSAAEDGLIRQYDLRENSKH  Novel protein
Q6FGN1_HUMAN:  (0190) RIVIPAHQAEILSCDWCKYNENLLVTGAVDCSLRGWDLRNVRQP  PEX7 protein
Q6JZZ5_HUMAN:  (0159) LSSYRAHAAQVTCVAASPHKDSVFLSCSEDNRILLWDTRCPKPA  Androgen receptor cofactor p44
```

```
Q6NZ53_HUMAN:  (0091) ENNYRGHGDSVDQLCWHPSNPDLFVTASGDKTIRIWDVRTTKCI  THOC3 protein
Q6PJI9_HUMAN:  (0014) VEYLAAHLSKIHGLDWHPDSEHILATSSQDNSVKFWDYRQPRKY  WDR59 protein
Q6UXN9_HUMAN:  (0098) YIRYFPGHSKRVVALSMSPVDDTFISGSLDKTIRLWDLRSPNCQ  WD40 protein
Q6ZQQ6_HUMAN:  (0558) FIETLPLHLCAITSFDVCLSLSLFVTGSADGSVRIWDFHGRLIA  CDNA FLJ46270 fis, clone TESTI4028042.
Q86TI4_HUMAN:  (0491) GELRRVFRGHTFIINCIQVHGQVLYTASHDGALRLWDVRGLRGA  LOC349136 protein
Q86XD6_HUMAN:  (0087) VHSLIGHRRTPWCVTFHPTISGLIASGCLDGEVRIWDLHGGSES  Hypothetical protein FLJ20294
Q86YQ0_HUMAN:  (0516) GHKEIINAIDGIGGLGIGEGAPEIVTGSRDGTVKVWDPRQKDDP  HZGJ
Q8IW98_HUMAN:  (0186) RAELQGHLGPVTAVEFCPWRAGTLISASEDRGFKVWD-HCTGSLI MGC43690 protein
Q8TBB7_HUMAN:  (0134) TLDVFAHEDAVYGLSVSPVNDNIFASSSDDGRVLIWDIRESPHG  WDR22 protein
Q8TBY9_HUMAN:  (0442) TEKTFNKLVGKFSQSIFHLNLTQILSATMEGKLVVWDIHRPPSS  WD repeat domain 66
Q8TCI4_HUMAN:  (0058) LRHTLTGHSGKVLSAKFLLDNARIVSGSHDRTLKLWDLRSKVCI  Hypothetical protein FLJ23854
Q9BRX9_HUMAN:  (0100) VVRKFRGHAGKVNTVQFNEEATVILSGSIDSSIRCWDCRSRRPE  Mitogen-activated protein kinase organizer 1
Q9BSW6_HUMAN:  (0183) VEYLAAHLSKIHGLDWHPDSEHILATSSQDNSVKFWDYRQPRKY  WDR59 protein
Q9BTV9_HUMAN:  (0159) FTRVLRGHTDYIHCLALRERSPEVLSGGEDGAVRLWDLRTAKEV  THO complex subunit 6 homolog
Q9BU59_HUMAN:  (0340) TLKEFRGHSSFVNEATFTQDGHYIISASSDGTVKIWNMKTTECS  Smu-1 suppressor of mec-8 and unc-52 homolog
Q9BWV9_HUMAN:  (0409) FIETLPLHLCAITSFDVCLSLSLFVTGSADGSVRIWDFHGRLIA  NYD-SP11
Q9C0C7_HUMAN:  (0093) VHSLIGHRRTPWCVTFHPTISGLIASGCLDGEVRIWDLHGGSES  KIAA1736 protein
Q9NUL4_HUMAN:  (0074) YEKTLYGHNLEISDVAWSSDSSRLVSASDDKTLKLWDVRSGKCL  CDNA FLJ11287 fis, clone PLACE1009596
Q9NXE7_HUMAN:  (0087) VHSLIGHRRTPWCVTFHPTISGLIASGCLDGEVRIWDLHGGSES  Hypothetical protein FLJ20294
Q9UFJ8_HUMAN:  (0178) CVHSYCEHGGFVTYVDFHPSGTCIAAAGMDNTVKVWDVRTHRLL  WD-repeat protein 51A
Q9UG25_HUMAN:  (0162) LLNLVDHTGVVRDLTFAPDGSLILVSASRDKTLRVWDLRDDGNM  Hypothetical protein DKFZp564A122
RAE1L_HUMAN:   (0264) TNTSAPQDIYAVNGIAFHPVHGTLATVGSDGRFSFWD-KDARTKL mRNA-associated protein mrnp 41
RFWD2_HUMAN:   (0547) SVASIEAKANVCCVKFSPSSRYHLAFGCADHCVHYYDLRNTKQP  Ring finger and WD repeat domain protein 2
RPTOR_HUMAN:   (1157) VQDIPTGADSCVTSLSCDSHRSLIVAGLGDGSIRVYDRRMALSE  Regulatory associated protein of mTOR
SCAP_HUMAN:    (1148) GSRVSHVFAHRGDVTSLTCTTSCVISSGLDDLISIWDRSTGIKF  Sterol regulatory element-binding protein cleavage-activating
protein
SPG16_HUMAN:   (0469) CRCTLYGHTDSVNSIEFFPFSNTLLTSSADKTLSIWDARTGICE  Sperm-associated antigen 16 protein
STB5L_HUMAN:   (0102) DCYCQHESGAAVLQLQFLINEGALVSASSDDTLHLWNLRQKRPA  Syntaxin-binding protein 5-like
STRN4_HUMAN:   (0392) GGGEVSLGDLADLTVTNDNDLSCDLSDSKDAFKKTWNPKFTLRS  Striatin-4
TAF5L_HUMAN:   (0501) LYKELRGHTDNITSLTFSPDSGLIASASMDNSVRVWDIRNTYCS  TAF5-like RNA polymerase II p300/CBP-associated factor 65 kDa
subunit 5L
TBL1R_HUMAN:   (0257) LASTLGQHKGPIFALKWNKKGNFILSAGVDKTTIIWDAHTGEAK  F-box-like/WD-repeat protein TBL1XR1
TBL1X_HUMAN:   (0269) LASTLGQHKGPIFALKWNRKGNYILSAGVDKTTIIWDAHTGEAK  F-box-like/WD-repeat protein TBL1X
TBL1Y_HUMAN:   (0267) LASTLGQHKGPIFALKWNKKGNYVLSAGVDKTTIIWDAHTGEAK  F-box-like/WD-repeat protein TBL1Y
TBL3_HUMAN:    (0169) TQAQPPGPGQELTHCTLAHTAGVVLTATADHNLLLYEARSLRLQ  WD-repeat protein SAZD
TEP1_HUMAN:    (2052) CGTELRGHEGPVSCCSFSTDGGSLATGGRDRSLLCWDVRTPKTP  Telomerase protein component 1
TF3C2_HUMAN:   (0605) FQCFLAHDQAVRTLQWCKANSHFLVSAGSDRKIKFWDLRRPYEP  General transcription factor 3C polypeptide 2
THOC3_HUMAN:   (0091) ENNYRGHGDSVDQLCWHPSNPDLFVTASGDKTIRIWDVRTTKCI  THO complex subunit 3
TSSC1_HUMAN:   (0176) ASLEGKGQLKFTSGRWSPHHNCTQVATANDTTLRGWDTRSMSQI  Protein TSSC1
WD51B_HUMAN:   (0177) CVNNFSDSVGFANFVDFNPSGTCIASAGSDQTVKVWDVRVNKLL  WD-repeat protein 51B
WDR12_HUMAN:   (0334) SLSLTSHTGWVTSVKWSPTHEQQLISGSLDNIVKLWDTRSCKAP  WD-repeat protein 12
WDR22_HUMAN:   (0134) TLDVFAHEDAVYGLSVSPVNDNIFASSSDDGRVLIWDIRESPHG  WD-repeat protein 22
WDR31_HUMAN:   (0052) AFQEYSPAHMDTVSVVAALNSDLCVSGGKDKTVVAYNWKTGNVV  WD-repeat protein 31
WDR37_HUMAN:   (0314) LVHSLTGHDQELTHCCTHPTQRLVVTSSRDTTFRLWDFRDPSIH  WD-repeat protein 37
WDR3_HUMAN:    (0666) HIQTLEGHHQEIWCLAVSPSGDYVVSSSHDKSLRLWE-RTREPLI WD-repeat protein 3
WDR47_HUMAN:   (0745) QGLHALSGHTGHILALYTWSGWMIASGSQDKTVRFWDLRVPSCV  WD-repeat protein 47
WDR48_HUMAN:   (0066) YIASMEHHTDWVNDIVLCCNGKTLISASSDTTVKVWNAHKGFCM  WD-repeat protein 48
```

```
WDR4_HUMAN:    (0180) ESFCLGHTEFVSRISVVPTQPGLLLSSSGDGTLRLWEYRSGRQL  WD-repeat protein 4
WDR57_HUMAN:   (0143) VKRLKGHTSFVNSCYPARRGPQLVCTGSDDGTVKLWDIRKKAAI  WD-repeat protein 57
WDR5_HUMAN:    (0120) CLKTLKGHSNYVFCCNFNPQSNLIVSGSFDESVRIWDVKTGKCL  WD-repeat protein 5
```

1.2. *Mus musculus* DWD-box proteins.

```
A16L1_MOUSE:   (0399) LRHTLTGHSGKVLSAKFLLDNARIVSGSHDRTLKLWDLRSKVCI  Autophagy-related protein 16-1
APAF_MOUSE:    (0873) KVADCRGHLSWVHGVMFSPDGSSFLTASDDQTIRVWETKKVCKN  Apoptotic protease-activating factor 1
ARC1A_MOUSE:   (0319) ETLHQNSITQVSIYEVDKQDCRKFCTTGIDGAMTIWDFKTLESS  Actin-related protein 2/3 complex subunit 1A
ARC1B_MOUSE:   (0320) DSLHKNSVSQISVLSGGKAKCSQFCTTGMDGGMSIWDVKSLESA  Actin-related protein 2/3 complex subunit 1B
DDB2_MOUSE:    (0234) LWNLRMHKKKVAHVALNPCCDWLLATASIDQTVKIWDLRQIKGK  DNA damage-binding protein 2
ERCC8_MOUSE:   (0178) SHILQGHRQEILAVSWSPRHDYILATASADSRVKLWDVRRASGC  DNA excision repair protein ERCC-8
FBXW5_MOUSE:   (0463) RAHRAYTPNDECFFIFLDVSRDFVASGAEDRHGYIWDRHYNICL  F-box/WD repeat protein 5
FBXW7_MOUSE:   (0535) LQTLQGPSKHQSAVTCLQFNKNFVITSSDDGTVKLWDLKTGEFI  F-box/WD repeat protein 7
FBXW8_MOUSE:   (0464) DKIALSLSAHQLGVSAVQMDDWKVVSGGEEGLVSVWDYRMNQKL  F-box/WD repeat protein 8
GBB1_MOUSE:    (0174) QTTTFTGHTGDVMSLSLAPDTRLFVSGACDASAKLWDVREGMCR  Guanine nucleotide-binding protein G(I)/G(S)/G(T) subunit beta 1
GBB2_MOUSE:    (0174) QTVGFAGHSGDVMSLSLAPDGRTFVSGACDASIKLWDVRDSMCR  Guanine nucleotide-binding protein G(I)/G(S)/G(T) subunit beta 2
GBB3_MOUSE:    (0175) QKTVFVGHTGDCMSLAVSPDYKLFISGACDASAKLWDVREGTCR  Guanine nucleotide-binding protein G(I)/G(S)/G(T) subunit beta 3
GBB4_MOUSE:    (0174) QTTTFTGHSGDVMSLSLSPDLKTFVSGACDASSKLWDIRDGMCR  Guanine nucleotide-binding protein subunit beta 4
GBB5_MOUSE:    (0230) QSFHGHGADVLCLDLAPSETGNTFVSGGCDKKAMVWDMRSGQCV  Guanine nucleotide-binding protein subunit beta 5
GRWD1_MOUSE:   (0299) MLTTATAHDGDVNVISWSRREPFLLSGGDDGALKVWDLRQFKSG  Glutamate-rich WD repeat-containing protein 1
KTNB1_MOUSE:   (0096) ILRTLMGHKANICSLDFHPYGEFVASGSQDTNIKLWDIRRKGCV  Katanin p80 WD40-containing subunit B1
LIS1_MOUSE:    (0370) CMKTLNAHEHFVTSLDFHKTAPYVVTGSVDQTVKVWECR-----  Platelet-activating factor acetylhydrolase IB subunit alpha
MEP50_MOUSE:   (0159) LNSYRAHAGQVTCVAASPHKDSVFLSCSEDSRILLWDTRCPKPA  Methylosome protein 50
NLE1_MOUSE:    (0362) PLARMTGHQALINQVLFSPDSRIVASASFDKSIKLWDGRTGKYL  Notchless homolog 1
NUP43_MOUSE:   (0209) ILSLTGDRVPLHCVDRHPDQQHVVATGGQDGMLSIWDVRQGTMP  Nucleoporin Nup43
PEX7_MOUSE:    (0185) RIVIPAHQTEILSCDWCKYNENLVVTGAVDCSLRGWDLRNVRQP  Peroxisomal targeting signal 2 receptor
PK1IP_MOUSE:   (0031) PVADFTHHSHTASLSVLASNSRYVVSGSKDETIHIYDMKRKVEH  p21-activated protein kinase-interacting protein 1
PLRG1_MOUSE:   (0402) GFIQNLSGHNAIINTLAVNADGVLVSGADNGTMHLWDWRTGYNF  Pleiotropic regulator 1
PRP19_MOUSE:   (0341) TKVTDETSGCSLTCAQFHPDGLIFGTGTMDSQIKIWDLKERTNV  Pre-mRNA-splicing factor 19
Q499G0_MOUSE:  (0177) CVNNFSDSVGFANFVDFNPNGTCIASAGSDHAVKIWDIRMNKLL  Hypothetical protein
Q4ADG5_MOUSE:  (0360) TKVTDETSGCSLTCAQFHPDGLIFGTGTMDSQIKIWDLKERTNV  Prp19 beta protein
Q54AE3_MOUSE:  (0175) QKTVFVGHTGDCMSLAVSPDYKLFISGACDASAKLWDVREGTCR  GTP-binding protein beta3 subunit
Q5DU30_MOUSE:  (0875) KVADCRGHLSWVHGVMFSPDGSSFLTASDDQTIRVWETKKVCKN  MKIAA0413 protein
Q5PPQ7_MOUSE:  (0212) EKAHEGARPMRAIFLADGNVFTTGFSRMSERQLALWNPKNMQEP  Coronin, actin binding protein 1C
Q5QNT7_MOUSE:  (0363) PLARMTGHQALINQVLFSPDSRIVASASFDKSIKLWDGRTGKYL  Novel WD40 repeat containing protein
Q5SW18_MOUSE:  (0371) CMKTLNAHEHFVTSLDFHKTAPYVVTGSVDQTVKVWECR-----  Platelet-activating factor acetylhydrolase, iso 1b, beta1 subunit
Q5XKB2_MOUSE:  (2060) CCAELRGHEGPVCCCSFSPDGGILATAGRDRNLLCWDMKIAQAP  Telomerase associated protein 1
Q69Z65_MOUSE:  (0212) VEYLAAHLSKIHGLDWHPDSEHIFATSSQDNSVKFWDYRQPRKY  MKIAA1923 protein
Q6A0A6_MOUSE:  (1147) GSRVSQTFAHRGDVTSLTCTASCVISSGLDDFISIWDRSTGIKL  MKIAA0199 protein
Q6GQT6_MOUSE:  (1146) GSRVSQTFAHRGDVTSLTCTASCVISSGLDDFISIWDRSTGIKL  SREBP cleavage activating protein
Q6NZK7_MOUSE:  (0183) VEYLAAHLSKIHGLDWHPDSEHIFATSSQDNSVKFWDYRQPRKY  Wdr59 protein
Q6PAN1_MOUSE:  (0072) GLAPAVDSQQSVTVVLFQDENTLVSAGAVDGIIKVWDLRKNYTA  2810047L02Rik protein
Q6ZPU3_MOUSE:  (0195) VQDIPTGADSCVTSLSCDSHRSLIVAGLGDGSIRVYDRRMALSE  MKIAA1303 protein
Q7TQK6_MOUSE:  (0087) VHSLIGHRRTPWCVTFHPTISGLIASGCLDGEVRIWDLHGGSES  Hypothetical protein D030051N19Rik
Q80UI6_MOUSE:  (0416) GSRVSQTFAHRGDVTSLTCTASCVISSGLDDFISIWDRSTGIKL  Scap protein
Q80VY1_MOUSE:  (0137) GHKEIINTIDGVGGLGIGEGAPEIVTGSRDGTVKVWDPRQKEDP  HZGJ-like protein
Q80WY1_MOUSE:  (0089) CFKEWMAHWNAVFDLAWVPGELKLVTAAGDQTAKFWDVRAGELM  Meth A retinoic-acid regulated nuclear matrix-associated protein
Q80WY2_MOUSE:  (0089) CFKEWMAHWNAVFDLAWVPGELKLVTAAGDQTAKFWDVRAGELM  Retinoic-acid regulated nuclear matrix-associated protein
```

```
Q8CIE6_MOUSE:  (0042) LIDKFDEHDGPVRGIDFHKQQPLFVSGGDDYKIKVWNYKLRRCL  Coatomer protein complex subunit alpha
Q8K265_MOUSE:  (0161) TGKVFKGHRNQVTCLSVSTDGSVLLSGSHDESVRLWDVKSKQCL  Wdr18 protein
Q8K2G5_MOUSE:  (0091) YIRYFPGHSKRVVALSMSPVDDTFISGSLDKTIRLWDLRSPNCQ  Wdr82 protein
Q8K335_MOUSE:  (0195) MLTTATAHDGDVNVISWSRREPFLLSGGDDGALKVWDLRQFKSG  Glutamate-rich WD repeat containing 1
Q8K3A5_MOUSE:  (0054) HIKTLSEAHEDCVNNIRFLDNRLFATSSDDTTIALWDLRKLNTK  WD repeat domain 32
Q8VEE8_MOUSE:  (0036) YIRYFPGHSKRVVALSMSPVDDTFISGSLDKTIRLWDLRSPNCQ  Wdr82 protein
Q91Z25_MOUSE:  (0325) DSLHKNSVSQISVLSGGKAKCSQFCTTGMDGGMSIWDVKSLESA  Arpc1b protein
RBBP4_MOUSE:   (0264) SHSVDAHTAEVNCLSFNPYSEFILATGSADKTVALWDLRNLKLK  Histone-binding protein RBBP4
RBBP7_MOUSE:   (0264) SHLVDAHTAEVNCLSFNPYSEFILATGSADKTVALWDLRNLKLK  Histone-binding protein RBBP7
SPG16_MOUSE:   (0477) CRYTLYGHTDSVNSIEFFPFSNILLTASADKTLSVWDARTGKCE  Sperm-associated antigen 16 protein
STB5L_MOUSE:   (0101) DCYCQHESGAAVLQLQFLINEGALVSASSDDTLHLWNLRQKRPA  Syntaxin-binding protein 5-like
TAF5L_MOUSE:   (0501) LFKELRGHTDSITSLAFSPDSGLIASASMDNSVRVWDIRSTCCN  TAF5-like RNA polymerase II p300/CBP-assoc fac 65 kDa subunit 5L
TBL1R_MOUSE:   (0257) LASTLGQHKGPIFALKWNKKGNFILSAGVDKTTIIWDAHTGEAK  F-box-like/WD repeat protein TBL1XR1
TBL2_MOUSE:    (0175) PEDFPKKHKAPIINIGIADTGKFIMTASSDTTVLIWNLKGQVLS  Transducin beta-like 2 protein
TBLX_MOUSE:    (0270) LASTLGQHKGPIFALKWNKKGNYILSAGVDKTTIIWDAHTGEAK  F-box-like/WD repeat protein TBL1X
TEP1_MOUSE:    (2060) CCAELRGHEGPVCCCSFSPDGGILATAGRDRNLLCWDMKIAQAP  Telomerase protein component 1
TF3C2_MOUSE:   (0601) FQCFLAHDQAVRTIQWCKANSHFLVSAGSDRKIKFWDLRRPYEP  General transcription factor 3C polypeptide 2
THOC3_MOUSE:   (0091) ENNYRGHGDSVDQLCWHPSNPDLFVTASGDKTIRIWDVRTTKCI  THO complex subunit 3
WD51B_MOUSE:   (0177) CVNNFSDSVGFANFVDFNPNGTCIASAGSDHAVKIWDIRMNKLL  WD repeat protein 51B
WDR12_MOUSE:   (0334) SLSLTSHTGWVTSVKWSPTHEQQLISGSLDNIVKLWDTRSCKAP  WD repeat protein 12
WDR22_MOUSE:   (0134) TLDVFAHEDAVYGLSVSPVNDNIFASSSDDGRVLIWDIRESPHG  WD repeat protein 22
WDR23_MOUSE:   (0299) TLQIESHEDDVNAVAFADISSQILFSGGDDAICKVWDRRTMRED  WD repeat protein 23
WDR31_MOUSE:   (0052) APQEYIPVHVDTVSVIATLNSDLCISGGKDKTAVAYNWKTGRMV  WD repeat protein 31
WDR37_MOUSE:   (0316) LVHSLTGHDQELTHCCTHPTQRLVVTSSRDTTFRLWDFRDPSIH  WD repeat protein 37
WDR47_MOUSE:   (0746) QGLHALSGHTGHILALYTWSGWMIASGSQDKTVRFWDLRVPSCV  WD repeat protein 47
WDR48_MOUSE:   (0159) TTSSLSGNKDSIYSLAMNQLGTIIVSGSTEKVLRVWDPRTCAKL  WD repeat protein 48
WDR4_MOUSE:    (0182) ESFCLGHTEFVSRILVVPSHPELLLSSSGDGTLRLWEYRSGRQL  WD repeat protein 4
WDR57_MOUSE:   (0144) VKRLKGHTSFVNSCYPARRGPQLVCTGSDDGTVKLWDIRKKAAV  WD repeat protein 57
WDR5_MOUSE:    (0120) CLKTLKGHSNYVFCCNFNPQSNLIVSGSFDESVRIWDVKTGKCL  WD repeat protein 5
WDTC1_MOUSE:   (0571) LVRVLQGDESIVNCLQPHPSYCFLATSGIDPVVRLWNPRPESED  WD and tetratricopeptide repeats protein 1
WSB1_MOUSE:    (0162) LLNLVDHIEMVRDLTFAPDGSLLLVSASRDKTLRVWDLKDDGNM  WD repeat and SOCS box-containing protein 1
```

1.3. *Drosophila melanogaster* DWD-box proteins

```
CAF1_DROME:    (0269) SHTVDAHTAEVNCLSFNPYSEFILATGSADKTVALWDLRNLKLK  Probable histone-binding protein Caf1
FBXW7_DROME:   (1227) LQTLSGPNKHHSAVTCLQFNSRFVVTSSDDGTVKLWDVKTGDFI  F-box/WD repeat protein 7
GBB1_DROME:    (0175) QVTSFLGHTGDVMALSLAPQCKTFVSGACDASAKLWDIREGVCK  Guanine nucleotide-binding protein subunit beta 1
L2DTL_DROME:   (0137) LNSYVGHTRSVKSAAFKRTDPAVFATGGRDGAILIWDIRANLNM  Protein lethal(2)denticleless
LIS1_DROME:    (0330) CLLTLSGHDNWVRGLAFHPGGKYLVSASDDKTIRVWDLRNKRCM  Lissencephaly-1 homolog
O18402_DROME:  (0289) SERRLAGHRQEVCGLKWSPDNQYLASGGNDNRLYVWNQHSVNPV  Fizzy-related protein
O76523_DROME:  (0126) KRCVGTFEQNNGKVYSMSVIDEKIVVATSDRKVLIWDLRKDGQL  Mitotic checkpoint control protein Bub3
O77285_DROME:  (0042) LLEKFDEHDGPVRGVAFHQQMPLFVSGGDDYKIKVWNYKQRRCI  Coatomer alpha subunit
Q24055_DROME:  (0014) LTKVIDTAEVGLTTAQFHPDGLIFGTGTVDSQVKIWDLKEQSNV  Gbp protein
Q4V4T3_DROME:  (0226) LMSIEAHASEALCCDWSHFDRNVLVTGGSDGLIRGWDLRKMRTH  IP11251p
Q4V560_DROME:  (0261) EREVCHRDPVNSVLWNNSKSGTEFFSGGSDGQVLWWDTRKLTEP  IP13643p
Q4V6K2_DROME:  (0229) LMSIEAHASEALCCDWSHFDRNVLVTGGSDGLIRGWDLRKMRTH  IP11351p
Q4V6Q4_DROME:  (00-1) -MSIEAHASEALCCDWSHFDRNVLVTGGSDGLIRGWDLRKMRTH  IP11451p
Q6NP36_DROME:  (0220) TPFQAYSGHTGHILSLYSWNNAMFVSGSQDQTIRFWDLRVNVSV  RE32047p
Q7JVX4_DROME:  (0257) TGTSGYQDIYAVNDIAFHPVHGTLVTVGSDGTFSFWD-KDARTKL LD40776p
Q7KTE5_DROME:  (0165) ALSLNAVCMSGATQVGFNRVSGNLLAAAHDGDLRIWDIRKGSCP  CG4705-PB, isoform B
Q86BR6_DROME:  (0395) LRHTLTGHSGKVMAAKYVQEPIKVVTGSHDRTLKIWDLRSIACI  CG31033-PC, isoform C
Q8IGK7_DROME:  (0157) TTSSLTGSKDSIYSLAMNPSGTVIVSGSTENILRIWDPRTCMRR  RE72568p
Q8MKW0_DROME:  (0028) PPTDSPQSVSICGVRFLDEGPHNILVGTTDGYVRLYDLRLRGEQ  CG12134-PB, isoform B
Q8MKZ5_DROME:  (0157) TTSSLTGSKDSIYSLAMNPSGTVIVSGSTENILRIWDPRTCMRR  CG9062-PB
Q8MSW6_DROME:  (0126) KRCVGTFEQNNGKVYSMSVIDEKIVVATSDRKVLIWDLRKMDSY  LD23540p
Q8MTB1_DROME:  (0266) PLEVSHRETTSALCWVHSKSNTEFYSGSLDGSIKYWDTRDLKMP  AT07549p
Q8SX92_DROME:  (0454) YNDENERGRVRLFSIAHHPYAPEFCVSGSDDILRVYDKRNLAKA  GH28796p
Q8SXJ6_DROME:  (0175) CLLTLSGHDNWVRGLAFHPGGKYLVSASDDKTIRVWDLRNKRCM  RE19540p
Q8SYL1_DROME:  (0307) MLTCEDAHQSDVNVISWNRNEPFIASGGDDGYLHIWDLRQFQSK  RE55020p
Q8T3W2_DROME:  (0100) VRVFGGHAKTINRLASQPGGENVFISAGRDDQVYMWDIRVKTHT  AT28277p
Q8T4D0_DROME:  (0487) LVGVLKDHSGPITSLDINYLDTEVISACTDGSCVIWDIKRMTRK  AT03371p
Q95TJ1_DROME:  (0210) LRHTLTGHSGKVMAAKYVQEPIKVVTGSHDRTLKIWDLRSIACI  LP08352p
Q960M2_DROME:  (0081) EIFKVPDAHTDSVNCIKFFDERLFATGSDDFTVALWDLRNMKQK  LD45447p
Q9BII5_DROME:  (0124) TLKVLRGHREDIYDLSWAPNSQFLVSGSVDNTAMLWDVHSGKSL  Chromatin assembly factor-1 p105 subunit
Q9V3B2_DROME:  (0341) LTKVIDTAEVGLTTAQFHPDGLIFGTGTVDSQVKIWDLKEQSNV  CG5519-PA
Q9V5C7_DROME:  (0552) SCIKRFDQECTILRAEFLDHGKFIISAASDGLLKLWNIKTNTCL  CG1671-PA
Q9V5E5_DROME:  (0098) PPTDSPQSVSICGVRFLDEGPHNILVGTTDGYVRLYDLRLRGEQ  CG12134-PA, isoform A
Q9V5L7_DROME:  (0124) TLKVLRGHREDIYDLSWAPNSQFLVSGSVDNTAMLWDVHSGKSL  CG12892-PA
Q9V5N6_DROME:  (0753) LNKSQAHHLTVRRLQFRPGKQLQLASCGEDHLVRIYDIKLT---  CG11887-PA
Q9V878_DROME:  (0130) CVKVLEGHSRYSFSCCFNPQANLLASTSFDETVRLWDVRTGKTL  CG10931-PA
Q9V8W2_DROME:  (0004) KILYKYEEPHGIGDVYFIWQKALLATTGTDGSVALYN-RQGQLVQ CG11237-PA
Q9V951_DROME:  (0259) RTHRMPGKDVNSVCFLHDKDPNVIIAGCDDGLLKVYDLRTTFRS  CG9945-PA, isoform A
Q9VAF9_DROME:  (0236) LRHTLTGHSGKVMAAKYVQEPIKVVTGSHDRTLKIWDLRSIACI  CG31033-PB, isoform B
Q9VAJ2_DROME:  (0126) KRCVGTFEQNNGKVYSMSVIDEKIVVATSDRKVLIWDLRKMDSY  CG7581-PA
Q9VAK0_DROME:  (0227) ELQQLTHHGAEVIAARFNRDGQMLLTGSFDHSAAIWDVRSKSLG  CG7568-PA
Q9VAT2_DROME:  (0081) EIFKVPDAHTDSVNCIKFFDERLFATGSDDFTVALWDLRNMKQK  CG1523-PA
Q9VCN9_DROME:  (0656) QLAELKDHSASISSLSWSTHNRHLATACSDGTLRLWDIKKLSPM  CG4448-PA
Q9VD52_DROME:  (0364) SRFTTRKMPFCVKFHPDNSKQHLFVAGTSDKKIICWDTRSGDIV  CG6015-PA
```

```
Q9VE73_DROME:  (0353) PAVSVFQGHTETVTSSVFARDDKVVSGSDDRTIKVWELRNMRSA  CG12333-PA
Q9VKK2_DROME:  (0165) ALSLNAVCMSGATQVGFNRVSGNLLAAAHDGDLRIWDIRKGSCP  CG4705-PA, isoform A
Q9VKQ3_DROME:  (0283) GIKTEISTNKSIFDASYSKLNRLILTASADKNLRLYDPRTNQGS  CG6724-PA
Q9VLN1_DROME:  (0100) YLRYFPGHTKKVISLCISPVEDTFLSGSLDKTLRLWDLRSPNCQ  CG17293-PA
Q9VML2_DROME:  (3275) GPKAEVQGERRKSSISGAKSLHEMKSATVEGQGSSYDPKSNEDE  CG14001-PA
Q9VPL0_DROME:  (0173) HAAHTLESPFQVTAVCFGDTGEQVISGGIDNEVKIWDIRKQAVL  CG3436-PA, isoform A
Q9VQD1_DROME:  (0100) VRVFGGHAKTINRLASQPGGENVFISAGRDDQVYMWDIRVKTHT  CG3515-PA
Q9VS00_DROME:  (0487) LVGVLKDHSGPITSLDINYLDTEVISACTDGSCVIWDIKRMTRK  CG10064-PA
Q9VSN7_DROME:  (0204) LMSIEAHASEALCCDWSHFDRNVLVTGGSDGLIRGWDLRKMRTH  CG6486-PA
Q9VTM3_DROME:  (0252) EREVCHRDPVNSVLWNNSKSGTEFFSGGSDGQVLWWDTRKLTEP  CG6053-PA
Q9VTY5_DROME:  (0219) WSINDAHGQMVRDLDCNPNKQCHLVTGGDDGYLRIWDCRMPKAP  CG10646-PA
Q9VU65_DROME:  (0051) RCIRFASHSAPVNGVAWSPKGNLVASAGHDRTVKIWEPKLRGVS  CG10191-PA
Q9VUN7_DROME:  (0266) DTRKLQTPLKVHFDHVSAVTDVDYSPTGKEFVSASYD-KTIRIYN CG7275-PA
Q9VVI0_DROME:  (0386) EVLHQEGHAKPVHCLSYHSDGSVLVTGGLDAFGRVWDLRTGRCI  CG6322-PA
Q9VVM7_DROME:  (0105) AHNGIINTIDAIGGTQIDCGAPEIVTGSRDGAVKVWDIRQGQAP  CG14353-PA
Q9VYQ9_DROME:  (0247) VIRHYHGHLSAVYSLALHPTIDVLATSGRDSTARIWDMRTKANV  CG1796-PA
Q9W091_DROME:  (0459) YNDENERGRVRLFSIAHHPYAPEFCVSGSDDILRVYDKRNLAKA  CG8001-PA
Q9W097_DROME:  (0282) SPTSQRDTNQVCFYSPLGKIYRTLKVPGTDITSLSWEGKSLRIA  CG2069-PA
Q9W0B8_DROME:  (0042) LLEKFDEHDGPVRGVAFHQQMPLFVSGGDDYKIKVWNYKQRRCI  CG7961-PA, isoform A
Q9W1G4_DROME:  (0170) TPFQAYSGHTGHILSLYSWNNAMFVSGSQDQTIRFWDLRVNVSV  CG2812-PA
Q9W1J3_DROME:  (0323) KTRAQGGLRTNAASCNFNRDATLIAAGCVDGSIQTWDTRKMFVN  CG5543-PA
Q9W1N4_DROME:  (0137) QPEEYAGHTGAIKRALFCRGDKCIISAAEDKTVRLWD-RMTGIEV CG3957-PA
Q9W2E7_DROME:  (0243) TGTSGYQDIYAVNDIAFHPVHGTLVTVGSDGTFSFWD-KDARTKL CG9862-PA
Q9W351_DROME:  (0264) MMQPLKRLGPPGSLLKWSPDNDWLFAATVDRVFRVWNCHQQWTT  CG16892-PA
Q9W3J1_DROME:  (0193) QSFHGHSGDVMAIDLAPNETGNTFVSGSCDRMAFIWDMRSGHVV  CG10763-PA
Q9W3K3_DROME:  (0328) PLAKLLCHSTAMSALAVEPKGQYLVTAGLDRAVKVWDIRMLVHD  CG2260-PA
Q9W3L0_DROME:  (0266) PLEVSHRETTSALCWVHSKSNTEFYSGSLDGSIKYWDTRDLKMP  CG1571-PA
Q9W4H9_DROME:  (0289) SERRLAGHRQEVCGLKWSPDNQYLASGGNDNRLYVWNQHSVNPV  CG3000-PA, isoform A
Q9XYF7_DROME:  (0126) KRCLGTFEQNNGKVYSMSVIDEKIVVATSDRKVLIWDLRKMDSY  WD-40 repeat protein
TAF5_DROME:    (0609) LVTTLLRHTSTVTTITFSRDGTVLAAAGLDNNLTLWDFHKVTED  Transcription initiation factor TFIID subunit 5
WDS_DROME:     (0147) SLKTLKGHSNYVFCCNFNPQSNLIVSGSFDESVRIWDVRTGKCL  Protein will die slowly
```

1.4. *Caenorhabditis elegans* DWD-box proteins

```
FZY1_CAEEL:    (0306) SWGGDNGHCRDVTALEWSADENMCVSGSSDRTAKIWDGRHVRGS  WD repeat-containing protein fzy-1
GBB1_CAEEL:    (0175) QCTAFTGHTGDVMSLSLSPDFRTFISGACDASAKLWDIRDGMCK  Guanine nucleotide-binding protein subunit beta 1
GBB2_CAEEL:    (0191) QNFHGHTGDVFAIDVPKCDTGNTFISAGADKHSLVWDIRSGQCV  Guanine nucleotide-binding protein subunit beta 2
LIN23_CAEEL:   (0374) LEFVRTLAGHRRGIACLQYRGRLVVSGSSDNTIRLWDIHSGVCL  F-box/WD repeat protein lin-23
LIN53_CAEEL:   (0257) GHCIDAHSAEVNCLAFNPYSEFILATGSADKTVALWDLRNLRMK  Probable histone-binding protein lin-53
LIS1_CAEEL:    (0365) CMKAIEAHEHFVSTVAFHQTSPFVITGSVDMSCKVWECR-----  Lissencephaly-1 homolog
NPP17_CAEEL:   (0123) AVVGTHDGPVKTCHWINGNNYQCLMTGSFDKTLRFWDMKNLPNQ  Nucleoporin-17
O45401_CAEEL:  (0048) QMQTLKGHKDLVYTVAWSHNGELFASGGADKLVILWNEKHEGTL  Hypothetical protein
O45604_CAEEL:  (0248) VKEYRHHNMGITSVDWNKADDRLVISSGCDGQVVIWNHETSEVL  Hypothetical protein
P90814_CAEEL:  (0183) NLEFERVHQVDIQNIGIAGNAKYLMSAALDNKICLYDLRGQLLQ  Hypothetical protein
P91867_CAEEL:  (0039) SWVGSSHSSSVEQVACSEKQPNLFASASADRNICVWDIRQSKPT  Hypothetical protein
PRP19_CAEEL:   (0329) KVSVEPGSQIAVHSIEFHPDGLIFGTGAADAVVKIWDLKNQTVA  PRP19/PSO4 homolog
PWP2_CAEEL:    (0351) YVMKQQAHSLRITTAEYSPDGSLMATGAEDGKVKIWNSRSSFCT  Periodic tryptophan protein 2 homolog
Q09649_CAEEL:  (0513) MGRKLTNHRQEVCGLKWSPDKQLLASGGNDNQLLVWNLRRNEPI  Hypothetical protein fzr-1
Q19211_CAEEL:  (0156) EPVKTYTNRYQQTAVTFNDSSDQVISGGIDNVLKVWDMRRDEIT  Hypothetical protein
Q19433_CAEEL:  (0662) MVQVLDRHTLDIRCLAQFTNGSVMFSASHDKSIRCWEKTDEILI  Hypothetical protein F13H8.2
Q19873_CAEEL:  (0323) PLVKILTHLSAVKGIAVDDQGNYMATTGLDRKCRIWDVRMFRQL  Hypothetical protein
Q22059_CAEEL:  (0131) SQVFFGHEGSVRSICFAPDDPNVFVTGGRDFQVKIWDMRVSTVK  Hypothetical protein
Q8IA70_CAEEL:  (0499) IQSMKGHTAPILGLYTWSQAGNQFVSCSQDKTIRFWDLRQQTAV  Hypothetical protein
Q93339_CAEEL:  (0371) CIMFLDGHTKEIHSVEWMPNGYEMITGSSDNSMKVWDLRMRRNT  Hypothetical protein
Q93759_CAEEL:  (0394) VARLRNHEATINGLSWAPHSGSHICTAGDDYQALIWDVHEMPKP  Hypothetical protein swan-2
Q95X41_CAEEL:  (0353) QSVAVFQGHQDSVTSVSFNTDYRIVSSSDDATVKIWDLRNMRTP  Hypothetical protein
Q95X42_CAEEL:  (0355) QSVAVFQGHQDSVTSVSFNTDYRIVSSSDDATVKIWDLRNMRTP  Hypothetical protein
Q95X65_CAEEL:  (0765) IQSMKGHTAPILGLYTWSQAGNQFVSCSQDKTIRFWDLRQQTAV  Hypothetical protein
Q95X66_CAEEL:  (0765) IQSMKGHTAPILGLYTWSQAGNQFVSCSQDKTIRFWDLRQQTAV  Hypothetical protein
Q9N4H7_CAEEL:  (0044) LLEKFDEHDGPVRGICFHHDQPIFVSGGDDYKIKVWNYKQKRCI  Hypothetical protein
Q9N533_CAEEL:  (0136) KSVFKSHERSATCLDWHATTPYILVSGSRDCTVKSYDMRVKDNH  Hypothetical protein
Q9NAN8_CAEEL:  (0294) CLATLQEHKSSVMAVEFNKNGNWLLTGGRDHLVKMYDIRMMKEM  Hypothetical protein
Q9TYV3_CAEEL:  (0308) VEECQKVAQTRYEAALEIAGGERLVSGSDDFTLFMWNPKETKQS  Hypothetical protein W07E6.2
Q9U1Q0_CAEEL:  (0200) LKIRDAHIHRTISMDFNPNLQHVIATCGDDGYVRIWDTRSTSSA  Hypothetical protein
RBA1_CAEEL:    (0256) QLTAVGHTAEVNCITFNPFSEYILATGSVDKTVALWDMRNMRKK  Probable histone-binding protein rba-1
YDEM_CAEEL:    (0411) SRSLFPASKVLDVATNMGASPSLFASGHFDKKLRFYDGRSTDPV  Hypothetical WD repeat protein F02E8.5
YH92_CAEEL:    (0288) CLRTMRGHTNYVFCCSFNPQSSLIASAGFDETVRVWDFKTGLCV  Hypothetical WD repeat protein ZC302.2
YKY4_CAEEL:    (0162) MTKTLKGHNNYVFCCNFNPQSSLVVSGSFDESVRIWDVKTGMCI  Hypothetical WD repeat protein C14B1.4
YRG5_CAEEL:    (0295) LKSYLVGSTVFDIVAKCGVSQSSFISSHFDKKVRFWDARSSDAT  Hypothetical WD repeat protein K06A1.5
YRIQ_CAEEL:    (0303) RTIVNAHEDDVNSVCFADLGSNLIYSAGDDGLVKVWDKRAWSDG  Hypothetical WD repeat protein D2030.9
```

1.5. *Arabidopsis thaliana* DWD-box proteins

```
GBB_ARATH:      (0196) GEFQSGHTADVLSVSISGSNPNWFISGSCDSTARLWDTRAASRA  Guanine nucleotide-binding protein beta subunit
IF32_ARATH:     (0184) QSDEEVGHKKDITSLCKAADDSHFLTGSLDKTAKLWDMRTLTLL  Eukaryotic translation initiation factor 3 subunit 2
KTNB1_ARATH:    (0092) IVRTLTGHRSNCISVDFHPFGEFFASGSLDTNLKIWDIRKKGCI  Katanin p80 WD40-containing subunit B1 homolog 1
MSI2_ARATH:     (0209) MFVYEGHESAIADVSWHMKNENLFGSAGEDGRLVIWDTRTNQMQ  WD-40 repeat protein MSI2
MSI3_ARATH:     (0210) MHVYEGHQSIIEDVAWHMKNENIFGSAGDDCQLVIWDLRTNQMQ  WD-40 repeat protein MSI3
MSI4_ARATH:     (0284) RGVYHGHEDTVEDVAFSPTSAQEFCSVGDDSCLILWDARTGTNP  WD-40 repeat protein MSI4
O22725_ARATH:   (0101) MVRAFTGHRSNCSAVEFHPFGEFLASGSSDANLKIWDIRKKGCI  F11P17.7 protein
O22785_ARATH:   (0360) ANVAKFDGHTGEVTAISFSENGYFLATAAEDGVRLWDLRKLRNF  Putative PRP19-like spliceosomal protein
O22826_ARATH:   (0130) IKKMAEHSSFVNSCCPTRRGPPLIISGSDDGTAKLWDMRQRGAI  Putative splicing factor
O82341_ARATH:   (0184) QSDEEVGHKEAITSLCKAADDSHFLTGSHDKTAKLWDMRTLTLI  Eukaryotic translation initiation factor 3 delta subunit
O82506_ARATH:   (0334) TPWCILSGHNKAVSYAKFLDNETLVTASTDNTLKLWDLKKTTHG  F2P3.13 protein
PRL1_ARATH:     (0293) QIFALSGHDNTVCSVFTRPTDPQVVTGSHDTTIKFWDLRYGKTM  PP1/PP2A phosphatases pleiotropic regulator PRL1
PRL2_ARATH:     (0286) MQIFVLPHDSDVFSVLARPTDPQVITGSHDSTIKFWDLRYGKSM  PP1/PP2A phosphatases pleiotropic regulator PRL2
Q2V435_ARATH:   (0385) ANVAKFDGHTGEVTAISFSENGYFLATAAEDGVRLWDLRKLRNF  Protein At2g33340
Q2V4K8_ARATH:   (0182) SHTLSGHRDGVMSVEWSTSSEWVLYTGGCDGAIRFWDIRRAGCF  Protein At1g27840
Q3E7F3_ARATH:   (0227) IIGTYVGHTEEVCGLKWSESGKKLASGGNDNVVHIWDRSLASSN  Protein At5g27945
Q3E906_ARATH:   (0209) IVETYLGHTEEVCGLKWSESGKKLASGGNDNVVHIWDHRSVASS  Protein At5g27570
Q3E9H4_ARATH:   (0304) DSLNLFCGKALNTVDVGGESSALIAAGGSDPILRVWDPRKPGTS  Protein At5g15550
Q3E9R4_ARATH:   (0196) GEFQSGHTADVLSVSISGSNPNWFISGSCDSTARLWDTRAASRA  Protein At4g34460
Q3E9R5_ARATH:   (0134) GEFQSGHTADVLSVSISGSNPNWFISGSCDSTARLWDTRAASRA  Protein At4g34460
Q3EBF5_ARATH:   (0184) QSDEEVGHKKDITSLCKAADDSHFLTGSLDKTAKLWDMRTLTLL  Protein At2g46280
Q3EBP5_ARATH:   (0385) ANVAKFDGHTGEVTAISFSENGYFLATAAEDGVRLWDLRKLRNF  Protein At2g33340
Q3ECF4_ARATH:   (0085) TVDTIGRHDDISTSIVYSYEKGEVISTGFDEKIKFWDTRQRESL  Protein At1g69400
Q3EDB9_ARATH:   (0382) CFITFTEHTNAVTALHFMADNHSLLSASLDGTVRAWDFKRYKNY  Protein At1g15440
Q42175_ARATH:   (0044) RLGTYRGHNGAVWCCDVSRDSSRLITGSADQTAKLWDVKSGKEL  G-protein
Q42339_ARATH:   (0001) CLAIMEKHFSAVTSIALSEDGLTLFSAGRDKVVNLWDLHDYSCK  Transducin homologue
Q4PSE4_ARATH:   (0243) IVETYLGHTEEVCGLKWSESGNKQASGGNDNVVHIWDRSLASSK  WD-40 repeat family protein
Q5HZ33_ARATH:   (0210) MHVYEGHQSIIEDVAWHMKNENIFGSAGDDCQLVIWDLRTNQMQ  At4g35050
Q5PNR9_ARATH:   (0286) MQIFVLPHDSDVFSVLARPTDPQVITGSHDSTIKFWDLRYGKSM  At3g16650
Q5PNT1_ARATH:   (0196) GEFQSGHTADVLSVSISGSNPNWFISGSCDSTARLWDTRAASRA  At4g34460
Q5XEV4_ARATH:   (0255) ARIKGIVVLTRNDSDGSLEDPYLIGSASSDGIIRVWDVRMAAKE  At1g65030
Q680F0_ARATH:   (0125) SHTLSGHRDGVMSVEWSTSSEWVLYTGGCDGAIRFWDIRRAGCF  MRNA, , clone: RAFL22-57-P16
Q6NLV4_ARATH:   (0282) ELCSLHGHKNIVLSVKWNQNGNWLLTASKDQIIKLYDIRTMKEL  At5g13480
Q7DLS8_ARATH:   (0251) VIRSYHGHLSGVYCLALHPTLDVLLTGGRDSVCRVWDIRTKMQI  PRL1 protein
Q84WM8_ARATH:   (0293) QIFALSGHDNTVCSVFTRPTDPQVVTGSHDTTIKFWDLRYGKTM  Putative PRL1 protein
Q84WQ9_ARATH:   (0210) MHVYEGHQSIIEDVAWHMKNENIFGSAGDDCQLVIWDLRTNQMQ  Putative WD-40 repeat protein
Q8GWC2_ARATH:   (0211) QSDEEVGHKEAITSLCKAADDSHFLTGSHDKTAKLWDMRTLTLI  Putative eukaryotic translation initiation factor 3 delta subunit
Q8GYY7_ARATH:   (0575) QVFANMHQEHINVVKFSNHSPFLFATSSFDKDVKLWDLRQEPSR  Hypothetical protein At4g34280/F10M10_50
Q8H177_ARATH:   (0255) ARIKGIVVFTRNDSDGSLEDPYLIGSASSDGIIRVWDVRMAAKE  Hypothetical protein At1g65030
Q8L4M1_ARATH:   (0192) IKMTFKGHSDYLHTVVSRSSASQILTGSEDGTARIWDCKTGKCV  Putative WD-40 repeat protein
Q8L7M8_ARATH:   (0314) VLRGHTGAVTAIAFSPRQASVYQLLSSSDDGTCRIWDARYSQWL  Putative WD-40 repeat protein
Q8L830_ARATH:   (0183) CLAIMEKHFSAVTSIALSEDGLTLFSAGRDKVVNLWDLHDYSCK  WD40-repeat protein
Q8LA29_ARATH:   (0085) TFDTIGRHDDIATSIVYSYEKGEVISTGFDEKIKFWDTRQRESL  Mitotic checkpoint protein, putative
Q8LA40_ARATH:   (0209) MFVYEGHESAIADVSWHMKNENLFGSAGEDGRLVIWDTRTNQMQ  Putative WD-40 repeat protein, MSI2
```

```
Q8LAL9_ARATH:  (0365) ELIGTLKMNGSVRSLAFSEDGKHLLSSCGDGQVYVWDLRTMKCL  Hypothetical protein
Q8LBC4_ARATH:  (0254) VLGSVSEKGKAITCLAYCADGNLLISGSEDGVVCVWDPKSLRHV  Hypothetical protein
Q8LBH5_ARATH:  (0159) ERDEHGGRRIWSVDYTLYNGSLLGASGSDDGTVQMWDPRNGGTL  Contains similarity to photomorphogenesis repressor protein
Q8LEL2_ARATH:  (0263) VISSLRGHKDYSFASAWHPNGLILATGNQDTTCRLWDIRNPSES  Hypothetical protein
Q8LF96_ARATH:  (0293) QIFALSGHDNTVCSVFTRPTDPQVVTGSHDTTIKFWDLRYGKTM  PRL1 protein
Q8LFX4_ARATH:  (0111) YLRYFKGHHDRVVSLSLCSGGECFISGSLDRTVLLWDQRVEKCQ  WD repeat protein-like
Q8LG28_ARATH:  (0310) TIGTLKGHLDYSFASAWHPNGVTFATGSQDKTCRIWDTRKLSES  WD-repeat protein-like
Q8LPI5_ARATH:  (0263) SLRTVAHTSDVNTVCFADESGNLILSGSDDNLCKVWDRRCFIGR  Putative WD-repeat protein
Q8RXA7_ARATH:  (0929) QLLEELKGHDSQVSCVKMLSGERVLTAAHDGTVKMWDVRTDMCV  Stomatal cytokinesis defective
Q8RXD8_ARATH:  (0111) YLRYFKGHHDRVVSLSLCSGGECFISGSLDRTVLLWDQRVEKCQ  WD repeat protein-like
Q8RYE4_ARATH:  (0307) PDGMPISVLRGHTGAVTAIAFSPRQASSDDGTCRIWDARYSQWL  Hypothetical protein At2g47410
Q8VYZ5_ARATH:  (0422) CFITFTEHTNAVTALHFMADNHSLLSASLDGTVRAWDFKRYKNY  Hypothetical protein At1g15440
Q8VZH9_ARATH:  (0444) GFISSWRAHDGYVTKLVAPESHLLVSSSLDKTLRIWDLRKSWTP  AT5g18530/T28N17_10
Q8VZS9_ARATH:  (0283) HVSKLKGHKSEICGLKWSSDNRELASGGNDNKLFVWNQHSTQPV  Putative Srw1 protein
Q8W117_ARATH:  (0338) LLKEFRGHTSYVNHAIFTSDGSRIITASSDCTVKVWDSKTTDCL  At1g73720/F25P22_14
Q93VK1_ARATH:  (0195) VQSFQWGTDSVISVRFNPGEPNLLATSASDRSITIYDLRLSSAA  AT4g28450/F20O9_130
Q93ZG3_ARATH:  (0182) SHTLSGHRDGVMSVEWSTSSEWVLYTGGCDGAIRFWDIRRAGCF  At1g27840/F28L5_15
Q93ZS6_ARATH:  (0204) TPTIAKGHKESVYALAMNDTGTMLVSGGTEKVLRVWDPRTGSKS  Hypothetical protein At3g05090
Q93ZT0_ARATH:  (00-4) ----MEKHFSAVTSIALSEDGLTLFSAGRDKVVNLWDLHDYSCK  Putative WD40-repeat protein
Q94AH2_ARATH:  (0093) VIRKFRGHDGEVNAVKFNDSSSVVVSAGFDRSLRVWDCRSHSVE  Hypothetical protein At5g64730
Q94BQ3_ARATH:  (0207) LADPPKQTLSLKSCDISATRPHLLLVGGSDAFARLYDRRMLPPL  Hypothetical protein At5g10940
Q94C55_ARATH:  (0162) TGVLIGHTGTVKSMCSHPTNSDLLVSGSRDGCFALWDLRCKSSS  Hypothetical protein At3g27640
Q94C94_ARATH:  (0137) LKILTGHRRTPWVVRFHPRHSEIVASGSLDHEVRLWNAKTGECI  Hypothetical protein At1g04140
Q94JT6_ARATH:  (0312) VIHGLEGHLDYSFSSAWHPNGQILATGNQDTTCRLWDVRNLSQS  At1g78070/F28K19_28
Q9C6N4_ARATH:  (0182) SHTLSGHRDGVMSVEWSTSSEWVLYTGGCDGAIRFWDIRRAGCF  Hypothetical protein F28L5.15
Q9C795_ARATH:  (0085) TVDTIGRHDDISTSIVYSYEKGEVISTGFDEKIKFWDTRQRESL  Mitotic checkpoint protein, putative
Q9C8W2_ARATH:  (0276) VISSLRGHKDYSFASAWHPNGLILATGNQDTACRLWDIRNPSES  Hypothetical protein T22A15.1
Q9C9T9_ARATH:  (0349) LLKEFRGHTSYVNHAIFTSDGSRIITASSDCTVKVWDSKTTDCL  Hypothetical protein F25P22.14
Q9CAF0_ARATH:  (0284) PLVQMQCHPGPVSSVAFHPNGHLMATSGKERKIKIWDLRKFEEV  Hypothetical protein F13M14.19
Q9FFY8_ARATH:  (0289) FVSKLVGHKSEVCGLKWSHDDRELASGGNDNQLLVWNNHSQQPI  Cell cycle switch protein
Q9FGG0_ARATH:  (0093) VIRKFRGHDGEVNAVKFNDSSSVVVSAGFDRSLRVWDCRSHSVE  Similarity to unknown protein
Q9FH64_ARATH:  (0108) YLRYFKGHHDRVVSLSLCSGGECFISGSLDRTVLLWDQRVEKCQ  WD repeat protein-like
Q9FKT5_ARATH:  (0058) DLELKGHTDSVDQLCWDPKHSDLVATASGDKSVRLWDARSGKCT  Gb|AAF54217.1
Q9FLX9_ARATH:  (0393) FVTVFRGHVGPVYQVSWSADSRLLLSGSKDSTLKIWEIRTKKLK  Notchless protein homolog
Q9FN19_ARATH:  (0356) LISTLSKHKGPIFSLKWNKKGDYLLTGSVDRTAVVWDVKAEEWK  Arabidopsis thaliana genomic DNA, chromosome 5, TAC clone:K8K14
Q9FND4_ARATH:  (0434) KFSGHRQSKYVIRSCFGGLDSSFIASGSEDSQVYIWNLKNTKPL  WD-repeat protein-like
Q9FT96_ARATH:  (0185) VVRTLTGHRSNCVSVNFHPFGEFFASGSLDTNLKIWDIRKKGCI  Katanin p80 subunit-like protein
Q9FXH4_ARATH:  (0182) SHTLSGHRDGVMSVEWSTSSEWVLYTGGCDGAIRFWDIRRAGCF  F6F9.19 protein
Q9FY53_ARATH:  (0231) VMPCNAGHGWDVKSVDWHPTKSLLVSGGKDQLVKLWDTRSGREL  Hypothetical protein T6I14_10
Q9FYL1_ARATH:  (0271) LVATLEKHKSAVNALALNDDGSVLFSGSCDRSILVWEREDTSNY  F21J9.19
Q9LEU6_ARATH:  (0207) LADPPKQTLSLKSCDISATRPHLLLVGGSDAFARLYDRRMLPPL  Hypothetical protein T30N20_210
Q9LF27_ARATH:  (0304) DSLNLFCGKALNTVDVGGESSALIAAGGSDPILRVWDPRKPGTS  Hypothetical protein T20K14_160
Q9LFE2_ARATH:  (0183) CLAIMEKHFSAVTSIALSEDGLTLFSAGRDKVVNLWDLHDYSCK  WD40-repeat protein
Q9LP54_ARATH:  (0184) TMIIPAHDFEILSCDWNKYDDCILATSSVDKTVKVWDVRSYRVP  Peroxisomal targeting signal type 2 receptor, Pex7p
Q9LPP3_ARATH:  (0272) PLVQMQCHPGPVSSVAFHPNGHLMATSGKERKIKIWDLRKFEEV  F18K10.11 protein
Q9LRZ0_ARATH:  (0864) MTTFMPPPPASTFLAFHPQDNNIIAIGMEDSSIHIYNVRVDEVK  Arabidopsis thaliana genomic DNA, chromosome 3, TAC clone:K20I9
Q9LTJ6_ARATH:  (0159) ERDEHGGRRIWSVDYTLYNGSLIGASGSDDGTVQMWDPRNGGTL  Similarity to photomorphogenesis repressor COP1
```

```
Q9LVF2_ARATH:  (0657) HLLTLEGHHAEIWCLAISNRGDFLVTGSHDRSMRRWDRSEEPFF  Arabidopsis thaliana genomic DNA, chromosome 3, P1 clone: MIL23
Q9LVX5_ARATH:  (0193) TGVLIGHTGTVKSMCSHPTNSDLLVSGSRDGCFALWDLRCKSSS  Similarity to unknown protein
Q9LXN4_ARATH:  (0109) AVMTLRGHTADVVDLNWSPDDSMLASGSLDNTVHIWNMRTGMCT  WD repeat domain protein
Q9LYK6_ARATH:  (0105) ILRYFKGHKDRVVSLCMSPINDSFMSGSLDRSVRLWDLRVNACQ  Hypothetical protein T15N1_20
Q9M0E5_ARATH:  (1072) LVAHLQEHRSAVNDIATSSDHSFFVSASDDSTVKVWDSRKLEKD  Hypothetical protein AT4g29380
Q9M1E5_ARATH:  (0192) RRHHSSSRIRLNSIAIDPRNSYYLAVGGSDEYARVYDTRRVQLA  Hypothetical protein F9K21.200
Q9M3B4_ARATH:  (0254) VLGSVSEKGKAITCLAYCADGNLLISGSEDGVVCVWDPKSLRHV  Hypothetical protein F2K15.40
Q9M9A6_ARATH:  (0025) CVATVGRCSSAILSLEYDDSTGILAAAGRDTVANIWDIRSGKQM  F27J15.17
Q9MAB0_ARATH:  (0206) TPTIAKGHKESVYALAMNDTGTMLVSGGTEKVLRVWDPRTGSKS  T12H1.5 protein
Q9SAI7_ARATH:  (0340) VFHWELHERRINSIDFNPQNPHVMATSSTDGTACLWDLRSMGAK  F23A5.6 protein
Q9SGZ4_ARATH:  (0386) VIHGLEGHLDYSFSSAWHPNGQILATGNQDTTCRLWDVRNLSQS  F28K19.28
Q9SIB8_ARATH:  (0121) LATASTDRTEKIWKTDGTLLQTFKASSGFDSLARVWDLRTARNI  Putative U4/U6 small nuclear ribonucleoprotein
Q9SJT9_ARATH:  (0042) LIDRFDEHEGPVRGVHFHNSQPLFVSGGDDYKIKVWNYKTHRCL  Coatomer alpha subunit
Q9SKW4_ARATH:  (0390) VISSLRGHKDYSFASAWHPNGLILATGNQDTACRLWDIRNPSES  F5J5.6
Q9SLN3_ARATH:  (0187) PDGMPISVLRGHTGAVTAIAFSPRQASSDDGTCRIWDARYSQWL  Putative WD-40 repeat protein
Q9SS57_ARATH:  (0275) ARIKGIVVLTRNDSDGSLEDPYLIGSASSDGIIRVWDVRMAAKE  F16G16.2 protein
Q9SXA3_ARATH:  (0091) MVRAFTGHRSNCSAVEFHPFGEFLASGSSDTNLRVWDTRKKGCI  T28P6.17 protein
Q9SY00_ARATH:  (0161) CVRMIKAHSMPISSVHFNRDGSLIVSASHDGSCKIWDAKEGTCL  Putative WD-repeat protein
Q9SZ03_ARATH:  (0315) LAQVLLKQENAVTALAVKSQSSIVYCGSSDGLVNYWERSKRSFT  Hypothetical protein AT4g34380
Q9SZA4_ARATH:  (0257) IVETYRGHTQEVCGLKWSGSGQQLASGGNDNVVHIWDRSVASSN  WD-repeat protein-like protein
Q9SZQ5_ARATH:  (0234) LLGSMSGHTSWVLSVDASPDGGAIATGSSDRTVRLWDLKMRAAI  Hypothetical protein F27B13.70
Q9T014_ARATH:  (0895) TPWCILSGHNKAVSYAKFLDNETLVTASTDNTLKLWDLKKTTHG  COP1 like protein
Q9T060_ARATH:  (0297) HVSKLKGHKSEICGLKWSSDNRELASGGNDNKLFVWNQHSTQPV  Srw1-like protein
Q9XF57_ARATH:  (0141) VRTFKEHAYCVYQAVWNPKHGDVFASASGDCTLRIWDVREPGST  Peroxisomal targeting signal type 2 receptor
Q9XI24_ARATH:  (0422) CFITFTEHTNAVTALHFMADNHSLLSASLDGTVRAWDFKRYKNY  F9L1.40 protein
Q9XIB2_ARATH:  (0325) LVQVLMKQENAVTALAVNLTDAVVYCGSSDGTVNFWERQKYLTH  F13F21.11 protein
Q9ZPY3_ARATH:  (2366) LWYIPKAHLGSVTKIATIPRTSLFLTGSKDGEVKLWDAKAAKLI  Hypothetical protein At2g46560
Q9ZT99_ARATH:  (0325) SLRTVAHTSDVNTVCFADESGNLILSGSDDNLCKVWDRRCFIGR  Putative WD-repeat protein
RAE1L_ARATH:   (0237) KCHRDGNDIYSVNSLNFHPVHGTFATAGSDGAFNFWDKDSKQRL  Rae1-like protein At1g80670
WDR50_ARATH:   (0365) ELIGTLKMNGSVRSLAFSEDGKHLLSSGGDGQVYVWDLRTMKCL  WD-repeat protein At5g14050
```

1.6. *Schizosaccharomyces pombe* DWD-box proteins

```
CORO_SCHPO:    (0167) VAHVSLKMDVMCQSMSFNADGTRLVTTSRDKKVRVWDPRTDKPV  Coronin-like protein crn1
GBB_SCHPO:     (0139) ISVLKGHEMDIVSLDFLPSNPNLFVTGGCDKLAKLWDLRAAYCC  Guanine nucleotide-binding protein beta subunit
IF32_SCHPO:    (0043) RLGTYEGHTGAIWTCDINKSSTLMVSGAADNTMRLWDVKTGKQL  Eukaryotic translation initiation factor 3 39 kDa subunit
MIP1_SCHPO:    (1170) TDVWKEHSSEIVNVEMQSSGMRELISASSDGEVKLWDIRMNHSL  WD-repeat protein mip1
O60097_SCHPO:  (0343) TESTTNNDNIKAPSESSSEESNIFLTTSIDGVMNVWDHRMVDSV  SPBC14C8.17c protein
O74340_SCHPO:  (0179) VTKFEWGADTLPVVKFNYTETSVLASAGMDRSIVIYDLRTSSPL  SPBC1A4.07c protein
O74855_SCHPO:  (0422) FLATLRGHVAAVYQCAWSTDSRLLVSSSQDTTLKVWDVRSKKMK  SPCC18.05c protein
O94244_SCHPO:  (0273) PKVIQAHSKAINAVAINPFNDYLLATASADKTVALWDLRNPYQR  Histone acetyltransferase type B subunit 2
O94527_SCHPO:  (0662) SYYGHCNVESIKNVNFYGQNDEYVMSGSDDGRFFIWD-KLNASIL SPBC609.03 protein
POF1_SCHPO:    (0302) FQQVALLEGHSSGVTCLQFDQCKLISGSMDKTIRIWNYRTSECI  F-box/WD-repeat protein pof1
POP1_SCHPO:    (0435) GVLIRSLEEHEGDVWTFEYVGDTLVTGSTDRTVRVWDLRTGECK  WD-repeat protein pop1
PRP46_SCHPO:   (0238) VIRHYHGHLSGVYALKLHPTLDVLVTAGRDAVARVWDMRTRQNV  Pre-mRNA-splicing factor prp46
Q96WV5_SCHPO:  (0044) LLDRFDGHDGPVRGIAFHPTQPLFVSGGDDYKVNVWNYKSRKLL  SPBPJ4664.04 protein
Q9C1X0_SCHPO:  (0131) FSPIQVLADAKDSVSSIDIAEHLIVTGSTDGTLRTYDIRKGTLS  SPBC713.05 protein
Q9P4X3_SCHPO:  (0256) PLVKMLTHRGPVRDLAVNRDGRYMVTAGADSLLKVWDLRTYKEL  SPAC959.03c protein
Q9USN3_SCHPO:  (0180) SMAVFEGHSSVIRGLTFEPTGSFLLSGSRDKTVQVWNIKKRSAV  Probable U3 small nucleolar RNA-associated protein 13
Q9USR0_SCHPO:  (0181) THSLSGHTGNVLAVDWCPKNEFVLASGSADGTCRLWDIRKVSSS  SPBC577.09 protein
Q9USZ0_SCHPO:  (0272) TYTYTGHRGKHIWSLVVSSANPIIYTGGNDGSVRSWDYKTRIQE  SPBC1306.02 protein
Q9UT39_SCHPO:  (0247) FQELPFSNNFHGGSTTFVPQGNFVIGSADDRTLNVWNLRHTFHH  SPAC824.04 protein
Q9UTC7_SCHPO:  (0298) ELLMQEGHSEGIFSIACQPDGSLVSSGGNDAIGRIWDLRSGKSI  SPAC227.12 protein
Q9Y7K5_SCHPO:  (0291) SVSAKLPHSDSVLTGSWHPNGNILATGGQDTTAKVWDIRALGKS  SPBC2A9.03 protein
SKB15_SCHPO:   (0228) GKILHEFTAHKKRVKSVYPVDDYLITASSDGSVCIWD-KDWNLVI Shk1 kinase-binding protein 15
SLP1_SCHPO:    (0295) QIGTLQGHSSEVCGLAWRSDGLQLASGGNDNVVQIWDARSSIPK  WD-repeat-containing protein slp1
SRW1_SCHPO:    (0365) YFRVLTAHRQEVCGLEWNSNENLLASGGNDNALMVWD-KFEEKPL WD-repeat-containing protein srw1
SWD1_SCHPO:    (0057) VSRVLTGHTRAIQSVCWSSCDRFLLTASRDWKCILWDLRDGSIV  Set1 complex component swd1
SWD2_SCHPO:    (0103) YLRYFPGHKQTVTSIDVSPADETFLSASLDNTIRLWDLRSPNCQ  Set1 complex component swd2
TAF5_SCHPO:    (0454) PLRVFAGHLSDVDCVTFHPNSAYVLTGSSDKTCRLWDVHRGHSV  Transcription initiation factor TFIID subunit 5
YAGE_SCHPO:    (0155) NVKIVQAHEMEVRDVAFSPNDSKFVTASDDGSLKVWNFHMSTEE  Hypothetical WD-repeat protein C12G12.14c in chromosome I
YCSB_SCHPO:    (0479) VCLNFTTTQKDINHATISNSGILVTSSGTDNQTFVWDSRKPDKP  Hypothetical WD-repeat protein C613.12c in chromosome III
YCSB_SCHPO:    (0537) DGANEEEVDAGINMAQWQPKGNLFVTGGSDGIVKVWDLRLNNPF  Hypothetical WD-repeat protein C613.12c in chromosome III
YDSB_SCHPO:    (0126) LYDFNEHSRAVHKLDISSFHPSYVLTASQDGLIKLWDYKESSST  Hypothetical WD-repeat protein C4F8.11 in chromosome I
YTM1_SCHPO:    (0347) SHTLSGHKNLVSGLSASPENPYMFASVSHDNTCRVWDVRATSGS  Microtubule-associated protein ytm1
CDT2_SCHPO:    (0281) HENSGRDCSITSATWLPQSTSQVISSCSANSALKLWDLRTVHTV  CDT2
```

1.7. *Saccharomyces cerevisiae* DWD-box proteins

```
CDC20_YEAST:   (0376) IVSTWAEHTGEVCGLSYKSDGLQLASGGNDNTVMIWDTRTSLPQ  APC/C activator protein CDC20
CDC4_YEAST:    (0412) KFLLQLSGHDGGVWALKYAHGGILVSGSTDRTVRVWDIKKGCCT  Cell division control protein 4
DIP2_YEAST:    (0153) VGLYKLRSHKDSITGFWCQGEDWLISTSKDGMIKLWDLKTHQCI  DOM34-interacting protein 2
GID7_YEAST:    (0664) QKYFGQKQQHFIIRSCFAYGNKLVMSGSEDGKIYIWDRIRGNLV  Glucose-induced degradation protein 7
GLE2_YEAST:    (0260) PGSNGQSLVYPVNSIAFHPLYGTFVTAGGDGTFNFWDKNQRHRL  Nucleoporin GLE2
HAT2_YEAST:    (0287) LHHMSGHEDAVNNLEFSTHVDGVVVSSGSDNRLMMWDLKQIGAE  Histone acetyltransferase type B subunit 2
MSI1_YEAST:    (0288) QSNREKHDGGVNSCRFNYKNSLILASADSNGRLNLWDIRNMNKS  Chromatin assembly factor 1 subunit p50
PEX7_YEAST:    (0212) NNFLVHSGLEALTCDFNKYRPYVVATGGVDNAIRIWDIRMLNKN  Peroxisomal targeting signal 2 receptor
PFS2_YEAST:    (0210) QERVLSGHHWDVKSCDWHPEMGLIASASKDNLVKLWDPRSGNCI  Polyadenylation factor subunit 2
PRP46_YEAST:   (0215) IIRDYYGHLSGVRTVSIHPTLDLIATAGRDSVIKLWDMRTRIPV  Pre-mRNA-splicing factor PRP46
PRP4_YEAST:    (0298) ELLLQEGHDKGVFSLSFQCDGSLVCSGGMDSLSMLWDIRSGSKV  U4/U6 small nuclear ribonucleoprotein PRP4
RRB1_YEAST:    (0313) QPFTVSNNKSIEDIQWSRTESTVFATAGCDGYIRIWDTRSKKHK  Ribosome assembly protein RRB1
TUP1_YEAST:    (0476) IVMILQGHEQDIYSLDYFPSGDKLVSGSGDRTVRIWDLRTGQCS  Glucose repression regulatory protein TUP1
WTM1_YEAST:    (0213) ILRTVHVPGTTVTHTVRFFDNHIFASCSDDNILRFWDTRTSDKP  Transcriptional modulator WTM1
YCW2_YEAST:    (0393) PIARMTGHQKLVNHVAFSPDGRYIVSASFDNSIKLWDGRDGKFI  Hypothetical WD-repeat protein YCR072C
YHY6_YEAST:    (1378) RAGNDKQGVWINNVHLQRGGYRELVSGATNGVVELWDIRSEDPV  Hypothetical 175.8 kDa wd protein in GND1-IKI1 intergenic region
YJL2_YEAST:    (0555) KSTLLTQRNERPSIGALQSFDAALATGTKDGVVRLWDLRSGKVI  Hypothetical 80.0 kDa wd protein in ASF1-CCT7 intergenic region
YK16_YEAST:    (0534) GKPVRLLEGHTDGITSLKFDSEKLVTGSMDNSVRIWDLRTSSIL  Hypothetical 74.7 kDa wd protein in DAL80-GAP1 intergenic region
YNA6_YEAST:    (0066) PVASFEGHRGNVTSVSFQQDNRWMVTSSEDGTIKVWDVRSPSIP  Hypothetical 34.0 kDa wd protein in SIS1-MRPL2 intergenic region
YTM1_YEAST:    (0367) QQQLIGHKNFVSSLDTCPENEYILCSGSHDGTVKVWDVRSTSPM  Microtubule-associated protein YTM1
```

REFERENCES

Andersen, J.L., Zimmerman, E.S., DeHart, J.L., Murala, S., Ardon, O., Blackett, J., Chen, J., and Planelles, V. 2005. ATR and GADD45alpha mediate HIV-1 Vpr-induced apoptosis. *Cell Death Differ* **12**(4): 326-334.

Angers, S., Li, T., Yi, X., MacCoss, M.J., Moon, R.T., and Zheng, N. 2006. Molecular architecture and assembly of the DDB1-CUL4A ubiquitin ligase machinery. *Nature* **443**(7111): 590-593.

Arai, T., Kasper, J.S., Skaar, J.R., Ali, S.H., Takahashi, C., and DeCaprio, J.A. 2003. Targeted disruption of p185/Cul7 gene results in abnormal vascular morphogenesis. *Proc Natl Acad Sci U S A* **100**(17): 9855-9860.

Arias, E.E. and Walter, J.C. 2005. Replication-dependent destruction of Cdt1 limits DNA replication to a single round per cell cycle in Xenopus egg extracts. *Genes & development* **19**(1): 114-126.

-. 2006. PCNA functions as a molecular platform to trigger Cdt1 destruction and prevent re-replication. *Nat Cell Biol* **8**(1): 84-90.

Bartz, S.R., Rogel, M.E., and Emerman, M. 1996. Human immunodeficiency virus type 1 cell cycle control: Vpr is cytostatic and mediates G2 accumulation by a mechanism which differs from DNA damage checkpoint control. *J Virol* **70**(4): 2324-2331.

Begum, N.A., Izumi, N., Nishikori, M., Nagaoka, H., Shinkura, R., and Honjo, T. 2006. Requirement of non-canonical activity of uracil DNA glycosylase for class switch recombination. *J Biol Chem*.

Bell, S.P. and Dutta, A. 2002. DNA replication in eukaryotic cells. *Annu Rev Biochem* **71**: 333-374.

Bondar, T., Mirkin, E.V., Ucker, D.S., Walden, W.E., Mirkin, S.M., and Raychaudhuri, P. 2003. Schizosaccharomyces pombe Ddb1 is functionally linked to the replication checkpoint pathway. *J Biol Chem* **278**(39): 37006-37014.

Bornstein, G., Ganoth, D., and Hershko, A. 2006. Regulation of neddylation and deneddylation of cullin1 in SCFSKP2 ubiquitin ligase by F-box protein and substrate. *Proc Natl Acad Sci U S A* **103**(31): 11515-11520.

Brzovic, P.S., Rajagopal, P., Hoyt, D.W., King, M.C., and Klevit, R.E. 2001. Structure of a BRCA1-BARD1 heterodimeric RING-RING complex. *Nature structural biology* **8**(10): 833-837.

Buchwald, G., van der Stoop, P., Weichenrieder, O., Perrakis, A., van Lohuizen, M., and Sixma, T.K. 2006. Structure and E3-ligase activity of the Ring-Ring complex of polycomb proteins Bmi1 and Ring1b. *Embo J* **25**(11): 2465-2474.

Cang, Y., Zhang, J., Nicholas, S.A., Bastien, J., Li, B., Zhou, P., and Goff, S.P. 2006. Deletion of DDB1 in mouse brain and lens leads to p53-dependent elimination of proliferating cells. *Cell* **127**(5): 929-940.

Cang, Y., Zhang, J., Nicholas, S.A., Kim, A.L., Zhou, P., and Goff, S.P. 2007. DDB1 is essential for genomic stability in developing epidermis. *Proc Natl Acad Sci U S A*.

Carrano, A.C., Eyther, E., Hershko, A., and Pagano, M. 1999. SKP2 is required for ubiquitin-mediated degradation of the CDK inhibitor p27. *Nat Cell Biol* **1**: 193-199.

Chen, L.-C., Manjeshwar, S., Lu, Y., Moore, D., Ljung, B.-M., Kuo, W.-L., Dairkee, S.H., Wernick, M., Collins, C., and Smith, H.S. 1998a. The human homologue for the Caenorhabditis elegans cul-4 gene is amplified and overexpressed in primary breast cancers. *Cancer Res* **58**: 3677-3683.

Chen, L.C., Manjeshwar, S., Lu, Y., Moore, D., Ljung, B.M., Kuo, W.L., Dairkee, S.H., Wernick, M., Collins, C., and Smith, H.S. 1998b. The human homologue for the Caenorhabditis elegans cul-4 gene is amplified and overexpressed in primary breast cancers. *Cancer research* **58**(16): 3677-3683.

Chu, G. and Chang, E. 1988. Xeroderma pigmentosum group E cells lack a nuclear factor that binds to damaged DNA. *Science* **242**(4878): 564-567.

Cope, G.A. and Deshaies, R.J. 2006. Targeted silencing of Jab1/Csn5 in human cells downregulates SCF activity through reduction of F-box protein levels. *BMC biochemistry* **7**: 1.

d'Azzo, A., Bongiovanni, A., and Nastasi, T. 2005. E3 ubiquitin ligases as regulators of membrane protein trafficking and degradation. *Traffic (Copenhagen, Denmark)* **6**(6): 429-441.

Das-Bradoo, S., Ricke, R.M., and Bielinsky, A.K. 2006. Interaction between PCNA and diubiquitinated Mcm10 is essential for cell growth in budding yeast. *Mol Cell Biol* **26**(13): 4806-4817.

Donaldson, T.D., Noureddine, M.A., Reynolds, P.J., Bradford, W., and Duronio, R.J. 2004. Targeted disruption of Drosophila Roc1b reveals functional differences in the Roc subunit of Cullin-dependent E3 ubiquitin ligases. *Molecular biology of the cell* **15**(11): 4892-4903.

Feldman, R.M.R., Correll, C.C., Kaplan, K.B., and Deshaies, R.J. 1997. A complex of Cdc4p, SKP1p, and Cdc53p/Cullin catalyzes ubiquitination of the phosphorylated CDK inhibitor Sic1p. *Cell* **91**: 221-230.

Ferreira, M.F., Santocanale, C., Drury, L.S., and Diffley, J.F. 2000. Dbf4p, an essential S phase-promoting factor, is targeted for degradation by the anaphase-promoting complex. *Mol Cell Biol* **20**(1): 242-248.

Furukawa, M., He, Y.J., Borchers, C., and Xiong, Y. 2003. Targeting of protein ubiquitination by BTB-Cullin 3-Roc1 ubiquitin ligases. *Nat Cell Biol* **5**: 1001-11007.

Furukawa, M., Ohta, T., and Xiong, Y. 2002. Activation of UBC5 Ubiquitin-conjugating Enzyme by the RING Finger of ROC1 and Assembly of Active Ubiquitin Ligases by All Cullins. *J Biol Chem* **277**(18): 15758-15765.

Furukawa, M. and Xiong, Y. 2005. BTB protein Keap1 targets antioxidant transcription factor Nrf2 for ubiquitination by the Cullin 3-Roc1 ligase. *Mol Cell Biol* **25**(1): 162-171.

Geyer, R., Wee, S., Anderson, S., Yates, J., and Wolf, D.A. 2003. BTB/POZ domain proteins are putative substrate adaptors for cullin 3 ubiquitin ligases. *Mol Cell* **12**(3): 783-790.

Goldenberg, S.J., Cascio, T.C., Shumway, S.D., Garbutt, K.C., Liu, J., Xiong, Y., and Zheng, N. 2004. Structure of the Cand1-Cul1-Roc1 complex reveals regulatory mechanisms for the assembly of the multisubunit cullin-dependent ubiquitin ligases. *Cell* **119**(4): 517-528.

Groisman, R., Kuraoka, I., Chevallier, O., Gaye, N., Magnaldo, T., Tanaka, K., Kisselev, A.F., Harel-Bellan, A., and Nakatani, Y. 2006. CSA-dependent degradation of

CSB by the ubiquitin-proteasome pathway establishes a link between complementation factors of the Cockayne syndrome. *Genes & development* **20**(11): 1429-1434.

Groisman, R., Polanowska, J., Kuraoka, I., Sawada, J., Saijo, M., Drapkin, R., Kisselev, A.F., Tanaka, K., and Nakatani, Y. 2003. The ubiquitin ligase activity in the DDB2 and CSA complexes is differentially regulated by the COP9 signalosome in response to DNA damage. *Cell* **113**(3): 357-367.

Gu, Q., Tan, M., and Sun, Y. 2007. SAG/ROC2/Rbx2 is a novel activator protein-1 target that promotes c-Jun degradation and inhibits 12-O-tetradecanoylphorbol-13-acetate-induced neoplastic transformation. *Cancer research* **67**(8): 3616-3625.

He, J., Choe, S., Walker, R., Di Marzio, P., Morgan, D.O., and Landau, N.R. 1995. Human immunodeficiency virus type 1 viral protein R (Vpr) arrests cells in the G2 phase of the cell cycle by inhibiting p34cdc2 activity. *J Virol* **69**(11): 6705-6711.

He, Y.J., McCall, C.M., Hu, J., Zeng, Y., and Xiong, Y. 2006. DDB1 functions as a linker to recruit receptor WD40 proteins to CUL4-ROC1 ubiquitin ligases. *Genes & development* **20**(21): 2949-2954.

Hershko, A. and Ciechanover, A. 1998. The ubiquitin system. *Annu Rev Biochem* **67**: 425-479.

Higa, L.A., Banks, D., Wu, M., Kobayashi, R., Sun, H., and Zhang, H. 2006a. L2DTL/CDT2 interacts with the CUL4/DDB1 complex and PCNA and regulates CDT1 proteolysis in response to DNA damage. *Cell Cycle* **5**(15): 1675-1680.

Higa, L.A., Wu, M., Ye, T., Kobayashi, R., Sun, H., and Zhang, H. 2006b. CUL4-DDB1 ubiquitin ligase interacts with multiple WD40-repeat proteins and regulates histone methylation. *Nat Cell Biol* **8**(11): 1277-1283.

Hochstrasser, M. 1996. Ubiquitin-dependent protein degradation. *Ann Rev Genet* **30**: 405-439.

-. 2006. Lingering mysteries of ubiquitin-chain assembly. *Cell* **124**(1): 27-34.

Holmberg, C., Fleck, O., Hansen, H.A., Liu, C., Slaaby, R., Carr, A.M., and Nielsen, O. 2005. Ddb1 controls genome stability and meiosis in fission yeast. *Genes & development* **19**(7): 853-862.

Hu, J., McCall, C.M., Ohta, T., and Xiong, Y. 2004. Targeted ubiquitination of CDT1 by the DDB1-CUL4A-ROC1 ligase in response to DNA damage. *Nat Cell Biol* **6**(10): 1003-1009.

Hu, J. and Xiong, Y. 2006. An evolutionarily conserved function of proliferating cell nuclear antigen for cdt1 degradation by the cul4-ddb1 ubiquitin ligase in response to DNA damage. *J Biol Chem* **281**(7): 3753-3756.

Huibregtse, J.M., Scheffner, M., Beaudenon, S., and Howley, P.M. 1995. A family of proteins structurally and functionally related to the E6-AP ubiquitin-protein ligase. *Proc Natl Acad Sci USA* **92**: 2563-2567.

Jackson, P., Eldridge, A.G., Freed, E., Furstenthal, L., Hsu, J.Y., Kaiser, B.K., and Reimann, J.D.R. 2000. The lore of the RINGs: substrate recognition and catalysis by ubiquitin ligases. *Trends in Cell Biology* **10**: 429-439.

Jentsch, S. 1992. The ubiquitin-conjugating system. *Annual review of Genetics* **26**: 179-207.

Jin, J., Arias, E.E., Chen, J., Harper, J.W., and Walter, J.C. 2006. A family of diverse Cul4-Ddb1-interacting proteins includes Cdt2, which is required for S phase destruction of the replication factor Cdt1. *Mol Cell* **23**(5): 709-721.

Kamura, T., Burian, D., Yan, Q., Schmidt, S.L., Lane, W.S., Querido, E., Branton, P.E., Shilatifard, A., Conaway, R.C., and Conaway, J.W. 2001. Muf1, a novel Elongin BC-interacting leucine-rich repeat protein that can assemble with Cul5 and Rbx1 to reconstitute a ubiquitin ligase. *J Biol Chem* **276**(32): 29748-29753.

Kamura, T., Koepp, D.M., Conrad, M.N., Skowyra, D., Moreland, R.J., Iliopoulos, O., Lane, W.S., Kaelin, W.G.J., Elledge, S.J., Conaway, R.C., Harper, J.W., and Conaway, J.W. 1999. Rbx1, a component of the VHL tumor suppressor complex and SCF ubiquitin ligase. *Science* **284**: 657-661.

Kamura, T., Maenaka, K., Kotoshiba, S., Matsumoto, M., Kohda, D., Conaway, R.C., Conaway, J.W., and Nakayama, K.I. 2004. VHL-box and SOCS-box domains

determine binding specificity for Cul2-Rbx1 and Cul5-Rbx2 modules of ubiquitin ligases. *Genes & development* **18**(24): 3055-3065.

Kamura, T., Sato, S., Haque, D., Liu, L., Kaelin, W.G., Jr., Conaway, R.C., and Conaway, J.W. 1998. The Elongin BC complex interacts with the conserved SOCS-box motif present in members of the SOCS, ras, WD-40 repeat, and ankyrin repeat families. *Genes & development* **12**(24): 3872-3881.

Kapetanaki, M.G., Guerrero-Santoro, J., Bisi, D.C., Hsieh, C.L., Rapic-Otrin, V., and Levine, A.S. 2006. The DDB1-CUL4ADDB2 ubiquitin ligase is deficient in xeroderma pigmentosum group E and targets histone H2A at UV-damaged DNA sites. *Proc Natl Acad Sci U S A*.

King, R.W., Deshaies, R.J., Peters, J.-M., and Kirschner, M.W. 1996. How proteolysis drives the cell cycle. *Science* **274**: 1652-1659.

Lai, M., Zimmerman, E.S., Planelles, V., and Chen, J. 2005. Activation of the ATR pathway by human immunodeficiency virus type 1 Vpr involves its direct binding to chromatin in vivo. *J Virol* **79**(24): 15443-15451.

Lammer, D., Mathias, N., Laplaza, J.M., Jiang, W., Liu, Y., Callis, J., Goebl, M., and Estelle, M. 1998. Modification of yeast Cdc53p by the ubiquitin-related protein Rub1p affects function of the SCF^{Cdc4} complex. *Genes & Dev* **12**: 914-926.

Latres, E., Chiaur, D.S., and Pagano, M. 1999. The human F box protein β-TrcP associates with the Cul1/SKP1 complex and regulates the stability of β-catenin. *Oncogene* **18**: 849-854.

Le Rouzic, E., Belaidouni, N., Estrabaud, E., Morel, M., Rain, J.C., Transy, C., and Margottin-Goguet, F. 2007. HIV1 Vpr arrests the cell cycle by recruiting DCAF1/VprBP, a receptor of the Cul4-DDB1 ubiquitin ligase. *Cell Cycle* **6**(2): 182-188.

Le Rouzic, E. and Benichou, S. 2005. The Vpr protein from HIV-1: distinct roles along the viral life cycle. *Retrovirology* **2**(1): 11.

Li, B., Ruiz, J.C., and Chun, K.T. 2002. CUL-4A is critical for early embryonic development. *Mol Cell Biol* **22**(14): 4997-5005.

Li, T., Chen, X., Garbutt, K.C., Zhou, P., and Zheng, N. 2006. Structure of DDB1 in complex with a paramyxovirus V protein: viral hijack of a propeller cluster in ubiquitin ligase. *Cell* **124**(1): 105-117.

Li, W., Tu, D., Brunger, A.T., and Ye, Y. 2007. A ubiquitin ligase transfers preformed polyubiquitin chains from a conjugating enzyme to a substrate. *Nature* **446**(7133): 333-337.

Liu, C., Poitelea, M., Watson, A., Yoshida, S.H., Shimoda, C., Holmberg, C., Nielsen, O., and Carr, A.M. 2005. Transactivation of Schizosaccharomyces pombe cdt2+ stimulates a Pcu4-Ddb1-CSN ubiquitin ligase. *Embo J* **24**(22): 3940-3951.

Liu, J., Furukawa, M., Matsumoto, T., and Xiong, Y. 2002. NEDD8 modification of CUL1 dissociates p120(CAND1), an inhibitor of CUL1-SKP1 binding and SCF ligases. *Mol Cell* **10**(6): 1511-1518.

Lo, S.C. and Hannink, M. 2006. CAND1-mediated substrate adaptor recycling is required for efficient repression of Nrf2 by Keap1. *Mol Cell Biol* **26**(4): 1235-1244.

Lyapina, S., Cope, G., Shevchenko, A., Serino, G., Tsuge, T., Zhou, C., Wolf, D.A., Wei, N., and Deshaies, R.J. 2001. Promotion of NEDD-CUL1 conjugate cleavage by COP9 signalosome. *Science* **292**(5520): 1382-1385.

Maya-Mendoza, A., Petermann, E., Gillespie, D.A., Caldecott, K.W., and Jackson, D.A. 2007. Chk1 regulates the density of active replication origins during the vertebrate S phase. *Embo J.*

Miao, H., Seiler, J.A., and Burhans, W.C. 2003. Regulation of cellular and SV40 virus origins of replication by Chk1-dependent intrinsic and UVC radiation-induced checkpoints. *J Biol Chem* **278**(6): 4295-4304.

Michel, J.J., McCarville, J.F., and Xiong, Y. 2003. A role for saccharomyces cerevisiae CUL8 ubiquitin ligase in proper anaphase progression. *J Biol Chem* **278**: 22828-22837.

Michel, J.J. and Xiong, Y. 1998. Human CUL-1, but not other cullin family members, selectively interacts with SKP1 to form a complex with SKP2 and cyclin A. *Cell Growth Differ* **9**(6): 435-449.

Montagnoli, A., Tenca, P., Sola, F., Carpani, D., Brotherton, D., Albanese, C., and Santocanale, C. 2004. Cdc7 inhibition reveals a p53-dependent replication checkpoint that is defective in cancer cells. *Cancer research* **64**(19): 7110-7116.

Myers, J.W., Jones, J.T., Meyer, T., and Ferrell, J.E., Jr. 2003. Recombinant Dicer efficiently converts large dsRNAs into siRNAs suitable for gene silencing. *Nat Biotechnol* **21**(3): 324-328.

Nag, A., Bondar, T., Shiv, S., and Raychaudhuri, P. 2001. The xeroderma pigmentosum group E gene product DDB2 is a specific target of cullin 4A in mammalian cells. *Mol Cell Biol* **21**(20): 6738-6747.

Neuwald, A.F. and Poleksic, A. 2000. PSI-BLAST searches using hidden markov models of structural repeats: prediction of an unusual sliding DNA clamp and of beta-propellers in UV- damaged DNA-binding protein. *Nucleic Acids Res* **28**(18): 3570-3580.

Nishitani, H., Lygerou, Z., Nishimoto, T., and Nurse, P. 2000. The Cdt1 protein is required to license DNA for replication in fission yeast. *Nature* **404**(6778): 625-628.

Nishitani, H., Sugimoto, N., Roukos, V., Nakanishi, Y., Saijo, M., Obuse, C., Tsurimoto, T., Nakayama, K.I., Nakayama, K., Fujita, M., Lygerou, Z., and Nishimoto, T. 2006. Two E3 ubiquitin ligases, SCF-SKP2 and DDB1-Cul4, target human Cdt1 for proteolysis. *Embo J.*

Ohta, T., Michel, J.J., Schottelius, A.J., and Xiong, Y. 1999. ROC1, a homolog of APC11, represents a family of cullin partners with an associated ubiquitin ligase activity. *Mol Cell* **3**: 535-541.

Oshikawa, K., Matsumoto, M., Yada, M., Kamura, T., Hatakeyama, S., and Nakayama, K.I. 2003. Preferential interaction of TIP120A with Cul1 that is not modified by NEDD8 and not associated with SKP1. *Biochemical and biophysical research communications* **303**(4): 1209-1216.

Patton, E.E., Willems, A., Sa, D., Kuras, L., Thomas, D., Craig, K.L., and Tyer, M. 1998. Cdc53 is a scaffold protein for multiple Cdc34/SKP1/F-box protein complexes that regulate cell division and methionine biosynthesis in yeast. *Genes & Dev* **12**: 692-705.

Petermann, E., Maya-Mendoza, A., Zachos, G., Gillespie, D.A., Jackson, D.A., and Caldecott, K.W. 2006. Chk1 requirement for high global rates of replication fork progression during normal vertebrate S phase. *Mol Cell Biol* **26**(8): 3319-3326.

Petroski, M.D. and Deshaies, R.J. 2005a. Function and regulation of cullin-RING ubiquitin ligases. *Nature reviews* **6**(1): 9-20.

-. 2005b. Mechanism of lysine 48-linked ubiquitin-chain synthesis by the cullin-RING ubiquitin-ligase complex SCF-Cdc34. *Cell* **123**(6): 1107-1120.

Pickart, C.M. 2001. Mechanisms Underlying Ubiquitination. *Annu Rev Biochem* **70**: 503-533.

-. 2004. Back to the future with ubiquitin. *Cell* **116**(2): 181-190.

Pickart, C.M. and Eddins, M.J. 2004. Ubiquitin: structures, functions, mechanisms. *Biochimica et biophysica acta* **1695**(1-3): 55-72.

Pintard, L., Willis, J.H., Willems, A., Johnson, J.L., Srayko, M., Kurz, T., Glaser, S., Mains, P.E., Tyers, M., Bowerman, B., and Peter, M. 2003. The BTB protein MEL-26 is a substrate-specific adaptor of the CUL-3 ubiquitin-ligase. *Nature* **425**(6955): 311-316.

Querido, E., Blanchette, P., Yan, Q., Kamura, T., Morrison, M., Boivin, D., Kaelin, W.G., Conaway, R.C., Conaway, J.W., and Branton, P.E. 2001. Degradation of p53 by adenovirus E4orf6 and E1B55K proteins occurs via a novel mechanism involving a Cullin-containing complex. *Genes & development* **15**(23): 3104-3117.

Rape, M., Reddy, S.K., and Kirschner, M.W. 2006. The processivity of multiubiquitination by the APC determines the order of substrate degradation. *Cell* **124**(1): 89-103.

Rapic-Otrin, V., Navazza, V., Nardo, T., Botta, E., McLenigan, M., Bisi, D.C., Levine, A.S., and Stefanini, M. 2003. True XP group E patients have a defective UV-damaged DNA binding protein complex and mutations in DDB2 which reveal the functional domains of its p48 product. *Hum Mol Genet* **12**(13): 1507-1522.

Re, F., Braaten, D., Franke, E.K., and Luban, J. 1995. Human immunodeficiency virus type 1 Vpr arrests the cell cycle in G2 by inhibiting the activation of p34cdc2-cyclin B. *J Virol* **69**(11): 6859-6864.

Roshal, M., Kim, B., Zhu, Y., Nghiem, P., and Planelles, V. 2003. Activation of the ATR-mediated DNA damage response by the HIV-1 viral protein R. *J Biol Chem* **278**(28): 25879-25886.

Schrofelbauer, B., Hakata, Y., and Landau, N.R. 2007. HIV-1 Vpr function is mediated by interaction with the damage-specific DNA-binding protein DDB1. *Proc Natl Acad Sci U S A* **104**(10): 4130-4135.

Schrofelbauer, B., Yu, Q., Zeitlin, S.G., and Landau, N.R. 2005. Human immunodeficiency virus type 1 Vpr induces the degradation of the UNG and SMUG uracil-DNA glycosylases. *J Virol* **79**(17): 10978-10987.

Selig, L., Benichou, S., Rogel, M.E., Wu, L.I., Vodicka, M.A., Sire, J., Benarous, R., and Emerman, M. 1997. Uracil DNA glycosylase specifically interacts with Vpr of both human immunodeficiency virus type 1 and simian immunodeficiency virus of sooty mangabeys, but binding does not correlate with cell cycle arrest. *J Virol* **71**(6): 4842-4846.

Senga, T., Sivaprasad, U., Zhu, W., Park, J.H., Arias, E.E., Walter, J.C., and Dutta, A. 2006. PCNA is a co-factor for Cdt1 degradation by CUL4/DDB1 mediated N-terminal ubiquitination. *J Biol Chem*.

Seol, J.H., Feldman, R.M.R., Zachariae, W., Shevchenko, A., Correll, C.C., Lyapina, S., Chi, Y., Galova, M., Claypool, J., Sandmeyer, S., Nasmyth, K., and Deshaies, R.J. 1999. Cdc53/cullin and the essential Hrt1 RING-H2 subunit of SCF define a ubiquitin ligase module that activates the E2 enzyme Cdc34. *Genes & Dev* **13**: 1614-1626.

Sharp, D.A., Kratowicz, S.A., Sank, M.J., and George, D.L. 1999. Stabilization of the MDM2 oncoprotein by interaction with the structurally related MDMX protein. *J Biol Chem* **274**(53): 38189-38196.

Skowyra, D., Craig, K., Tyers, M., Elledge, S.J., and Harper, J.W. 1997. F-box proteins are receptors that recruit phosphorylated substrates to the SCF ubiquitin-ligase complex. *Cell* **91**: 209-219.

Skowyra, D., Koepp, D.M., Kamura, T., Conrad, M.N., Conaway, R.C., Conaway, J.W., Elledge, S.J., and Harper, J.W. 1999. Reconstitution of G1 cyclin ubiquitination with complexes containing SCF^{Grr1} and Rbx1. *Science* **284**: 662-665.

Sondek, J., Bohm, A., Lambright, D.G., Hamm, H.E., and Sigler, P.B. 1996. Crystal structure of a G-protein beta gamma dimer at 2.1A resolution. *Nature* **379**(6563): 369-374.

Stebbins, C.E., Kaelin, W.G., Jr., and Pavletich, N.P. 1999. Structure of the VHL-ElonginC-ElonginB complex: implications for VHL tumor suppressor function. *Science* **284**(5413): 455-461.

Stewart, S.A., Poon, B., Jowett, J.B., and Chen, I.S. 1997. Human immunodeficiency virus type 1 Vpr induces apoptosis following cell cycle arrest. *J Virol* **71**(7): 5579-5592.

Sugasawa, K., Okuda, Y., Saijo, M., Nishi, R., Matsuda, N., Chu, G., Mori, T., Iwai, S., Tanaka, K., Tanaka, K., and Hanaoka, F. 2005. UV-induced ubiquitylation of XPC protein mediated by UV-DDB-ubiquitin ligase complex. *Cell* **121**(3): 387-400.

Syljuasen, R.G., Sorensen, C.S., Hansen, L.T., Fugger, K., Lundin, C., Johansson, F., Helleday, T., Sehested, M., Lukas, J., and Bartek, J. 2005. Inhibition of human Chk1 causes increased initiation of DNA replication, phosphorylation of ATR targets, and DNA breakage. *Mol Cell Biol* **25**(9): 3553-3562.

Talis, A.L., Huibregtse, J.M., and Howley, P.M. 1998. The role of E6AP in the regulation of p53 protein levels in human papillomavirus (HPV)-positive and HPV-negative cells. *JBiolChem* **273**: 6439-6445.

Tan, M., Gallegos, J.R., Gu, Q., Huang, Y., Li, J., Jin, Y., Lu, H., and Sun, Y. 2006. SAG/ROC-SCF beta-TrCP E3 ubiquitin ligase promotes pro-caspase-3 degradation as a mechanism of apoptosis protection. *Neoplasia (New York, NY* **8**(12): 1042-1054.

Tan, P., Fuches, S.Y., Angus, A., Wu, K., Gomez, C., Ronai, Z., and Pan, Z.-Q. 1999. Recruitment of a ROC1-CUL1 ubiquitin ligase by SKP1 and HOS to catalyze the ubiquitination of IkBα. *Mol Cell* **3**: 527-533.

Tanimura, S., Ohtsuka, S., Mitsui, K., Shirouzu, K., Yoshimura, A., and Ohtsubo, M. 1999. MDM2 interacts with MDMX through their RING finger domains. *FEBS letters* **447**(1): 5-9.

Tarpey, P.S., Raymond, F.L., O'Meara, S., Edkins, S., Teague, J., Butler, A., Dicks, E., Stevens, C., Tofts, C., Avis, T., Barthorpe, S., Buck, G., Cole, J., Gray, K., Halliday, K., Harrison, R., Hills, K., Jenkinson, A., Jones, D., Menzies, A., Mironenko, T., Perry, J., Raine, K., Richardson, D., Shepherd, R., Small, A., Varian, J., West, S., Widaa, S., Mallya, U., Moon, J., Luo, Y., Holder, S., Smithson, S.F., Hurst, J.A., Clayton-Smith, J., Kerr, B., Boyle, J., Shaw, M., Vandeleur, L., Rodriguez, J., Slaugh, R., Easton, D.F., Wooster, R., Bobrow, M., Srivastava, A.K., Stevenson, R.E., Schwartz, C.E., Turner, G., Gecz, J., Futreal, P.A., Stratton, M.R., and Partington, M. 2007. Mutations in CUL4B, which encodes a ubiquitin E3 ligase subunit, cause an X-linked mental retardation syndrome associated with aggressive outbursts, seizures, relative macrocephaly, central obesity, hypogonadism, pes cavus, and tremor. *American journal of human genetics* **80**(2): 345-352.

Tsvetkov, L.M., Yeh, K.H., Lee, S.J., Sun, H., and Zhang, H. 1999. p27(KIP1) ubiquitination and degradation is regulated by the SCF(SKP2) complex through phosphorylated Thr187 in p27. *CurrBiol* **17**: 661-664.

Ulane, C.M. and Horvath, C.M. 2002. Paramyxoviruses SV5 and HPIV2 assemble STAT protein ubiquitin ligase complexes from cellular components. *Virology* **304**(2): 160-166.

Unsal-Kacmaz, K., Chastain, P.D., Qu, P.P., Minoo, P., Cordeiro-Stone, M., Sancar, A., and Kaufmann, W.K. 2007. The human Tim/Tipin complex coordinates an Intra-S checkpoint response to UV that slows replication fork displacement. *Mol Cell Biol* **27**(8): 3131-3142.

Wang, H., Zhai, L., Xu, J., Joo, H.Y., Jackson, S., Erdjument-Bromage, H., Tempst, P., Xiong, Y., and Zhang, Y. 2006. Histone H3 and H4 ubiquitylation by the CUL4-DDB-ROC1 ubiquitin ligase facilitates cellular response to DNA damage. *Mol Cell* **22**(3): 383-394.

Wertz, I.E., O'Rourke, K.M., Zhang, Z., Dornan, D., Arnott, D., Deshaies, R.J., and Dixit, V.M. 2004. Human De-etiolated-1 regulates c-Jun by assembling a CUL4A ubiquitin ligase. *Science* **303**(5662): 1371-1374.

Wimuttisuk, W. and Singer, J.D. 2007. The Cullin3 ubiquitin ligase functions as a Nedd8-bound heterodimer. *Molecular biology of the cell* **18**(3): 899-909.

Woodward, A.M., Gohler, T., Luciani, M.G., Oehlmann, M., Ge, X., Gartner, A., Jackson, D.A., and Blow, J.J. 2006. Excess Mcm2-7 license dormant origins of replication that can be used under conditions of replicative stress. *The Journal of cell biology* **173**(5): 673-683.

Xu, L., Wei, Y., Reboul, J., Vaglio, P., Shin, T.H., Vidal, M., Elledge, S.J., and Harper, J.W. 2003. BTB proteins are substrate-specific adaptors in an SCF-like modular ubiquitin ligase containing CUL-3. *Nature* **425**(6955): 316-321.

Yasui, K., Arii, S., Zhao, C., Imoto, I., Ueda, M., Nagai, H., Emi, M., and Inazawa, J. 2002. TFDP1, CUL4A, and CDC16 identified as targets for amplification at 13q34 in hepatocellular carcinomas. *Hepatology* **35**(6): 1476-1484.

Yu, X., Yu, Y., Liu, B., Luo, K., Kong, W., Mao, P., and Yu, X.F. 2003. Induction of APOBEC3G ubiquitination and degradation by an HIV-1 Vif-Cul5-SCF complex. *Science* **302**(5647): 1056-1060.

Zhang, J.G., Farley, A., Nicholson, S.E., Willson, T.A., Zugaro, L.M., Simpson, R.J., Moritz, R.L., Cary, D., Richardson, R., Hausmann, G., Kile, B.J., Kent, S.B., Alexander, W.S., Metcalf, D., Hilton, D.J., Nicola, N.A., and Baca, M. 1999. The conserved SOCS box motif in suppressors of cytokine signaling binds to elongins B and C and may couple bound proteins to proteasomal degradation. *Proc Natl Acad Sci U S A* **96**(5): 2071-2076.

Zhang, S., Feng, Y., Narayan, O., and Zhao, L.J. 2001. Cytoplasmic retention of HIV-1 regulatory protein Vpr by protein-protein interaction with a novel human cytoplasmic protein VprBP. *Gene* **263**(1-2): 131-140.

Zhang, Y., Morrone, G., Zhang, J., Chen, X., Lu, X., Ma, L., Moore, M., and Zhou, P. 2003. CUL-4A stimulates ubiquitylation and degradation of the HOXA9 homeodomain protein. *EMBO J* **22**(22): 6057-6067.

Zhao, L.J., Mukherjee, S., and Narayan, O. 1994. Biochemical mechanism of HIV-I Vpr function. Specific interaction with a cellular protein. *J Biol Chem* **269**(22): 15577-15582.

Zheng, J., Yang, X., Harrell, J.M., Ryzhikov, S., Shim, E.H., Lykke-Andersen, K., Wei, N., Sun, H., Kobayashi, R., and Zhang, H. 2002a. CAND1 binds to unneddylated CUL1 and regulates the formation of SCF ubiquitin E3 ligase complex. *Mol Cell* **10**(6): 1519-1526.

Zheng, N., Schulman, B.A., Song, L., Miller, J.J., Jeffrey, P.D., Wang, P., Chu, C., Koepp, D.M., Elledge, S.J., Pagano, M., Conaway, R.C., Conaway, J.W., Harper, J.W., and Pavletich, N.P. 2002b. Structure of the Cul1-Rbx1-SKP1-F boxSKP2 SCF ubiquitin ligase complex. *Nature* **416**(6882): 703-709.

Zhong, W., Feng, H., Santiago, F.E., and Kipreos, E.T. 2003. CUL-4 ubiquitin ligase maintains genome stability by restraining DNA-replication licensing. *Nature* **423**(6942): 885-889.

Zimmerman, E.S., Chen, J., Andersen, J.L., Ardon, O., Dehart, J.L., Blackett, J., Choudhary, S.K., Camerini, D., Nghiem, P., and Planelles, V. 2004. Human immunodeficiency virus type 1 Vpr-mediated G2 arrest requires Rad17 and Hus1 and induces nuclear BRCA1 and gamma-H2AX focus formation. *Mol Cell Biol* **24**(21): 9286-9294.

Zou, Y., Liu, Q., Chen, B., Zhang, X., Guo, C., Zhou, H., Li, J., Gao, G., Guo, Y., Yan, C., Wei, J., Shao, C., and Gong, Y. 2007. Mutation in CUL4B, which encodes a member of cullin-RING ubiquitin ligase complex, causes X-linked mental retardation. *American journal of human genetics* **80**(3): 561-566.